# mRNA binding to organellar surfaces as mode of cellular surveillance

Dissertation

zur Erlangung des Doktorgrades

der Naturwissenschaften

vorgelegt beim Fachbereich Biowissenschaften

der Johann Wolfgang-Goethe-Universität

in Frankfurt am Main

von

**Bo Zhang**

aus Zheng Zhou

**Frankfurt am Main 2022**

**(D30)**

vom Fachbereich Biowissenschaften der Johann Wolfgang-Goethe-Universität als Dissertation angenommen.


Dekan:           Prof. Dr. Sven Klimpel



Erster Gutachter:    Prof. Dr. Enrico Schleiff

Zweiter Gutachter:   Prof. Dr. Jörg Soppa



Datum der Disputation: ……………………….

# ABSTRACT

Generally speaking, protein import into mitochondria and chloroplasts is a post-translational process during which the precursor proteins destined for mitochondria or chloroplasts are translated with cytosolic ribosomes and targeted. The previous results showed that the isolated chloroplasts can import *in vitro* synthesized proteins and the absence of ribosomes in the immediate area around chloroplasts in electron microscopy (EM) images. However, none of the EM images were recorded in the presence of a translation elongation inhibitor. Also, the observation showed that ribosomes stably bind to purified liver mitochondria *in vitro*, and the first indication of chloroplast localization of mRNAs encoding plastid proteins in *Chlamydomonas rheinhardtii*, which challenge the post-translational import and support the co-translational process. Therefore, in this study, the association of the ribosomes to the isolated chloroplasts was analyzed, a binding assay was established and showed that naked ribosomes are not considerably bound to chloroplasts.

Additionally, mRNA localize in close vicinity to mitochondria also challenged post-translation protein import. Global analysis of transcripts bound to mitochondria in yeast or human revealed that around half of the transcripts of mitochondrial proteins displayed a high mitochondrial localization. The observed association of mRNAs with chloroplast fractions and the *in vivo* analysis of the distribution of mRNAs was used as base to formulate the hypothesis that mRNA can bind to chloroplast surface. Therefore, in this study, the mRNA binding assay was established and revealed that mRNAs coding for the mitochondrial cytochrome c oxidase copper chaperone COX17 showed unspecific binding to the chloroplasts. The mRNA coding for chloroplast outer envelope transport protein OEP24 and mRNA coding for the essential nuclear protein 1 (ENP1) showed specific binding, and OEP24 has a 3-fold higher affinity than ENP1 mRNA. Moreover, the BY2-L (*Nicotiana tabacum* non-green cell culture) could confer the highest enhancement of OEP24 mRNA binding efficiency than the COX17 and ENP1 mRNA and the preparation of the BY2-L was optimized. Afterwards, the feasibility to fix the interaction between mRNA and the proteins on the surface of chloroplasts was confirmed. OEP24 mRNA showed more efficiency in the UV-crosslinking. Following, the pull-down with antisense locked nucleic acid (LNA)/DNA oligonucleotides was established which could be used for the further investigation of the proteins involved in the mRNA binding to the chloroplasts.

# 1  TABLE OF CONTENTS

# INDEX OF FIGURES

# INDEX OF TABLES

# ABBREVEATIONS AND UNITS

<u>Non-standard abbreviations</u>

| | | | |
|---|---|---|---|
| ATP | adenosine triphosphate | P body | processing body |
| CHART | capture hybridization analysis of RNA targets | PB-ER | protein body ER |
| ChIRP | chromatin isolation by RNA purification | PB-I/II | ER-derived protein body 1/2 |
| Cis-ER | cisternal ER | Puf | pumilio family binding factor |
| COX | cytochrome c oxidase | RAP | RNA affinity purification |
| ENP1 | essential nuclear protein 1 | RBPs | RNA binding proteins |
| eRIC | enhanced RNA interactome capture | RIC | RNA interactome capture |
| GTP | guanosine triphosphate | RNP | ribonucleoprotein |
| IM | inter membrane | RPL5 | Ribosomal protein of the large subunit 5 |
| LHC | light harvesting complex | RPL10 | Ribosomal protein of the large subunit 10 |
| LNA | locked nucleic acid | RPS3 | Ribosomal protein of the small subunit 3 |
| MS | mass spectrometry | RPS10 | Ribosomal protein of the small subunit 10 |
| MS2-BioTRAP | MS2 *in vivo* biotin-tagged RAP | TOC | translocase of the outer membrane of chloroplasts |
| NPC | nuclear pore complex | TOM | translocase of the outer membrane of mitochondria |
| OEP24 | outer envelope transport protein with the size of 24kDa | TRIP | tandem RNA isolation procedure |
| OM | outer membrane | UDP | uridine diphosphate |
| PAIR | peptide-nucleic-acid-assisted identification of RBPs | UTR | untranslated region |

## Units

| | | | |
|---|---|---|---|
| μg | microgram, $10^{-6}$ g | mL | milliliter, $10^{-3}$ L |
| μL | microliter, $10^{-6}$ L | mM | millimolar, $10^{-3}$ M |
| μM | micromolar, $10^{-6}$ M | nm | nanometer, $10^{-9}$ m |
| °C | degree Celsius | rpm | round per minute |
| g | relative centrifugal force | sec | second |
| h | hour | min | minute |
| kDa | kilo Dalton, $10^3$ Da | u | unit |
| M | molar | vol. | volume |
| mA | milliampere, $10^{-3}$ A | v/v | volume per volume |
| mg | milligram, $10^{-3}$ g | w/v | weight per volume |
| w/w | weight per weight | | |

# ZUSAMMENFASSUNG

Die eukaryotische Zelle ist in Kompartimente unterteilt, diese nennt man Organellen. Zu den Organellen gehören das Cytoplasma, Bestandteile des Endomembransystems (ER, Golgi-Apparat, Plasmamembran), Mitochondrien, Chloroplasten und Peroxisomen. Im Gegensatz zu tierischen Zellen, enthalten Pflanzenzellen zwei Energie generierende Organelle: Chloroplasten und Mitochondrien. Beide dieser Organellen stammen von einem Gram-negativen prokaryotischen Vorläuferorganismus ab. Ein starkes Argument für die Gültigkeit dieser Endosymbiontentheorie ist das Vorhandensein von β-Fass Proteinen in der Membran von Mitochondrien und Chloroplasten. Diese Proteine bestehen aus parallelen, alternierenden β-Faltblättern, welche sich zu einer zylindrischen Struktur falten und Metaboliten oder ungefalteten Proteinen als Membrandurchgang dienen. Im Laufe der Evolution wurden viele Gene, die ursprünglich im Vorläuferorganismus lokalisiert waren, in den Nukleus überführt. Aktuelle Schätzungen gehen davon aus, dass ca. 4.500 protein-codierende Gene vom Cyoanobakterienvorläufer des Chloroplasten in das nukleäre Genom der Wirtszelle transferiert wurden. Während dieser Gentransfer eine zentralisierte Kontrolle der Genexpression ermöglichte, zog er auch die Entwicklung von Zielführungs- und Importmachanismen für nukleär codierte Gene nach sich.

Die intrazelluläre Verteilung von Proteinen, die für alle eukaryotischen Zellen gemein und essentiell ist, wird hauptsächlich von zwei Mechanismen vermittelt, dem co-translationalen- und dem post-translationalen Importprozess. Der erstgenannte Prozess setzt voraus, dass Proteintranslokation und Proteintranslation eng aneinandergekoppelt sind, während im post-translationalen Importprozess die Proteinsynthese nicht mechanisch an die Proteintranslokation angegliedert ist.

Der Proteinimport in Mitochondrien ist ein post-translationaler Prozess, während dem das Vorläuferprotein, welches für Mitochondrien bestimmt ist, an cytosolischen Ribosomen translatiert und dann zielgeführt wird. Diese Vorstellung jedoch, wird von Fällen mitochondrialem Proteinimports in Frage gestellt, die womöglich co-translational erfolgen, was durch die Beobachtung gestützt wird, dass mRNA mit cytoplasmatischen Polysomen in direkter Nähe von Mitochondiren gefunden werden kann. Darüber hinaus wurde beobachtet, dass Ribosomen *in vitro* stabil an aufgereinigte Mitochondiren der Leber binden und durch GTP, sowie einen Transitpeptid, reguliert wurden, was die Existenz von co-translationalen Translokationswegen für den Import von Protein in Mitochondrien weiter untermauert. Ebenso ist der Proteinimport in Chloroplasten ein post-translationaler Prozess. Dies wurde überzeugend bestätigt durch die Befunde, dass isolierte Chloroplasten *in vitro* synthetisierte

Proteine importieren können und auf EM-Bildern ein ribosomen-freier Bereich direkt um den Chloroplasten erkennbar ist. Jedoch gaben Kollegen an, dass keines der EM-Bilder unter der Zugabe von Inhibitoren der Translationselongation aufgenommen wurde.

Abgesehen von der Beobachtung, dass Ribosomen mit Mitochondrien assoziieren, wurde die Vorstellung des post-translationalen Proteinimports auch von der engen Positionierung von mRNA zu Mitochondrien in Frage gestellt. Eine globale Analyse von Transkripten, die an Mitochondrien aus Hefe oder Mensch gebunden hatten, ergab, dass etwa die Hälfte der Transkripte von mitochondrialen Proteinen in hohem Maße eine mitochondriale Lokalisation zeigten. Darüber hinaus ist die mRNA der Glyceraldehyd-3-Phosphat-Dehydrogenase (GAPDH) befähigt an isolierte Mitochondrien zu binden, während die Länge der 3'UTR die Assoziationseffizienz der VDAC3 mRNA mit Mitochondrien beeinflusst.

**Ribosomen binden an Chloroplasten**

Die Abwesenheit von Ribosomen in der direkten Umgebung eines Chloroplasten, die auf EM-Bildern zu sehen ist, wurde nicht in Gegenwart eines Translationselongationsinhibitors aufgenommen. Daher wurde die Assoziation von Ribosomen mit Chloroplasten neu bewertet. Antikörper, die spezifisch die cytosolischen Ribosomen von *Arabidopsis* erkennen, wurden genutzt, um die Detektion von cytosolischen Ribosomen der verschiedenen Organismen *Pisum sativum* (PsL), BY2-Zellkultur (*Nicotiana tabacum* nicht-grüne Zellkultur) und *Triticum aestivum* (Weichweizenkeimling, WGL) zu testen. Hierbei enthielten die isolierten Chloroplasten die Proteine cytosolischer Ribosomen. Verschiedene Behandlungen wurden durchgeführt, um die Ribosomen aus den isolierten Chloroplasten zu entfernen. Weder 300 mM Salz noch 5 mM EDTA reduzierten die Menge an Ribosomen signifikant. 1 mM Puromycin, ein Antibiotikum, das eine verfrühte Termination der Translation einleitet, hingegen verursachte eine geringfügige Reduktion der Menge an cytosolischen Ribosomen. Wenn das BY2-Lysat unter den gleichen Bedingungen zentrifugiert wird, die für die Re-Isolierung der Chloroplasten benutzt wurden (5,000 xg, 1 min, 4 °C), pelletierten die Ribosomen nicht. Dies änderte sich auch nicht durch die Zugabe von ATP oder GTP. Dieser Ansatz konnte genutzt werden, um zu untersuchen, ob Ribosomen eng mit der Chloroplastenoberfläche interagieren oder nicht. Jedoch verstärkte die Gegenwart von ATP diese Interaktion, während GTP keinen Einfluss auf die Bindungsfähigkeit hatte. Außerdem führte die Beigabe von mRNA zur Bildung von Polysomen, welche unter den genutzten Zentrifugationsbedingungen pelletierten.

Abgesehen von den Proteinen, wurde auch rRNA als Indikator zur Analyse der Interaktion genutzt. Hierfür wurde die gesamte RNA des Lysats und der Chloroplasten isoliert und über

ein natives Gel visualisiert. 25SrRNA und 5.8SrRNA wurden nur in der cytosolischen Fraktion visualisiert und 23SrRNA wurde nur in den isolierten Chloroplasten visualisiert. Die rRNA von cytosolischen Ribosomen wurde in der Fraktion der isolierten Chloroplasten quantitativ nicht dargestellt. Die cytosolische 5.8SrRNA als Indikator zeigte, dass nackte Ribosomen im Wesentlichen nicht an die Chloroplasten gebunden waren.

## mRNA bindet an Chloroplasten
## Bindung der mRNAs an Chloroplasten

Da die Bindung von mRNAs an Chloroplasten noch nicht untersucht wurde, wurden drei mRNAs ausgewählt, die für das Transportprotein OEP24 der äußeren chloroplastidären Hüllmembran, das Kupferchaperon COX17 der mitochondrialen Cytochrom-c-Oxidase und das essenzielle Kernprotein 1 (ENP1) kodieren. Die entsprechende Gensequenz umfasst die codierende Sequenz (CDS) und 3'-UTR-Region, die jeweils eine Länge von 843 bp, 400 bp bzw. 1587 bp aufweisen. Die mRNAs wurden nicht unter denselben Bedingungen pelletiert, die für die Re-Isolierung der Chloroplasten verwendet wurden (5,000xg, 1 min, 4 °C). Mit dieser Methode konnte untersucht werden, ob die mRNAs mit der Oberfläche der Chloroplasten interagieren. Mit zunehmender Menge an den Chloroplasten zugesetzten mRNAs kam es zu einer stärkeren Bindung aller drei mRNAs an Chloroplasten. Allerdings unterschieden sich die Bindungsmuster der drei mRNAs. COX17 zeigte eine konzentrationsabhängige unspezifische Bindung, die im Allgemeinen durch ein lineares Verhalten beschrieben wird. OEP24 und ENP1 zeigten eine Kombination der spezifischen und unspezifischen Komponenten der Bindung, die mit der Bindung von COX17 vergleichbar ist. In Anbetracht der erhaltenen Dissoziationskonstante von OEP24 ($K_D = 50 \pm 20$ nM) und ENP1 ($K_D = 160 \pm 50$ nM) hat OEP24 zudem eine 3-fach höhere Affinität als ENP1-mRNA.

Die Interaktion der mRNAs mit der Oberfläche des Chloroplasten ist teilweise nicht elektrostatisch, da sich die Bindungskapazität in Anwesenheit von zusätzlich 75 mM oder 150 mM NaCl nicht drastisch verändert. Darüber hinaus wurde bestätigt, dass die unspezifische Bindung auf die Lipidoberfläche mit den inneren Hüllversikeln als Kompetitor gerichtet wurde. Die Ergänzung von inneren Hüllvesikeln während der mRNA-Bindung an die Chloroplasten verringert die Interaktion der COX17-mRNA. Darüber hinaus reduziert die Ergänzung von inneren Hüllvesikeln während der Bindung von ENP1- oder OEP24-mRNA an Chloroplasten deren Interaktion, obwohl die Reduktion der ENP1-mRNA-Bindung stärker ausgeprägt ist.

Die Konkurrenz für die unspezifische Bindung deckte eine spezifische Interaktion der OEP24-mRNA mit den Chloroplastenoberflächen auf. Der Bindungsassay mit COX17, dem

Kompetitor, zeigte eine konzentrationsabhängige unspezifische Bindung. Die Bindungsassays mit OEP24 und ENP1 wiesen die spezifischen Komponenten der Bindung auf, die mit der Bindung von COX17 verglichen werden konnten. Angesichts der erhaltenen Dissoziationskonstante von OEP24 (KD= 90 ± 20 nM) und ENP1(KD = 320 ± 200 nM) hat OEP24 eine 3-fach höhere Affinität als ENP1-mRNA. Weiterhin ist die Bindung von mRNAs an Chloroplasten unabhängig von der Zugabe von ATP. Die mit Thermolysin behandelten Chloroplasten könnten die Bindungskapazität erhöhen.

Die Funktion des BY2-L auf die mRNA-Bindung wurde analysiert. Die Menge der Hüllvesikel beeinflusste die Wirkung von BY2-L auf die Bindungskapazität. Je mehr Hüllvesikel vorhanden waren, desto geringer war die Bindungskapazität. Durch Zentrifugation (50,000xg, 15 min) konnte die Menge an Hüllvesikeln reduziert werden, was zu einer Erhöhung der Bindungskapazität führte. Es wurde eine geeignete Methode zur Herstellung von BY2-L entwickelt, die die Bindungskapazität heraufsetzt. Die BY2-L sollten 9 Tage lang inkubiert und mit dem Gewichtsverhältnis des TR-Puffers (1:6) lysiert werden, gefolgt von einer 15-minütigen Zentrifugation mit 50,000xg. Mit dem optimierten BY2-L wurde die spezifische Bindung von OEP24 und ENP1 erhöht. Die Anreicherung der spezifischen Bindung von ENP1 betrug das 0.5-Fache, während die Anreicherung der spezifischen Bindung von OEP24 das 3.2-Fache betrug. Die höchste Anreicherung der spezifischen Bindung von OEP24 aus BY2-L bestätigt die Existenz der zytosolischen Faktoren, die am mRNA-Targeting zu den Chloroplasten involviert sind.

## UV-Crosslinking fixierte die Interaktion zwischen mRNAs und Proteinen

Aufgrund der geringen Effizienz der UV-Vernetzung *in vivo* und der Absorptionsfähigkeit der Chloroplasten für UV-Strahlung wurde die Verwendung von ultraviolettem Licht zur Fixierung der Interaktion zwischen mRNAs und Chloroplasten noch nicht beleuchtet. In dieser Arbeit konnte die Interaktion zwischen mRNAs und Proteinen an der Oberfläche des Chloroplasten durch die UV-Vernetzung stark fixiert werden. Die Ausbeute der RNA-Isolierung wurde durch die irreversible Interaktion zwischen mRNAs und Proteinen verringert, da die mit Proteinen quervernetzten mRNAs in der organischen Phase statt in der wässrigen Phase verblieben. Die Effizienz der UV-Vernetzung von OEP24 ist höher als die von COX17.

## Optimale Hybridisierungstemperatur für die LNA-Primer

Die LNA-Primer wurden über die Dehydrierungsreaktion zwischen den carboxyaktivierten Oberflächen der Magnetic Beads und den 3'-Aminomodiferen der LNA-Primer an die Beads gekoppelt. Die gekoppelten Beads konnten die an die Oberfläche der Chloroplasten

gebundenen spezifischen mRNAs hybridisieren. Für die optimale Hybridisierung der LNA$_{OEP24}$ wurde äquimolare COX17-mRNA als Kontrolle verwendet. Die LNA$_{OEP24}$ fing deutlich mehr OEP24-mRNA ein als sowohl COX17-mRNA als auch 16SrRNA und die höchste Bindungseffizienz trat bei 56 °C auf. Die höchste Anreicherung von OEP24 gegenüber der COX17-Kontrolle betrug das 17-Fache und die von 16SrRNA das fast 24-Fache bei 40 °C im Test-Setup.

Für die optimale Hybridisierung der LNA$_{COX17}$ wurde äquimolare OEP24-mRNA als Kontrolle verwendet. Die LNA$_{COX17}$ fing deutlich mehr COX17-mRNA ein als sowohl OEP24-mRNA als auch 16SrRNA und die höchste Bindungseffizienz trat bei 52 °C auf. Die beste Anreicherung von COX17 gegenüber der OEP24-Kontrolle betrug jedoch das 20-Fache und von 16SrRNA das fast 56-Fache bei 40 °C im Test-Setup.

Die Prä-Elution wurde verwendet, um die unspezifische Bindung im Pull-Down-Assay gründlich zu entfernen. Verglichen mit der COX17-mRNA-Kontrolle und der endogenen 16SrRNA waren die OEP24-mRNAs bei allen getesteten Temperaturen stark angereichert, insbesondere wenn die Hybridisierung bei 56 °C durchgeführt wurde. Die LNA$_{OEP24}$ erreichte die beste Anreicherung von OEP24 gegenüber der COX17-Kontrolle von fast 800-Fachen und 16SrRNA von fast 1600-Fachen bei 40 °C im Test-Setup.

In ähnlicher Weise war die Ziel-COX17-mRNA im Vergleich zur OEP24-mRNA-Kontrolle und der endogenen 16SrRNA bei allen getesteten Temperaturen stark angereichert, insbesondere wenn die Hybridisierung bei 48 °C durchgeführt wurde. Die LNA$_{COX17}$ erreichte die beste Anreicherung von COX17 gegenüber der OEP24-Kontrolle um fast das 1250-Fache und von 16SrRNA um fast das 250-Fache bei 48 °C im Test-Setup. Die Temperatur bei 48 °C wurde für weitere Pull-Down-Tests mit LNA$_{COX17}$ gewählt. Daher ist 40 °C die optimale Hybridisierungstemperatur für LNA$_{OEP24}$ und 48 °C ist die richtige Temperatur für die Pull-Down-Tests mit LNA$_{COX17}$.

**Die Analyse von RNAs und Proteinen in der Elution aus LNA $_{OEP24}$-Capture-Assay**

Bevor die Massenspektrometrie-Analyse der Elution durchgeführt wurde, wurden RNAs und Proteine analysiert. Die Probe mit Crosslinking (CL-Probe) beinhaltete eine signifikant geringere Menge an OEP24-mRNA im Vergleich zu der Probe ohne Crosslinking (Nicht-CL-Probe). Die Menge der 16SrRNA wies jedoch keinen Unterschied zwischen der CL-Probe und Nicht-CL-Probe. Für den Nachweis von Proteinen wurden die Werte der Absorbtion bei OD$_{260}$ und OD$_{280}$ ermittelt, um die Menge an RNAs und Proteinen zwischen der CL- und Nicht-CL-Probe zu vergleichen. In der CL-Probe lag der A260-Wert bei 0.827, was fast dem A260-Wert von 0.78 in der Nicht-CL-Stichprobe entsprach. Allerdings lag der A280-Wert in der CL-Probe

bei 1.482 und damit deutlich über dem A280-Wert von 0.397 in der Nicht-CL-Probe, was darauf hinweist, dass mRNAs in der CL-Probe mit mehr Proteinen quervernetzt wurden. Darüber hinaus betrug das Absorptionsverhältnis A260/A280 in der Nicht-CL-Probe 1.96, während es in der CL-Probe 0.558 betrug, was ebenfalls darauf hindeutet, dass in der Elution mit UV-Crosslinking mehr Proteine vorhanden waren. Dies könnte also den Erfolg des Pull-Down-Assays mit den LNA Primern bestätigen, bei dem die mit mRNAs interagierenden Proteine eingefangen wurden.

# 1. INTRODUCTION

## 1.1. Endosymbiotic theory in plant cells

The eukaryotic cell is organized into compartments, which are called organelles. These are cytoplasm, constituents of the endomembrane system (ER, Golgi, plasma membrane), mitochondria, chloroplasts. Each serve as specialized reaction centers within the cell and their function is essential for cellular homeostasis. In contrast to animal cells, plant cells contain two energy-generating organelles, chloroplasts and mitochondria. Chloroplasts are a differentiated form of plastids, a group of organelles with diverse functions in plant cells. They are most abundant in the green tissues of plants and perform amino acid and lipid metabolism, iron-sulfur cluster formation, oxygenic carbon fixation, and photophosphorylation via photosynthesis (Wang and Benning, 2011). In contrast, mitochondria are present in all eukaryotic cells and produce adenosine triphosphate through oxidative phosphorylation and perform important functions in apoptosis, lipid and fatty acid metabolism as well as iron-sulfur cluster assembly (Saraste, 1999; Lill and Mühlenhoff, 2008).

Today it is an accepted hypothesis that both organelles originate from gram-negative prokaryotic progenitor organisms, which were swallowed by a larger eukaryotic cell and in which were subsequently integrated into the cellular system of the host organism (Mirus and Schleiff, 2012; Ku et al., 2015). Mitochondria were the first endosymbiotic organelle, which originated from a α-proteobacterium taken up by a eukaryotic cell, generating the first heterotrophic cell and the last eukaryotic common ancestor (LECA) of all fungal and animal cells (Zimorski et al., 2014). Later on, the mitochondria-containing single cell organism absorbed a singular cyanobacterium, which resulted in the rising to the progenitor of contemporary plant cells (Timmis et al., 2004).

One additional strong argument for the validity of the endosymbiotic theory is the presence of β-barrel proteins in the outer membrane of mitochondria and chloroplasts (reviewed in Jores and Rapaport, 2017). These proteins are composed of parallel, alternating β-sheets that fold into a cylindrical structure which serve as gateways for metabolites or unfolded proteins (Mirus et al., 2010). During the course of evolution many genes originally resident in the progenitor relocated to the nucleus. For example, current estimations assume that around 4,500 protein-coding genes were relocated from the cyanobacterial progenitor of chloroplasts to the nuclear genome (Martin et al., 2002). Therefore, contemporary plastids only retain around 120 protein-encoding genes in their distinct genome, which encode e.g. prokaryotic ribosome subunits, photosystem components and highly hydrophobic membrane proteins (Daley and Whelan, 2005; Leliaert and Lopez-Bautista, 2015). Mitochondria still contain around 10-40 protein

encoding genes in their chondroma (Gray, 1999). While the gene transfer resulted in a centralized control of gene expression, it prompted the development of targeting and import mechanisms for nuclear-encoded genes (Sommer and Schleiff, 2014).

## 1.2. Protein translocation to subcellular compartments

### 1.2.1 The general principle of protein translocation

Recently the discussion of mRNA instead of protein transport is demerging. As for the protein transport, it is common and essential for all eukaryotic cells to intracellularly distribute proteins, which are mainly mediated by two mechanisms: co-translational and post-translational import processes. The former process requires protein translocation to be tightly coupled to translation; however, in the post-translational import process protein synthesis is not mechanically linked to protein translocation (reviewed in Schleiff and Becker, 2011).

In spite of the structural and functional diversity of protein-translocation machineries in different organelles, there are general principles:

1) cytosolic synthesis of a precursor protein containing an organelle-specific signal which could guide the protein to the different organelles and recognized by the cytosolic factors; 2) transport to the target membrane in an import-competent form by cytosolic factors such as the signal-recognition particle (SRP) for the co-translational pathway and chaperones for the post-translational pathway; Also the signal for targeting could localize in the mRNA sequence, a cis-acting sequence which is called localization element (LE) or Zipcode (Jambhekar et al., 2007). 3) the signal is recognized by the receptors on the organelle surface and then mediated by the targeting factors which transferred the protein to the receptor. 4) transport across the membrane by a translocation channel; 5) an energy force that drives translocation; In mitochondria, the energy force is the affinity chain that precursor proteins show increasing affinity for receptors following the recognition order; In chloroplasts, the import reaction is promoted by the GTP binding and hydrolysis 6) processing and folding of the precursor protein occurring inside the target organelle after import.

### 1.2.2 Protein translocation at the endoplasmic reticulum (ER)

It is an accepted hypothesis that the main pathway delivering proteins to the ER is the Signal recognition particle (SRP) pathway mediating the co-translational targeting of translating ribosomes (Saraogi and Shan, 2011). This process is initiated when the signal sequence of an emerging nascent polypeptide from a translating ribosome is recognized by the SRP, which stalls translation and forms a ribosome-nascent chain complex (RNC). Afterwards, the RNC

is delivered to the target membrane through the interaction between SRP and SRP receptor (SR). Then, the RNC is transferred to the Sec61 complex, which facilitates the translocation of the polypeptide across or into the membrane as soon as the translation process is resumed. Meanwhile, SRP and SR are released from each other and targeted for another subsequent round (Junne et al., 2010; Gogala et al., 2014).

### 1.2.3 Proteins translocation to endosymbiotically derived organelles

Currently, it is accepted that protein import into mitochondria and chloroplasts is a post-translational process during which the precursor proteins destined for mitochondria or chloroplasts are translated with cytosolic ribosomes and targeted. To confer high fidelity of the transport process, three prerequisites are required: 1) specific signals within the synthesized precursor; 2) soluble cytosolic factors; 3) receptor proteins on the organelle surface (reviewed in Schleiff and Becker, 2011).

The majority of the precursor proteins importing into the mitochondrial matrix or chloroplast stroma contain a cleaveable N-terminal sequence called a presequence or transit peptide, respectively. This signal sequence comprises the information sufficient for proper targeting and recognition by the membrane receptors on the surface of the organelle (Gakh et al., 2002). Both targeting sequences show the variable length and diverse primary structure, but tend to form an amphiphilic α-helix and show an overall positive charge (Huang et al., 2009), which suggested that it is not a specific sequence motif but rather a physicochemical feature or a certain structural motif that is recognized by the import receptors. The targeting signals of mitochondrial and chloroplast show differences in the starting position of the amphiphilic α-helix and overall hydrophobicity (Huang et al., 2009). Additionally, the abundance of arginines are enriched in mitochondrial signals, which form part of the recognition sites for the processing peptidase. In contrast, the targeting signal of chloroplast is enriched in hydroxylated amino acids, which could be phosphorylation targets of cytosolic kinases (Martin et al., 2006). Thus, this diversity in the targeting information could help distinguish and drive targeting to either mitochondrial or chloroplast.

It is thought that the transport of the preprotein to mitochondrial and chloroplast is regulated by cytosolic soluble factors, which include chaperones such as heat-shock protein 70 (Hsp70). Hsp70 can bind to preproteins, to maintain the unfolded import-competent state of the precursor proteins. Hsp70 could function alone or together with the other cytosolic factors such as 14-3-3 proteins or Hsp90 (May and Soll, 2000). 14-3-3 proteins bind to phosphoserine to modulate biochemical processes such as protein translocation. As for the chloroplast precursor proteins, the phosphorylated transit peptides could bind with Hsp70 and 14-3-3

protein to form a 'guidance' complex, which facilitates the transport of proteins to the chloroplasts. Phosphorylation dependent transport has not been directly shown for mitochondria, but the mitochondrial import-stimulating factor (MSF), a 14-3-3 protein family member, enhances protein translocation into mitochondria (Hachiya et al., 1994). Apart from these chaperones, there are several other factors which can guide precursor proteins to mitochondria or chloroplasts. For example, arylhydrocarbon-receptor-interacting protein (AIP), which is responsible for protein targeting to subcellular compartments and ankyrin-rich protein 2A (AKR2A), which is important for the integration of chloroplast outer membrane proteins containing an α-helical membrane anchor (Bae et al., 2008; Dhanoa et al., 2010).

After the association of the cytosolic soluble factors with precursor proteins, the precursor proteins is transported to the outer membrane and the transfer across the outer membrane of mitochondria and chloroplasts is catalyzed by the translocase complexes, the translocase of the outer membrane of mitochondria (TOM) and the translocase of the outer membrane of chloroplasts (TOC) (Hill et al., 1998; Schnell et al., 1994). Both complexes consist of receptors that function and face the cytosol  (Tom20, Tom70 and Tom22 as well as Toc34, Toc159 and Toc64) and two β-barrel pore forming channel proteins Tom40 and Toc75 (Chacinska et al., 2009; Schleiff et al., 2003). Based on the resistance to detergent, the core complex was assigned. The TOM core complex consists of Tom40, Tom22 and their small partners Tom5, Tom6 and Tom7 (Bausewein et al., 2017); the TOC core complex consists of Toc159, Toc34 and Toc75 (Schleiff et al., 2003). The receptor proteins Tom70 and Tom20, and Toc64, are more loosely associated. TOM 20 is critical for the normal architecture of the TOM complex, while Toc34 affects the stability of the TOC complex by phosphorylation and its GTPase activity (Becker et al., 2004; reviewed in Schleiff and Becker, 2011).

There are two main approaches for both mitochondria and chloroplasts in which the precursor proteins bind to the translocase complexes (reviewed in Schleiff and Becker, 2011). Most precursor proteins are directly guided by the presequence to the receptor Tom20 or Toc34 of the translocons. However, the precursors which form the 'guidance complex' with Hsp70/Hsp90 bind to the peripherally associated Tom70 or Toc64 subunits, which contain a clamp-type tetratricopeptide repeat (TPR) domain (Young et al., 2003; Qbadou et al., 2006). This TPR domain which is exposed to the cytosol is required in the docking of the Hsp70/Hsp90 chaperones. Additionally, Toc64 contains an amidase-like domain which functions in precursor-protein binding to the intermembrane-space site (Qbadou et al., 2007). Therefore, the type of the receptor subunit that is involved is determined by the import signal and whether the precursor is associated with a cytosolic chaperone. With the help of Tom 70 and Toc 64, the precursor proteins are transferred to the TOMcore or TOCcore complexes for translocation, respectively (Yamamoto et al., 2009; Qbadou et al., 2007).

However, the organellar β-barrel proteins do not contain typical N-terminal cleavable targeting signals. Still they are targeted to the outer organellar membrane where they are recognized by surface exposed translocation complexes (Machettira et al., 2012; Ulrich et al., 2012; Jores et al., 2016). Recently, an *in vitro* import reaction showed that the mitochondrial β-barrel membrane protein VDAC1 can distinguish between chloroplasts and mitochondria. This specific targeting process depends on hydrophobicity of the last β-hairpin of the β-barrel (Kutik et al., 2008; Jores et al., 2016). Furthermore, the characterization of Klinger et al (2019) of the final two strands of mitochondrial and chloroplasts OM β-barrel proteins, showed that amino acids with hydrophilic residues are more prevalent in plastidic proteins then in mitochondrial β-barrel proteins. Therefore, it is accepted that the hydrophobicity profile of the penultimate β-strand is the defining regulatory element of mitochondrial targeting, while an additional hydrophilic amino acid residue is necessary for mitochondrial targeting. Interestingly, the β-barrel protein OEP24 in chloroplasts outer membrane is imported into both organelles *in vitro* (Ulrich et al., 2012; reviewed in Jores and Rapaport, 2017). However, no similar signal which facilitates the targeting of β-barrel proteins to chloroplasts was reported. Therefore, there might be another mechanism which ensures the proper targeting of β-barrel protein during chloroplasts biogenesis.
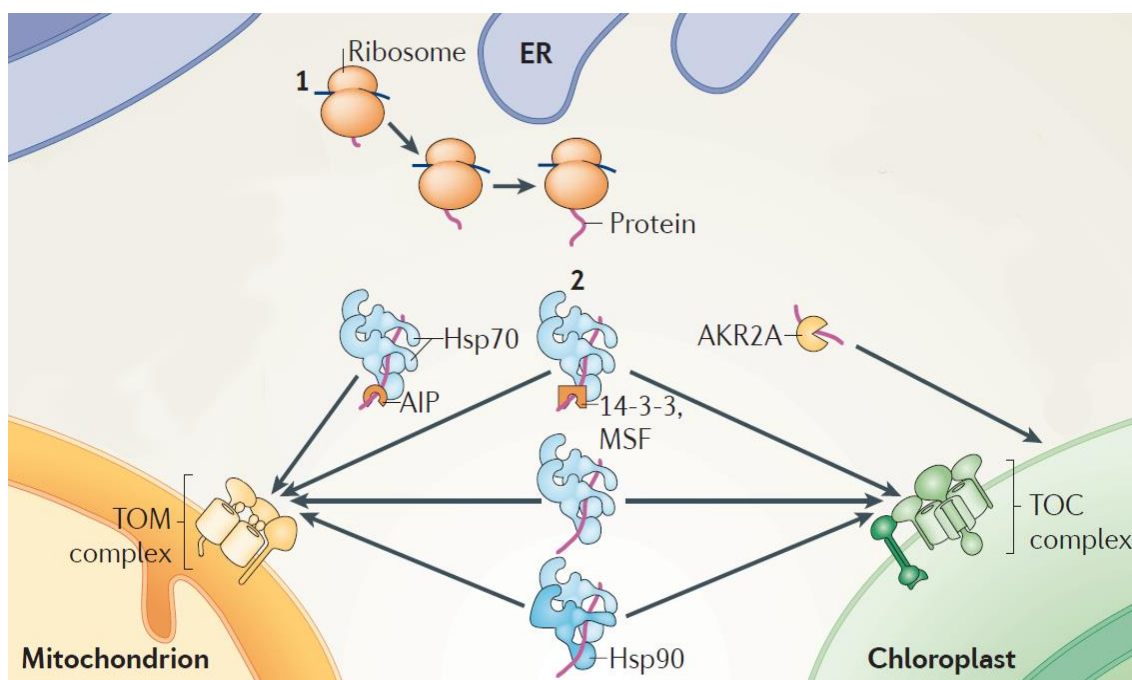


**Figure 1-1 The main precursor-protein transport pathways from the cytosol to organelles.**
Post-translational protein transport is performed on cytosolically synthesized ribosomes **(1)** and facilitated by cytosolic factors **(2)** that bind the polypeptide chain and shuttle the protein to the respective organelle. Hsp70 works in concert with various other protein factors like Hsp90, 14-3-3 proteins and AIP to guide translated polypeptides to their respective organellar translocon. AKR2A is responsible for the integration of chloroplast outer membrane proteins containing an α-helical membrane anchor. Adapted and modified from Schleiff and Becker, 2011.

## 1.2.4 mRNA-based protein targeting

In addition to peptide-based targeting processes, messenger RNA (mRNA) themselves are recognized and transported to specific destination sites within the cell for local synthesis of the corresponding proteins (Tian and Okita, 2014). The emergence of mRNA localization, driven by the cis-acting elements is an alternative mechanism for the protein targeting throughout the eukaryotic species including metazoans, yeast, algae, and higher plants (Tian and Okita, 2014).

Compared with the classical peptide sequence-based targeting, mRNA-based targeting pathway includes several advantages. 1) avoiding the protein from intracellular regions in which it would be toxic, 2) exclude the requirement for other targeting mechanisms, 3) guarantee the efficient translational responses to various abiotic or biotic conditions, 4) allowing the mediation of the protein synthesis stimulated by the requirement for the product, 5) offering economic benefits by not localizing many copies of a protein translated from a single mRNA (reviewed in Weis et al., 2013).

The components of the mRNA-based localization included the cis-acting sequence called a localization element (LE) or Zipcode within the RNA sequence (Jambhekar et al., 2007). The length of the Zipcodes range from a few nucleotides to highly complex and redundant sequences of up to 1kb (Ainger et al., 1997). It is highly accepted that most Zipcodes are located within the 3'UTR leading to the specific localization of mRNA (Kraut-Cohen et al., 2010). The other components of the mRNA-based localization are the RNA-binding proteins which associate with the cis-acting sequence and mediate the localization to different organelles (reviewed in Weis et al., 2013).

### *1.2.4.1 mRNA targeting to Mitochondria*

As for the mitochondrial targeting, the peptide based mode is the most prevalent. However, this post-translation mode of protein import was challenged with the examples of an obligate co-translational mitochondrial protein import, supported by the evidence that mRNAs together with cytoplasmic polysomes localize in close vicinity to mitochondria (Kellems et al., 1972; Kellems et al., 1974; Kellems et al., 1975).

Initially, several researchers found that ribosomes are associated with the mitochondria in cell fractionation assay (Kellems et al., 1974). The stability in response to KCL concentrations showed significant differences between this mitochondrial associated ribosomes and free ribosomes in cytoplasm, which showed that the mitochondria-localized ribosomes are of cytoplasmic nature (80S) and were able to be linked to the mitochondria via the nascent peptide chain. Additionally, the existence of the specific binding sites for ribosomes were

proposed, supported by the evidence that mitochondria washed by EDTA could interact with 80S ribosomes in a Mg2+ dependent manner (Kellems et al., 1975). Afterwards, the vicinity of polysomes in mitochondria was observed with EM analyses in yeast spheroplasts. In the 1970s, researches showed that mitochondrial mRNA is enriched in polysomes translating mitochondrial proteins in specific enzymatic assays, which not only corroborated the initial results but also support this RNA dependent association (Kellems et al., 1975).

In the 2000s, the global analysis of transcripts bound to mitochondria in yeast or human revealed that around half of the transcripts of mitochondrial proteins displayed a high mitochondrial localization (Marc et al., 2002). For example, transcripts from proteins of the cytochrome oxidase complex, like *COX17*. These analyses proposed that co-translational import might be the predominant pathway for proteins encoded by the genes of prokaryotic origin (Marc et al., 2002). Moreover, this observation was subsequently extended from yeast to higher mammals. A tight binding of ribosomes to mitochondria was observed and thought to be regulated by GDP/GTP and the presequence in the nascent chain (Crowley et al., 1998). Later on, the import of adenylate kinase 2 into rat mitochondria was inhibited by the cycloheximide treatment (80S ribosome inhibitor); and the mitochondrial association of mammalian ribosomes requires Mg2+ ions and surface proteins, which could further support the existence of the co-translational import (Nobumoto et al., 1998).

Currently, it was reported that the Puf (Pumilio-Fem-3 binding factor) protein family and TOM complexes play critical roles in the mRNA localization to mitochondrial (reviewed in Weis et al., 2013). Puf proteins containing several repeats of a RNA-binding domain Pumilio existed in yeast. There are six members in the PUF protein family. Each of the Puf proteins can bind to a large set of distinct and functionally related mRNAs (Gerber et al., 2004; Gu et al., 2004). The novel and conserved sequence in 3'-untranslated regions of the mRNA bound by Puf3p, Puf4p, and Puf5p was identified. Additionally, *in vitro* the Puf6 protein could bind to the 3' UTR of Ash1 mRNA and subsequently repress its translation in the transport to the cytoplasm (Gu et al., 2004). Interestingly, the Puf6 protein could also be copurified with She2p-mRNPs complexes in which Ash1 mRNA was detected (Shen et al., 2009). The Puf3 protein colocalizes with mitochondria at the periphery of the outer membrane which is consistent with the function in the localization of transcripts to the mitochondrial surface (Saint-Georges et al., 2008; Gerber et al., 2004)  For instance, In Δpuf3 yeast strains, COX17 enrichment at mitochondria is greatly diminished when compared to the wild-type strain (Saint-Georges et al., 2008). Moreover, this protein could bind to the consensus RNA motif in 3' UTR of 270– 300 nuclear genes which encode the mitochondrial proteins. Puf3 also functions in the regulation of mitochondrial biogenesis and motility in budding yeast which was proved by the observation of altered morphology and abnormal motility of mitochondria in Δpuf3-strain

(Saint-Georges et al., 2008). Two classes of mitochondria bound mRNAs were uncovered with microarray based analysis in the Δpuf3-strain. Class I mRNA are Puf3p dependent as its mislocalization was observed in the deletion strains; Class II mRNAs are Puf3p independent in the localization process. Additionally, this classification analysis showed that nearly 40% of the mRNAs were associated with the mitochondrial surface in a Puf3p-independent manner. Both classes have the common requirement of translation while associated with mitochondria.

In addition to the Puf protein family, the TOM complex itself undoubtedly plays an important role in mRNA targeting to the mitochondrial surface (Michaud et al., 2010; Eliyahu et al., 2010). In yeast, the deletion of the Tom20 leads to the mislocalization of several mRNAs encoding mitochondrial proteins (Eliyahu et al., 2010). The translating ribosomes are required for these mitochondrial protein encoding mRNAs, which indicates that for mitochondrial mRNA localization by Tom20, the mitochondrial presequence rather than the cis-element in 3'UTR of its transcript is necessary (Eliyahu et al., 2010). Surprisingly, TOM70 mRNA localization to mitochondria was neither affected in TOM20 deletion strain nor affected by cycloheximide treatment. These results are consistent with the findings that some mRNAs are translational independent in the localization to mitochondria, which might be facilitated by receptors like the Puf3 protein or other yet unidentified candidates (Saint-Georges et al., 2008). Interestingly, the localization of certain mRNAs was significantly influenced by the deletion of Tom6, Tom7 or Tom70 (Gadir et al., 2011). In plants, the evidence from the co-isolation assays have shown the co-purification of various mitochondrial transcripts and cytosolic proteins with mitochondria, which illustrates the ability of binding to the mitochondrial surface (Michaud et al., 2010). It has also been shown that the glyceraldehyde-3-phosphate dehydrogenase (GAPDH) mRNA is able to bind to isolated mitochondria treated with proteinase K *in vitro*,
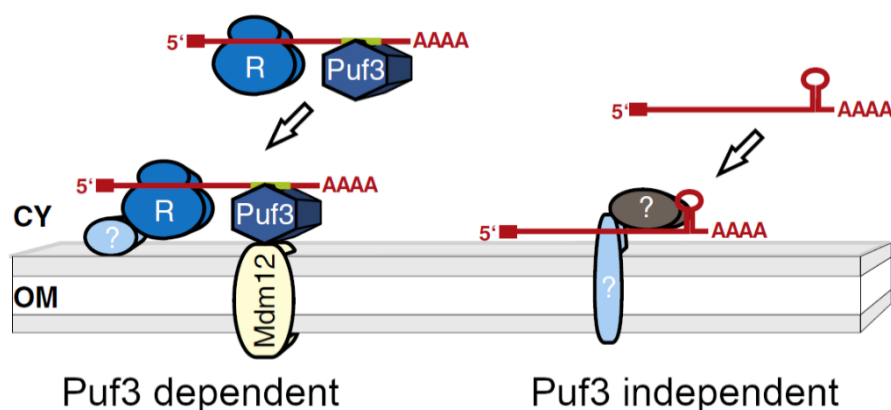


**Figure 1-2 Modes of direct association of mRNAs with mitochondria.** Puf3-dependent mitochondrial localized mRNAs feature a 3'UTR zipcode which serves as the binding site for Puf3. Subsequently, Puf3 facilitates the enrichment at the mitochondrial surface via an interaction with Mdm12. Puf3-independent mRNAs are targeted to mitochondria by still unidentified factors. Obtained from Weis et al., 2013.

which indicates that Tom 40 could interact with mRNA in the absence of *trans*-acting protein factors (Michaud et al., 2014a). Later on, the same group found that the length of the 3'UTR influences the efficiency of VDAC3 association with mitochondria (Michaud et al., 2014b). Thereby, various TOM complex components are involved in the targeting of mRNA to mitochondria.

### 1.2.4.2 mRNA targeting to chloroplast

Compared with the studies in mitochondria, there is much less known about mRNA targeting to chloroplasts. The notion of the protein targeting to the chloroplast was thought to be an entirely post-translation process, which was confirmed by the findings that the isolated chloroplasts can import *in vitro* synthesized proteins and the absence of ribosomes in the immediate area around chloroplasts in EM images (Ulrich et al., 2012; Carde et al., 1982; Uniacke and Zerges, 2009). However, some findings started to challenge this convinced notion. Firstly, the ribosomes in the chloroplast of *C. reinhardtii* are membrane-bound, approximately 50% are held only by electrostatic interactions, which indicated that polysomes are tethered to membranes by proteins that bind chloroplast mRNAs, ribosomes, or both (Margulies and Michaels, 1974). Secondly, chloroplasts can directly import nuclear-transcribed RNAs encoding the eukaryotic initiation factor 4E (eIF4E), and the eIF4E mRNA was found located within the stromal compartment of chloroplast (Nicolai et al., 2007). The strongest evidence against the post-translation import is the finding that LhcIIA mRNAs encoding the light harvesting complex II (LHCII) subunits in Chlamydomonas are enriched on the cytoplasmic border of the chloroplast basal region (Uniacke and Zerges, 2009). However, this localization pattern was abolished by treatment with puromycin, which prematurely releases the association of the ribosome. Therefore, the targeting of LHCII subunits to chloroplasts in *C. rheinahrdii* must be translation dependent, confirming the existence of a co-translational pathway (Uniacke and Zerges, 2009).

## 1.3 RNA-binding proteins

RNA-binding proteins (RBPs) interact with RNAs to form dynamic ribonucleoprotein (RNP) complexes that regulate the fate and function of RNA at virtually every step of its life cycle (Glisovic et al., 2008). Therefore, RBPs affect the structure and interactions of the RNAs and are key players in their biogenesis, stability, function, transport and cellular localization (Glisovic et al., 2008). In the plant field, RBPs also function in every aspect of RNA biology, such as splicing, RNA modification, localization, folding and editing. The RBPs not only

influence each of these processes, but also contribute greatly to the process of the development and stress response in plants (Lee and Kang 2016).

## 1.3.1 The function of the RNA-binding proteins in plant mRNA localization

In the plant field, the function of the mRNA-binding proteins in the mRNA localization has been well revealed in *Oryza sativa* endosperm cells (Hamada et al., 2003; Tian and Okita, 2014). In rice, two major storage proteins prolamin and glutelin are synthesized on the ER, transported across the ER membrane into the lumen and folded in different compartments of the ER (Hamada et al., 2003). Afterwards, prolamin proteins are kept as intracisternal inclusions of the ER and generate the ER-derived protein body 1(PB-I). Glutelin on the other hand is transported to protein storage vacuoles (PSVs) via the Golgi apparatus to form PB-II (Tian et al., 2018). The differential localization of the individual mRNA on the ER contribute to the segregation of these two proteins. Since glutelin mRNAs are predominantly detected on the protein body ER (PB-ER), whereas prolamin mRNAs are present on the cisternal-ER (Cis-ER) (Tian and Okita, 2014). During this process, AU-rich zipcode sequences in the 3'UTR of those mRNA facilitate the localization of glutelin and prolamin mRNA and the deletion of those sequence caused the mis-localization (Washida et al., 2009). Also, RBP-P plays a critical role in this localization of both mRNA. Since the mutation of essential amino acids in RBP-P resulted in the reduction of the binding efficiency between RBP-P and its targets, which subsequently lead to the mislocalization of glutelin and prolamin mRNA (Tian et al., 2018, 2019).

## 1.3.2 The method to identify the RNA-binding proteins

Considering the critical role of RBPs in cellular function, it is very essential to elucidate the composition of RBPs bound to the interest RNA (Bach-Pages et al., 2020). However, these dynamic interactions are often transient which challenge the identification of the important proteins binding with the given RNA (Ramanathan et al., 2019). Generally speaking, the methods for the RNA-binding proteins could be classified into two categories: *In vitro* methods commonly are used to study RNAs and proteins outside the context of an intact cell. *In vivo* approaches are used to investigate RNA–protein interactions in the cellular environment and are subdivided according to whether cross-linking is used. Each *in vitro* and *in vivo* RNA centric method has particular strengths and drawbacks (Table 1-1), which makes it important to select a method tailored to the biological question being addressed (Ramanathan et al., 2019).

### 1.3.2.1 *In vitro* methods

*In vitro*-transcribed (IVT) RNA containing a tag that binds to resin is commonly used in *in vitro* methods. Once the RNA is associated with the resin, cellular extract was incubated with RNA, and the stringent washing steps are conducted to define the RBPs bound to the IVT RNA bait (Faoro et al., 2014). The obvious advantages of this method is speed and ease. The particular advantage is the possibility of mutagenesis studies which could identify the specific RNA nucleotides and protein amino acids involved in the binding of a given RNA–protein pair. The disadvantage is that IVT RNA might lack the identical modification or structure of the RNA in cellular condition. Numerous tags have been developed for *in vitro* methods, including End-labeled biotinylated RNA (Zheng et al., 2016), RNA aptamer tags (Hartmuth et al., 2004; Hogg et al., 2007), S1 aptamer tag (Leppek et al., 2014). As a category of methods, *in vitro* pulldowns overall are particularly useful for characterizing the binding of specific known RNA–protein interactions (Ramanathan et al., 2019).

### 1.3.2.2 *In vivo* methods

*In vivo* methods, protein-RNA cross-linking could be used to identify the *in vivo* interaction by purifying the bait RNA under denaturing condition, after the stringent washing to remove the unspecific interactions, the cross-linked proteins can be identified. Formaldehyde is a small, bifunctional cross-linker that readily permeates cells and cross-links macromolecules within 2 Å, which could create a reversible covalent linkage. This covalent linkage could be created in protein–protein, protein–DNA, and protein–RNA complexes (Sutherland et al., 2008). UV light cross-links protein to nucleic acid at zero distance and forms an irreversible covalent bond (Li et al., 2014; Beckmann et al., 2017). Each cross-linking method shows different advantages and disadvantages. Since UV light is a zero-distance cross-linker which could not cross-link protein-protein interactions. It is a more specific cross-linker than formaldehyde. However, the efficiency of UV cross-linking is lower than formaldehyde (Li et al., 2014). Both cross-linking method have preferences. UV cross-linking has a slight uridine biases and double-stranded RNA is known to be poorly cross-linked (Sugimoto et al., 2012; Kim et al., 2019). The efficiency of UV cross-linking differs by amino acid, the structure and surface area of the protein-RNA interaction and other factors (Meisenheimer et al., 1997). However, the current knowledge of cross-linking efficiency remains incomplete and further research is still needed to make progress on this essential problem. In contrast, strongly nucleophilic lysine residues are preferentially crosslinked in formaldehyde cross-linking (Hoffman et al., 2015). Since formaldehyde generates cross-linking not only between proteins but also between protein and RNA, and thus it is difficult to differentiate proteins that directly contact RNA from those that are complexed with directly bound proteins.

Several *in vivo* methods use either formaldehyde or UV crosslinking. Chromatin isolation by RNA purification (ChIRP) (Chu et al., 2011; Chu et al., 2015) and capture hybridization analysis of RNA targets (CHART) (Simon et al., 2011), use formaldehyde to cross-link RNA to proteins. CHART requires an additional RNase H assay to identify accessible sites for probes, whereas ChIRP does not require prior knowledge of RNA accessibility and uses shorter, 20-mer oligonucleotide probes (Chu et al., 2011; Simon et al., 2013). These biotinylated probes hybridize with RNA in the cell and are captured with streptavidin beads for proteomic analysis. Methods that use UV cross-linking include RNA affinity purification (RAP) (McHugh et al., 2018; Hacisuleyman et al., 2014), peptide-nucleic-acid-assisted identification of RBPs (PAIR) (Zeng et al., 2006), MS2 *in vivo* biotin-tagged RAP (MS2- BioTRAP) (Tsai et al., 2011), and tandem RNA isolation procedure (TRIP) (Matia-González et al., 2017). Although they share a common UV cross-linking approach, these methods differ in experimental setup. RAP uses long, 120-oligonucleotide probes to pull down RNA–RBP complexes after crosslinking and has been used to study noncoding RNAs such as Xist and FIRRE (McHugh et al., 2015; Hacisuleyman et al., 2014). PAIR uses peptide nucleic acid probes with cell penetrating peptides to gain entry into cells and hybridize to RNA, after which the RNA is purified, along with bound RBPs (Zeng et al., 2006). MS2-BioTRAP uses the interaction between MS2 hairpin loop and MS2 coat protein to tether protein to RNA (Parrott et al., 2008). Both MS2 hairpin RNA and MS2 coat protein are expressed in the same cell and form a stable complex, enabling the fusion MS2 coat protein to be used as a handle to purify the MS2-containing RNA after UV cross-linking (Tsai et al., 2011). The ectopic expression of MS2-tagged RNA might not reflect physiological levels of RNA, which can potentially impair the accuracy of downstream proteomic analysis. TRIP is used to study polyadenylated RNA and uses a dual purification: poly(A) RNA is purified first, and then biotinylated antisense oligonucleotides (ASOs) are used to hybridize with the RNA of interest in the poly(A) mixture by base pairing, after which the RNA–ASO complex is purified with streptavidin beads (Matia-González et al., 2017).

A recently developed approach termed RNA interactome capture (RIC) can systematically and comprehensively identify the proteins that interact with polyadenylated RNAs in living cells (Bach-Pages et al., 2020). RIC employs ultraviolet (UV) irradiation of cells to promote RNA-to-protein crosslinking, followed by capture of poly(A) RNAs with oligo(dT) under denaturing conditions. Proteins crosslinked to isolated poly(A) RNA are identified by quantitative mass spectrometry (Castello et al., 2013). Later on, enhanced RNA interactome capture (eRIC) was developed, a method based on the use of locked nucleic acid (LNA)-modified (Figure1-4) capture probe and more stringent capture and washing conditions (Rogell et al., 2017; Perez-Perri et al., 2018; Perez-Perri et al., 2021). eRIC markedly increases capture specificity,

reduces material requirement, and improves signal-to-noise ratios compared to precedent techniques. eRIC is particularly suitable for the detection of unconventional RBPs and the identification of dynamic changes among the RNA-bound proteome (Perez-Perri et al., 2018; 2021).

**Table 1 Comparison of RNA-centric methods**

| Method | Advantages | Disadvantages |
|---|---|---|
| Biotinylated RNA | Strong binding of biotin-end-labeled RNA with streptavidin beads | *In vitro*; potentially biased toward abundant proteins in cell extracts |
| S1 aptamer | Easy elution of RBP complex from streptavidin beads with biotin | *In vitro*; potentially biased toward abundant proteins |
| RAP | *In vivo*; high specificity with UV cross-linking and long oligonucleotide probes (120 nt) | High input cell numbers |
| TRIP | *In vivo*; high specificity with UV cross-linking | Two capture steps with poly(A) and biotinylated ASO capture decrease efficiency |
| PAIR | *In vivo*; high specificity with UV cross-linking | Cost and effort for production of peptide nucleic acid |
| MS2-BioTRAP | *In vivo*; high specificity with UV cross-linking | Requires MS2 conjugation to RNA, transfection/infection of RNA and labeler protein, and high input cell numbers |
| CHART | *In vivo* | Additional RNase H step to identify accessible sites for probes; high input cell numbers |
| ChIRP | *In vivo*; no prior knowledge of RNA accessibility required for probe design | Short probes may pull down similar sequence fragments; high input cell numbers |

# 2 OBJECTIVES

The protein based post-translational import has been extensively studied in the past. As isolated chloroplasts can import *in vitro* synthesized proteins and the absence of ribosomes in the immediate area around chloroplasts in EM images. However, none of the EM images were recorded in the presence of a translation elongation inhibitor (Uniacke et al., 2009). Additionally, previous findings showed that ribosomes stably bind to purified liver mitochondria *in vitro* (Crowley et al., 1997). Therefore, the first objective of this work is to check if ribosomes are able to bind to the chloroplasts.

The post-translation protein transport notion was further challenged by the other evidences that mRNAs localize in close vicinity to mitochondria. Global analysis of transcripts bound to mitochondria in yeast or human revealed that around half of the transcripts of mitochondrial proteins displayed a high mitochondrial localization (Marc et al., 2002). Also, the glyceraldehyde-3-phosphate dehydrogenase (GAPDH) mRNA is able to bind to isolated mitochondria treated with proteinase K *in vitro*, which indicated Tom 40 could interact with mRNA in the absence of *trans*-acting protein factors (Michaud et al., 2014a). A subsequent study by the laboratory of Prof. Schleiff (personal communication) revealed a high accumulation of mRNAs coding for chloroplast proteins at the chloroplast surface. Therefore, the second objective is to conduct the mRNA binding to chloroplasts *in vitro.*

A third question arises from the widely used model system for protein import: the incubation of synthesized proteins with isolated chloroplasts. This system omits cytosolic factors. Thus, the importance of such factors needed to be explored. Since the BY2-L could be used for the translation *in vitro* (Buntru et al., 2014), BY2-L can serve as model for a cytosolic environment which might contain factors involved in mRNA targeting to chloroplasts. Therefore, following the remained question in the former objective, another objective is to further analyze the effects of the BY2-L on the established mRNA binding assay.

Regarding the great functions of the RBPs in the biology process, it is beneficial to identify the RBPs in the process of the mRNA targeting to chloroplasts. The current method RNA interactome capture (RIC) is broadly used to identify the repertoire of RBPs. However, applying RIC to plant tissues containing the chloroplasts is challenging since the UV-crosslinking efficiency can be reduced due to the additional secondary metabolites and the presence of UV-absorbing pigments such as chlorophyll (Köster et al., 2019). Thus, another objective is to identify putative RBPs by UV-crosslinking to fix the interaction between mRNA and proteins in the surface of the chloroplasts.

# 3. MATERIALS

## 3.1. Oligonucleotides

The oligonucleotides used in this research were purchased from Eurofins Genomics GmbH (Ebersberg, Germany), and preserved in 100 µM stock solution and are presented in the following tables.

**Table 3-1 Oligonucleotides used for PCR to T7 promoter insertion, clone the CDS and 3'UTR of the target gene.**

| Name | Sequence (5' → 3') |
|------|--------------------|
| Fw_COX17 | ATGACTGATCAGCCAGCACAAAATG |
| Rv_COX17 | TTGAAAAGATGGTTTCTTTTTA |
| Fw_OEP24 | ATGGCGATGAAGGCTTCTATCAAAG |
| Rv_OEP24 | CGTTGTTTAATTTTTATTCTTGAAC |
| Fw_ENP1 | ATGGCGAAGAAGCGAGATCG |
| Rv_ENP1 | GAACCACCTACATGAACCGA |
| T7 primer | TAATACGACTCACTATAGGGCCACCATGG |

**Table 3-2 Oligonucleotides used for qRT-PCR to analyse the RNA amount in the elution.**

| Name | Sequence (5' → 3') |
|------|--------------------|
| qRT_OEP24_F | ATGGCGATGAAGGCTTCTAT |
| qRT_OEP24_R | TACAGCGAGAGCGAGACC |
| qRT_COX17_F | TGATCAGCCAGCACAAAT |
| qRT_COX17_R | GCTTCTTGGTATCAGGGCA |
| qRT_16srRNA_F | AAAGGAGGTGATCCAGTCG |
| qRT_16srRNA_R | ACCTTAACCGCAAGGAGG |

**Table 3-3 LNA/DNA mixmer oligonucleotides used for the pull-down assay**

| Name | Sequence (5' → 3') | Modification |
|------|--------------------|--------------|
| LNA$_{COX17}$ | ACCTTCTGCTCGGAGACAAAT | 3AmMO |
| LNA$_{OEP24}$ | TCAGCTCTGTATGAATGTAA | 3AmMO |

3AmMO: 3´end aminomodifier

## 3.2 Chemicals, media and buffers

The chemicals used in this study were ordered from Sigma-Aldrich (München, Germany), VWR (Darmstadt, Germany), Merck (Darmstadt, Germany) and Roth (Karlsruhe, Germany) in analytical purity grade. All the buffers were prepared based on the Sambrook and Russell (2001) and autoclaved or filtered through a 0.22 µm sterile filter, if required. The Murashige Skoog (MS) which contains 0.44 % (v/w) MS salts, 0.3 % (v/w) gelrite and 20 mM 2-(N-Morpholino) ethanesulfonic acid (MES)/KOH pH 5.7 was used to grow the plants. Standard buffers and media were prepared following the (Sambrook and Russel, 2001) and autoclaved, if it is necessary.

## 3.3 Kits and enzymes

The DNeazy kit used for the DNA extraction from the agarose gels and RNA isolation from plant tissue were bought from VWR (Darmstadt, Germany). The RevertAid kit which was used for reverse transcription were purchased from the Thermo Fischer Scientific (Frankfurt, Germany). Thermolysin was purchased from Sigma Aldrich (München, Germany). Enzymes including Restriction endonucleases, T4-DNA-ligases which were used for the molecular cloning methods were obtained from Thermo Fisher Scientific (Frankfurt, Germany). Enzymes used for the plant work were purchased from Duchefa Biochemie (Haarlem, Netherland).

## 3.4 Organisms used in this study

**Table 3-4 Bacterial strains and plant used in this study**

| Organism | Strain | Genotype | Source |
|---|---|---|---|
| *Escherichia coli* | DH5α | F⁻ Φ80*lac*ZΔM15 Δ(*lac*ZYA-*arg*F)U169 *rec*A1 *end*A1 *hsd*R17 ($r_K^-$, $m_K^+$) *pho*A *sup*E44 *thi*-1 *gyr*A96 *rel*A1 λ⁻ | Invitrogen, Carlsbad, USA |
| *Pisum sativum* | | Wildtype | |

## 3.5 Antibodies

**Table 3-5 Antibodies used in this study**

| Name | source | dilution |
|------|--------|----------|
| αRPS3 | raised | 1:5000 |
| αRPS10 | raised | 1:2000 |
| αRPL5 | raised | 1:5000 |
| αRPL10 | raised | 1:5000 |
| αActin | Sigma | 1:5000 |
| αToc34 | raised | 1:5000 |

# 4. METHODS

## 4.1 Molecular biological and biochemical methods

### 4.1.1 Standard molecular cloning techniques

The basic experimental execution of the analytical and preparative DNA restriction reactions, transformation, the growth of the bacteria, plasmid isolation and polymerase chain reaction (PCR) were achieved following the instruction as described (Sambrook and Russell, 2001). The Phusion High Fidelity Polymerase (NEB, Ipswich, USA) was used to amplify the fragment, during which 50-100 ng template was used in addition to 1.5 µl mononucleotides (2 mM stock), 0.2 U Phusion High Fidelity Polymerase and 1.5 µl forward and reverse oligonucleotide (10 µM stock). Regarding the elongation speed of the Phusion High Fidelity Polymerase, the elongation time was calculated based on the length of the fragment. Annealing temperature was dependent on the base composition of the primers. The separation of the amplification was conducted based on the electrophoresis using Tris-Taurin-EDTA (TTE) as the running buffer under the condition of the voltage limitation at 30 V/cm (Mülhardt, 2013). If necessary, the separated fragments were extracted with using a Gel Extraction Kit (Omega Bio-Tek, Nocross, USA).

### 4.1.2 RNA extraction using TRIzol

This protocol is suitable for the both protoplasts and leaves. 350 µL Trizol was used for 0.3-0.4 Mio protoplasts or for 70 mg leaves. The leaves were frozen with liquid $N_2$ and smashed with mortar and pestle before the Trizol was added. Afterwards, the samples were vortexed. Then the samples were incubated at RT for 5 min to dissolve the nucleoprotein complexes. 70 µL chloroform was added and samples were vortexed for 1 min, then the samples were incubated 5 min at RT. After the incubation, the samples were subjected to centrifugation 12,000xg at 4 °C for 15 min. The aqueous (RNA containing) phase was gently transferred to a new tube (please note: the interphase should not be touched in order to avoid the additional contamination from chloroform and protein). Then, 175 µL isopropanol were added into the collected aqueous phase and vortexed for 20 sec. The mixture was incubated 10-20 min at RT (time can be extended to 45 min to improve the yield. However, 10 min is still sufficient). Afterwards, the samples were subjected to centrifugation at max speed for 10 min at 4 °C to pellet the RNA. The supernatant was discarded and the RNA pellet was carefully collected. In order to wash the pellet, 350 µL 70 % EtOH was added and the pellet was resuspended by vortexing. The pellet was spun down at max speed for 5 min at 4 °C, and the supernatant was

discarded. The 70 % EtOH wash step was repeated twice. After the last wash step, the supernatant was removed by decanting and the extra supernatant was spun down using tabletop centrifuge and removed with 20 µL tips. Finally, the fresh RNA was dried 4 min at 55 °C and solubilized with nuclease free water and the concentration was determined by Nanodrop.

### 4.1.3 T7 promoter insertion and *in vitro* transcription

Before transcription, the T7 promoter region was inserted into the fragment of choice by PCR reaction with the T7 primer (Table 3-1). Then, the mRNA was *in vitro* transcripted with the HiScribe T7 High Yield RNA Synthesis Kit, following the 20 µL reaction system, including 2 µL 10X Reaction Buffer, 2 µl ATP (100 mM), 2 µl GTP (100 mM), 2 µl UTP (100 mM), 2 µl CTP (100 mM). 1 µg Template DNA, 2 µl T7 RNA Polymerase Mix were used and the final volume was filled up to 20 µL with Nuclease-free water. The mixture was thoroughly mixed and spun down in microfuge, then the mixture was incubated at 37 °C for 2 h.

### 4.1.4 Reverse transcription and qRT-PCR reaction

The reversed transcription was conducted with the Random Hexamer primer to generate cDNA following the procedures below: 1 µL of the random primer was added into each RNA sample, and heated at 70 °C for 5 min. Afterwards, the samples were kept on ice for 5 min. Meanwhile, the 9 µL reaction mix containing (4 µL 5x Reaction Buffer, 2 µL 10x dNTPs, 1 µL RevertAid Reverse Transcriptase, 2 µL ddH2O) was prepared. Then, the mixture was added to the sample, and mixed with peptide. Afterwards, the sample was incubated at 25 °C for 10 min, then the sample was transformed into heater and incubated at 42 °C for 1 h. Finally, the sample was heated and incubated at 70 °C for 15 min. Before the qRT-PCR, the cDNA was diluted with 180 µL ddH2O. The diluted cDNA was used to conduct the qRT-PCR in a appliedbiosystems machine.

### 4.1.5 Sodium-dodecyl sulfate polyacrylamide gel electrophoresis

Sodium dodecyl sulfate polyacrylamide gel electrophoresis was used to separate the proteins which included two different methods Tris-Glycine or Tris-Tricin according to the applications requirements. Tris-glycine-PAGE was conducted following the instruction of Laemmli (1970) in gels containing 12 % (v/v) Rotiphorese Gel 30 (Roth, Karlsruhe, Germany), while Tris-Tricin-PAGE was executed following the instruction of Schägger (2006) in 12 % (v/v) Rotiphorese Gel 30. Prior to the samples loading, samples were added with 6x SDS-Urea loading buffer (8 M urea, 8 % SDS, 1 mM ß-ME, 0.025 % (w/v) bromphenolblue) and treated with 90 °C heating

for 10 min or diluted with 4x Schägger buffer followed by denaturation at 65 °C for 10 min. After the heat treatment, samples were subjected to immunodetection (Schägger, 2006).

### 4.1.6 Antibody for the protein detection

Once the proteins were separated by the denatured SDS gel electrophoresis, they were transferred to the nitrocellulose membranes following the instruction of the semi-dry method (Towbin et al., 1979) under the condition of 1mA/cm$^2$ for 1 h and 15 min. After the transferring, the transformed membrane was stained with 0.008 % (w/v) Direct Blue 71 (DB71) (Zeng et al., 2013). The stained membrane was destained in DB71 destaining solution (150 mM NaHCO$_3$ and 50% ethanol), and blocked using 5 % (w/v) dried milk powder in phosphate buffered saline Tween 20 (PBS-T) at RT for 1 h. Primary antibodies were prepared in the corresponding dilution shown in Table 3-5 in 5% milk dissolved with PBS. The membrane was incubated with the primary antibodies overnight at 4 °C. The membrane was thoroughly washed before the secondary antibody which was diluted of 1:25000 in PBS dissolved milk was added for 1 h room temperature incubation. Once the washing was finished with PBS, the membranes were wetted with Western Lightning™ Plus-ECL reagent (PerkinElmer) and exposure on Fuji Medical X-Ray Super RX-N films (Fujifilm, Tokio, Japan). If necessary, membranes were stripped with 200 mM NaOH for 1 h at RT.

## 4.2 Cell biological methods

### 4.2.1 Isolation of the cytosolic lysate from the *P. sativum*

The cytosolic lysate from the *P. sativum* was isolated from leaves. Leaf material was frozen with liquid nitrogen and grinded by a MM300 cell mill. The powder was collected into a new tube, and Lysis buffer (50 mM Tris pH 7.5, 50 mM NaCl, 2 mM MgCl$_2$, 1 mM β-mercaptoethanol, 1 % Protease Inhibitor Cocktail (PIC), 10 mM Ribonucleoside Vanadyl Complex (VRC) (heated before use) was added and vortexed. Then, the tube was centrifugated at max speed for 10 min, at 4 °C. Afterwards, the supernatant was collected for the further research.

### 4.2.2 BY-2 lysate preparation

BY2-L culture (*N. tabacum*) were centrifuged for 10 min at 500xg in RT (acceleration 9, deceleration 4). After the centrifugation, the supernatant was discarded and the pellet was collected. The cell pellet was resuspended with MCP solution (20mM MES PH 5.7; 400mM

Mannitol; 20mM KCl; 10 mM $CaCl_2$; 0.1% BSA; 3% Rohament; 0.2% Rohapect; 5mM ß-Mercaptoethanol) and was incubated for 2 h in the original culture flask under 25 °C to lyse the cell walls. The BY2-L protoplasts were centrifugated at 800xg (acceleration 9, deceleration 4) for 15 min at RT. Meanwhile, the stepwise Percoll-gradient (70 % 8 mL, 40 % 8 mL, 30 % 8 mL, 15 % 8 mL) was prepared. After the centrifugation, the supernatant was discarded and the pellet was resuspended with mannitol buffer (700 mM Mannitol, 20 mM $MgCl_2$, 5mM KOH/PIPES) by gently shaking and inverting, and the resuspension was layered on the prepared Percoll-gradient with cut tips. Then, the Percoll-gradient was centrifugated in swinging-bucket rotor at 12,000xg for 1.5 h). The top layer was discarded with jet pump. The protoplasts at lowest interface were collected and transferred into a new tube. The protoplasts were resuspended with mannitol buffer, then spun down through a 8 ml 40 % percoll cushion for purification under 12,000xg, 25 °C, 5 min. The protoplasts pellets were washed with the mannitol buffer, and centrifuged for 5 min (500xg and 25 °C) to pellet the protoplasts. The pellets were diluted with TR-buffer (20mM LiOH/HEPES, 2mM DTT, 60 mM K-Acetat, 0.5 mM $MgCl_2$ supplemented with one tablet per 10 mL of Complete EDTA-free Protease Inhibitor) with the weight ration 1:3. Then the pellet was resuspended by vortexing. The protoplasts were disrupted by a glass Teflon-homogenizer (homogenizer Potter S., B. Braun, Melsungen, Germany) and a Drilling machine (TB135CE, TIP Werkzeuge, 400 rpm) stroking (20 strokes/min; 2 min). The broken cells were centrifuged for 10 min at 500xg and 4 °C to remove the nuclei and non-disrupted cells, and the supernatant was collected into the new tube. 0.5 mM $CaCl_2$ and 75 U/ml Nuclease S7 (micrococcal Nuclease, Thermo Fisher Scientific, Massachusetts, USA) were added into the supernatant and the supernatant was incubated for 15 min at 20 °C. Then, 2 mM EGTA was added into the solution to inactivate the nuclease by chelating $Ca^{2+}$. Finally, the solution was frozen in liquid nitrogen and stored at -80 °C.

Moreover, based on the general preparation of BY2-L shown above, various BY2-L were also prepared by different procedures to probe the function of BY2-L in the binding assay. The BY2 cell culture either incubated for 7 d or 9 d before harvesting were referred as BYL-7d and BYL-9d, respectively. In the process of lysing BY2 cell cultures, different amount of TR buffer were added. The 7 d incubated cell lysed with the TR buffer of weight ratios (1:3) and (1:6) was noted as BYL-7d (1:3) and BYL-7d (1:6), respectively. The 9 d incubated cells lysed with the TR buffer of weight ratios (1:3) and (1:6) was noted as BYL-9d (1:3) and BYL-9d (1:6), respectively.

Also, the BY2-L which reduced the binding efficiency were subjected to centrifugation at different speeds 2,000xg, 7,000xg and 15,000xg for 10 min, and the supernatant was collected after the centrifugation. The collected supernatant was further used for the binding assay. In

order to remove envelope vesicles, the BY2-L was subjected to 50,000xg 15 min centrifugation, and the supernatant was collected for the binding assay.

### 4.2.3 Isolation of the chloroplast and chloroplast inner envelope from *P. sativum*

The chloroplasts were isolated from leaves of 7-8 days old *Pisum sativum* plants following the protocol in (Bionda and Schleiff, 2010). The chlorophyll content was measured according to (Arnon, 1949). Chloroplast inner envelope vesicles were isolated following (Simm et al., 2013). Protein concentrations of the chloroplast and chloroplast envelope fractions were determined by Amido Black (Popov et al., 1975).

### 4.2.4 Proteolytic digestion and various washing strategies

Isolated chloroplasts were directly used for the following treatments. In the proteolytic digestion, chloroplasts were incubated with thermolysin at a concentration of 120 µg/ml in wash buffer (50 mM HEPES/KOH pH 7.6, 330 mM sorbitol). Then, 1 mM $CaCl_2$ was supplemented to activate the digestion, and the sample was kept on ice in the dark for 30 min. The digestion was inactivated with 10 mM EDTA, and the chloroplasts were pelleted at 800xg for 1 min for further research.

For various washing strategies, 50 µg Chlorophyll were taken and diluted to the final volume 1 mL in wash buffer containing 1 M NaCl, 5 mM EDTA, 1 mM puromycin. The dilution was kept on the ice for 2 min, and the chloroplasts were spun down (800xg, 1 min), the wash step was repeated one more time. Afterwards, the Schägger buffer was added to the pellet. After 3 min heating at 95 °C the pellet was subjected to the SDS-gel running.

### 4.2.5 Assays with isolated chloroplast

#### 4.2.5.1 The Ribosome binding assay

Cytosolic lysate (20 µg total protein) of BY2-L culture (*N. tabacum*) from section 4.2.2 or PsL (*P. sativum*) from section 4.2.1 were prepared. Meanwhile, the *P. sativum* chloroplast (50 µg total protein) from section 4.2.3 were isolated. 250 µL mixture containing ATP (1.2 mM), 25 µL 10×HMS, 52,5 µL Premix (20 mM K-Gluconat, 10 mM Methionin, 10 mM Cystein, 10 mM $NaHCO_3$, 20 % BSA), 20 µg Cytosolic lysate, 50 µg total protein of chloroplasts was prepared. And the 250 µL mixture was incubated for 10 min at 25 °C. Then, the mixture was loaded on the 750 µL 40 % Percoll gradient, and the gradient was centrifuged at 5,000×g, 1 min with a swing out rotor. After the centrifugation, the supernatant was discarded and the re-isolated

chloroplasts were loaded onto SDS-PAGE from section 4.1.5 followed by Western blotting and immunostaining from section 4.1.6 with the indicated antibodies. (ii) RNA from the re-isolated chloroplasts were extracted and subjected to the agarose or PAGE gel and stained with ethidium bromide.

### 4.2.5.2 The mRNA binding assay

The standard volume for the mRNA binding assay was 100 µL, including water, 5 mM ATP, 21 µL import mix (1 M K-Gluconat, 250 mM Methionin, 250 mM Cystein, 1 M $NaHCO_3$, 20 % BSA), 10×HMS, 1 mM $K_2HPO_4$, 20 % BY2-L (if required) 2.5 µL Ribolock, mRNA from the *in vitro* transcription, 50 µg chlorophyll. The mixture was gently mixed with cut 100 µL pipet tips. The mixture was incubated at 25 °C for 10 min, during which the tube was gently shaken. After 10 min incubation, the 100 µL was loaded on the 2 mL 40 % percoll cushion with cut tips, and centrifugated (5,000xg, 4 min) with swing out rotor (Accel:7, Decel:3). The supernatant was discarded and the pellet was resuspended with wash buffer (50 mM HEPES/KOH pH 7.6, 330 mM sorbitol, containing 2.5µL Ribolock), the pellet was spun down (800xg, 1 min) and kept on the ice for the further analysis.

## 4.3 Capturing the RNA interactome

### 4.3.1 Coupling LNA primers to beads

The LNA-containing primers ($LNA_{OEP24}$ and $LNA_{COX17}$) were coupled with the magnetic beads via free carboxylic groups around the surface. The coupling steps of the LNA probes to the beads were described below and takes around 8h.

Step 1: Calculation of the amounts of LNA probes and the carboxylated beads which are required: Normally, each 10 nmol of probe (100 µL of a 100 µM solution) should be coupled to the 5 mg of beads (100 µL of the original 50 mg/mL bead suspension). Please note: LNA primer coupled beads could be recycled at least five times without significant loss in performance.

Step 2: Two tubes containing the lyophilized ($LNA_{OEP24}$ and $LNA_{COX17}$) probes were spun down (10,000xg, 25 °C, 10 s), then 1 mL nuclease free water was added to dissolve the powder and the final 100 µM concentration was obtained. Afterwards, the tubes were vortexed for 1 min, briefly spun down (10,000xg, 25 °C, 5 s), the solution were aliquoted into 10 tubes and stored at -80 °C for at least several years.

Step 3: 5 mg of beads were washed three times (100 μL of the original 50 mg/mL bead suspension) with 5 volumes (500 μL) of 2-(N-morpholino) Ethanesulfonic acid MES buffer (pH 6).

Step 4: 500 μL of a 20 mg/mL solution of the coupling activator N-(3-dimethylaminopropyl)-N′-ethylcarbodimide hydrochloride EDC-HCl in MES buffer was freshly prepared. A small aliquot (~20 μL) of the EDC-HCl solution was transferred into a new 1.5 mL tube, serving as a blank to calculate the coupling efficiency.

Step 5: The beads washed in step 3 were collected with magnet and the supernatant was discarded.

Step 6: 10 nmol of probe (100 μL of 100 μM probe solution) with 500 μL activator EDC-HCl were combined together. A small aliquot (~20 μL) of the probe-EDC-HCl solution was transferred to a new 1.5 mL tube, used to estimate the coupling efficiency.

Step 7: 600 μL of probe–EDC-HCl solution (step 6) with 5 mg of beads (step 5) were mixed and resuspended.

Step 8: The mixture was incubated for 5 h at 50 °C and 800 rpm with a thermal block and occasionally spin down (10,000xg, 25 °C, 10 s) the liquid left on the lid. After the 5 h incubation, the beads were collected with magnet. A small aliquot (~20 μL) of supernatant was collected to measure the coupling efficiency.

Step 9: The three (~20 μL) test samples from steps 4, 6 and 9 were preserved and kept at room temperature for further evaluation.

Step 10: The LNA primer coupling beads were washed twice with 500 μL (5 volume) of PBS.

Step 11: The residual carboxyl residues of the beads were inactivated with 1.5 mL of 200 mM ethanolamine, pH 8.5, via an incubation 1 h at 37 °C and 800 rpm incubation.

Step 12: After the inactivation, the LNA primer-coupled beads were washed three times with 500 μL of 1 M NaCl and recovered with magnet.

Step 13: The washed beads were collected and resuspended with 100 μL of PBS supplemented with 0.1 % (vol/vol) PBS–Tween 20. The coupled beads could be preserved at 4 °C for at least 3 months.

Step 14: The coupling efficiency was calculated by measuring the probe concentration in the probe–EDC-HCl solution collected before (step 4) and after (step 9) in a Nanodrop device at 260-nm wavelength. The EDC-HCl solution without probes from step 4 was served as a blank. A robust drop in the absorbance after coupling should be observed.

### 4.3.2 UV-crosslinking to capture the RNA-protein interaction

The interaction between the mRNA and the protein of chloroplast was fixed with the UV-crosslinking following the steps below.

The pellet of the chloroplast obtained from the mRNA binding assay from section 4.2.5.2 were resuspended with wash buffer (330 mM Sorbit, 50 mM KOH/HEPES pH 7.6, 3 mM $MgCl_2$) then the suspension was evenly placed on the small petri dishes. These were placed into the UV-crosslinking machine (UV Stratalinker 2400), and the Auto program was conducted to crosslink mRNA and proteins in the surface of chloroplasts. The chloroplasts were resuspended after each crosslinking execution. After the UV-crosslinking, the chloroplasts were spun down (800xg, 1 min) and the supernatant was discarded. The chloroplasts pellet was kept on the ice for the further research.

### 4.3.3 Pull-down assay with LNA primers

For the capture of the bound mRNA to the chloroplast surface, the isolated pellet from the mRNA binding assay was resuspended with the lysis buffer (20 mM Tris-HCl pH 7.5, 500 mM LiCl, 0.5 % LiDS (w/v,), 1 mM EDTA, 5 mM DTT (freshly added), Complete Protease Inhibitor Cocktail (freshly added)), and kept on the ice for 10 min. Then, the LNA-coupled beads were added into the lysate and 2.5 µL Ribolock (Sigma) was added into every 100 µL lysate. The mixture was incubated for 2 h with 600 rpm shaking in the thermal cycle at optimal hybridization temperature (52 °C for $LNA_{OEP24}$ and 48 °C for $LNA_{COX17}$), and the samples were mixed every 15 min by inverting the tubes six times. After the 2 h incubation, the Lysate and beads mixture was cooled down at room temperature for 5 min. Then, the beads were collected with magnet. Afterwards, beads were washed 5 min at RT by gentle rotation with the buffers containing reducing concentrations of LiCl and LiDS from Lysis buffer (20 mM Tris-HCl pH 7.5, 500 mM LiCl, 1 mM EDTA, 5 mM DTT, 0.5 % (w/v) LiDS, Complete Protease Inhibitor Cocktail (freshly added)), Buffer 1 (20 mM Tris-HCl pH 7.5, 500 mM LiCl, 1 mM EDTA, 5 mM DTT, 0.1 % (w/v) LiDS, Complete Protease Inhibitor Cocktail (freshly added)), Buffer 2 (20 mM Tris-HCl pH 7.5, 500 mM LiCl, 1 mM EDTA, 5 mM DTT, 0.02 % (v/v) NP40, Complete Protease Inhibitor Cocktail (freshly added)) to Buffer 3 (20 mM Tris-HCl (pH 7.5), 200 mM LiCl, 1 mM EDTA, 5 mM DTT, 0.02 % (v/v) NP40, Complete Protease Inhibitor Cocktail (freshly added)) two times with each buffer (Castello et al. 2013). Pre-elution was performed in 220 µL of nuclease-free water (Ambion) for 5 min at 40 °C and 800 rpm. Afterwards, the bead suspension was divided into two aliquots, one of 200 µL for the RNase-mediated elution for protein analysis and one of 20 µL that was heat-eluted for RNA/DNA analyses (Perez-Perri et al., 2018).

### 4.3.4 Recycling of LNA2.T-coated beads.

The LNA-coupled magnetic beads could be recycled at least five times. Before recycling the beads, the associated RNase A/T1 must be eluted by heat. It is recommended to recycle the beads no later than 1 day after the pull-down assy.

100 µL of the used beads were resuspended in 300 µL of nuclease-free water and transferred into a 1.5 mL low binding tube. The resuspension was incubated at 95 °C with the thermal cycler at 900 rpm for 5 min. The beads were collected immediately before the samples were cooled down. The supernatant was discarded. Then, the beads were washed with 5 volumes of nuclease-free water three times, and the magnet was used to collect the beads. Afterwards, the beads were washed with 5 volumes of lysis buffer for three times. The beads could be used immediately after washing or be kept in PBS supplemented with 0.1 % (vol/vol) PBS–Tween 20 for longer-term storage (up to 3 months) at 4 °C.

# 5. RESULTS

## 5.1. Analysis of ribosomes binding to chloroplasts surface

### 5.1.1 Analysis of ribosomes on the surface of the isolated chloroplasts

Since the scientifically well described post-translational import was challenged by the previous findings that ribosomes stably bind to purified liver mitochondria *in vitro* (Crowley et al., 1997). Though, isolated chloroplasts can import *in vitro* synthesized proteins and the absence of ribosomes in the immediate area around chloroplasts in EM images. However, colleagues stated that none of the EM images were recorded in the presence of a translation elongation inhibitor (Uniacke et al., 2009). Therefore, the first objective is to investigate if the ribosomes could bind to the chloroplasts.

The analysis of the association of ribosomes on the surface of the isolated chloroplasts was conducted with antibodies. Firstly, the antibodies against the four ribosomal proteins RPS3, RPS10 (proteins of the small subunit 3 and 10, respectively), RPL5, and RPL10 (proteins of the large subunit 5 and 10, respectively) were tested for the specificity. Since the antibodies were generated from the *Arabidopsis thaliana*, the specificity of the antibodies for the other organisms should be tested. To do this, the antibodies were tested in the lysate isolated from the different organisms. As shown in (Fig. 5.1A), the four antibodies recognized proteins in the cytosolic lysates isolated from *Arabidopsis thaliana* (Alt) or *Pisum sativum* (PsL), from BY2-cell culture (*Nicotiana tabacum* non-green cell culture), or from *Triticum aestivum* germ (wheat germ, WGL). This result confirmed the specificity of the antibodies and the existence of ribosomes in these lysates. Having confirmed the specificity and selectivity of the antibodies for the different systems, chloroplasts from *P. sativum* were isolated (Fig. 5.1B). These were either treated with the protease thermolysin to remove all surface-exposed proteins and protein complexes (lane 2, 3) or were kept on ice (lane 4, 5). The efficiency of the thermolysin treatment was confirmed by the immunostaining with antibodies against Toc34. Toc34 is a membrane-embedded outer envelope protein with a cytosolic exposed GTPase domain. The binding of ribosomes was probed with the antibodies tested (Fig. 5.1A). The repetitive results demonstrated that the thermolysin treatment resulted in degradation of Toc34, which confirmed the functionality of the protease treatment (Fig. 5.1B, lanes 2, 3, lowest panel). Using the ribosomal antibodies, the observation showed both, the antibodies against RPS10 and RPL5, an unspecific signal (marked by a asterisk). However, these unspecifically detected proteins were not thermolysin sensitive. Thus, these were proteins protected at least by the outer envelope membrane and did not represent components of cytosolic ribosomes. In turn,

the protein detected by the antibodies and migrating at the same molecular weight as the ribosomal protein in the cytosolic lysate isolated from *P. sativum* was protease-sensitive (Fig. 5.1B, lanes 2, 3, second and third panel). Moreover, the protein band detected by antibodies against RPS10 or RPL5, respectively, was increased in a loading concentration-dependent manner (Fig. 5.1B, lanes 4, 5, second and third panel). Thus, the first evidence was shown that ribosomes were bound to chloroplasts, although at the low concentration at least after chloroplast isolation.

To substantiate the finding that ribosomes were bound to the chloroplasts surface, several treatments were performed to remove the ribosomes from the outer envelope membrane. However, neither the addition of 300 mM salt nor 5 mM EDTA significantly removed the ribosomes content as exemplified for the signal obtained with antibodies against RPS10 (Fig. 5.1C). This suggested that the interaction of the ribosomes might be specifically manifested by a membrane-bound protein serving as a receptor or by translation. Hence, 1 mM puromycin was added, an antibiotic that caused premature chain termination during translation (Pestka, 1971). This drug was used to probe whether the interaction of the ribosomes was due to its translational activity (Liu and Spremulli, 2000). While the chloroplasts cross-reactive band did not show any change after the addition of puromycin, a mild reduction of the abundance of cytosolic ribosomes was observed as judged from the occurring signal with the antibodies against RPS10 and RPL5 (Fig. 5.1D). However, this reduction was very moderate and suggested that if at all, only a small portion of the ribosomes were dependent on translation for their interaction with chloroplasts.

### 5.1.2 Analysis of ribosomes binding to chloroplasts with binding assay

As the detection of the ribosomes on the surface of the isolated chloroplasts was conducted. Next, the binding assay was developed and used to probe the association of the ribosomes with the chloroplasts. The theory of the binding assay was that the ribosomes and chloroplasts could be separated by the procedure of centrifugation through the 40 % percoll cushion. During the binding analysis, chloroplasts were generally collected by centrifugation. If BY2-L was centrifuged under the same condition as used for re-isolation of chloroplasts (5,000xg, 1 min, 4 °C), the ribosomes were not pelleted as judged from the absence of a signal for RPS10 in the pellet (Fig. 5.2A). This did also not change by the addition of ATP or GTP. Hence, the approach could be used to investigate whether non-translating ribosomes present in the BY2-L tightly interacted with the chloroplasts surface. Based on the established binding assay, the isolated chloroplasts were incubated with BY2-L in the presence of ATP or GTP followed by re-isolation of the chloroplasts to analyze a putative interaction (Fig. 5.2B). Based on the
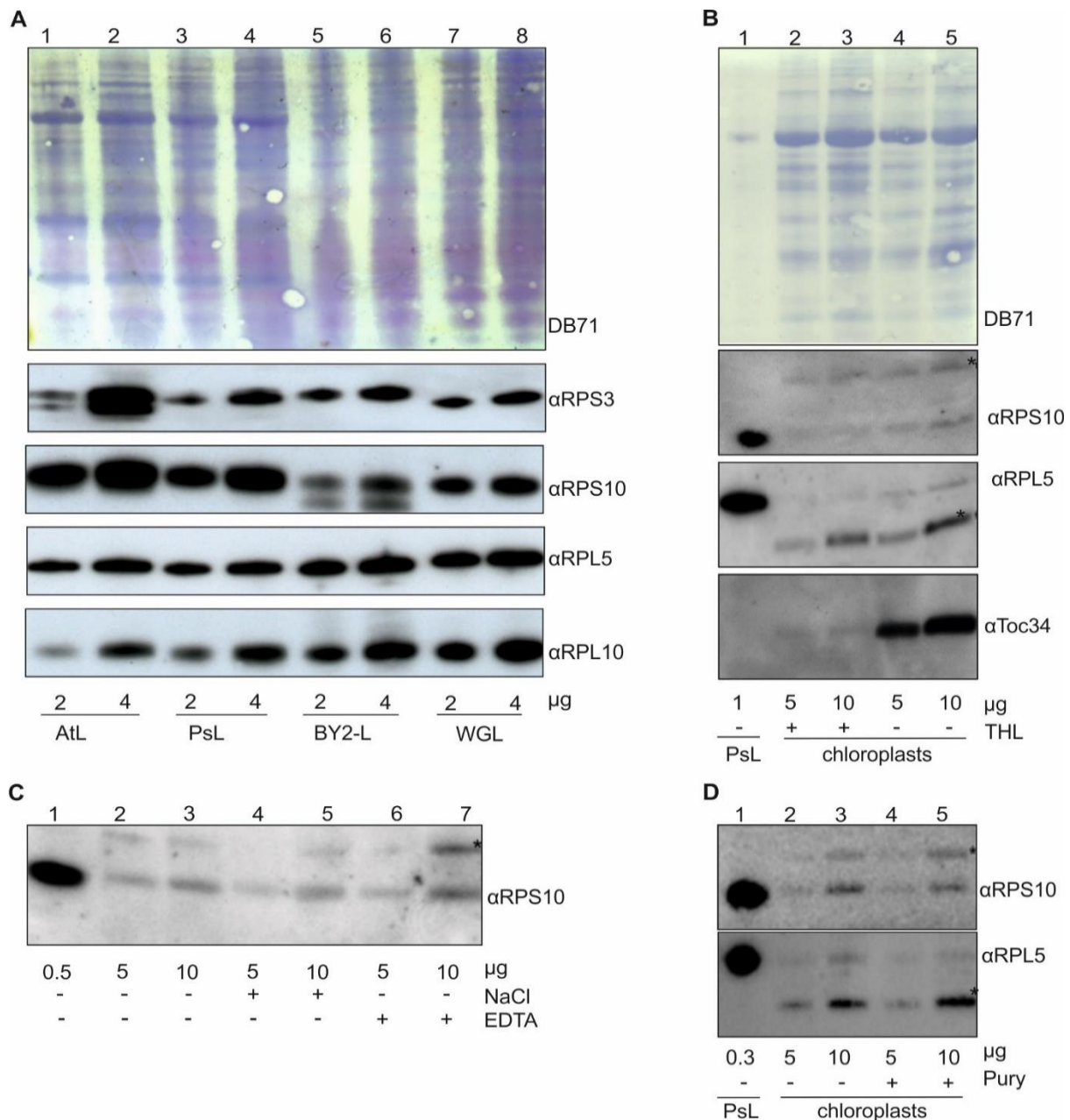
**Figure 5-1 Proteins of the cytosolic ribosomes are present in isolated chloroplasts fraction**
(A) Cytosolic lysate was isolated from *A. thaliana* (AtL), *P. sativum* (PsL), BY2-cell culture (*N. tabacum*, BY2-L) or from *T. aestivum* (Wheat germ, WGL) and 2 or 4 µg protein was subjected to SDS-PAGE followed by Western blotting with the antibodies indicated on the right. As loading control, the DB71 stain of the blotting membrane is shown. Note: the double band observed for RPS3 in *A. thaliana* lysate and for RPS10 in BY2 Lysate most likely represent the detection of the different paralogs present. (B) Chloroplast (lanes 2-5) were isolated from *P. sativum* according to standard protocols (Bionda and Schleiff, 2010). Chloroplasts were subsequently incubated with 20 µg thermolysin (THL) for 30 min on ice (lane 2, 3). After re-isolation through a Percoll cushion by centrifugation, 5 or 10 µg total proteins were loaded onto SDS-PAGE followed by Western blotting and immunostaining with the indicated antibodies. Lane 1 shows 1 µg of the lysate for control of the migration of ribosomal proteins. (C) Chloroplast (lanes 2-7) were isolated from *P. sativum* as in (B) and incubated with 300 mM NaCl (lane 4, 5) or 5 mM EDTA (lane 6, 7). After re-isolation, 5 or 10 µg total proteins were loaded onto SDS-PAGE followed by Western blotting and immunostaining with RPS10 antibodies. Lane 1 shows 0.5 µg of the lysate. (D) Isolated chloroplast (lanes 2-5) were three times incubated with 1 mM puromycin (Pury) for 1 min followed by re-isolation (lane 4, 5). 5 or 10 µg total proteins were loaded onto SDS-PAGE followed by Western blotting and immunostaining with RPS10 or RPL5 antibodies. Lane 1 shows 0.3 µg of the lysate. The asterisk in B, C and D marks a band that is recognized by the antibody in addition to the cytosolic ribosomal protein.
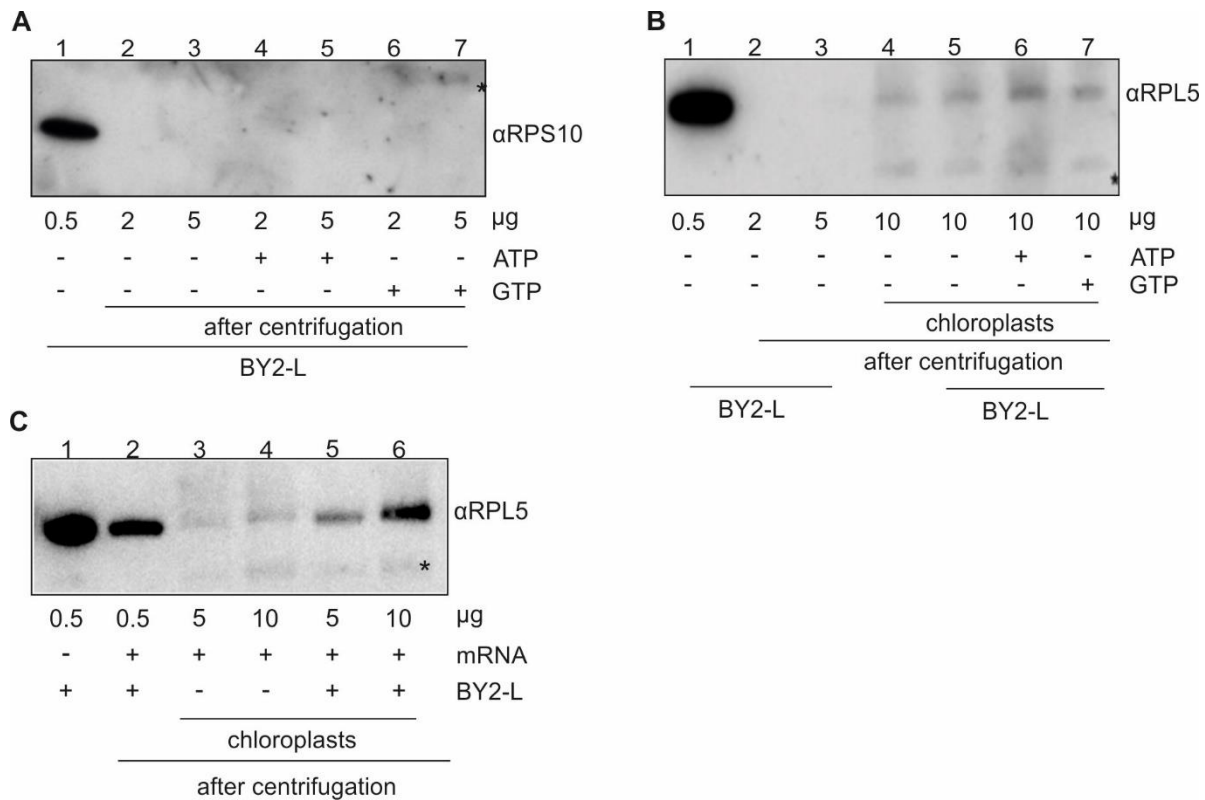
45

**Figure 5-2 RPL5 present in lysate partially co-precipitated with chloroplast**

(A) Cytosolic lysate from BY2-cell culture (*N. tabacum*, BY2-L, 0.5 μg lane 1) were incubated with 1 mM ATP (lane 4, 5) or 1m mM GTP (lane 6, 7). After incubation, the lysate was centrifuged at 5.000 x g for 1 min at 4 °C. 2 or 5 μg of the proteins in the pellet were subjected to SDS-PAGE followed by Western blotting with antibodies against RPS10. (B) Cytosolic lysate from BY2-cell culture (*N. tabacum*, BY2-L, 0.5 μg lane 1) were incubated with 1 mM ATP (lane 6) or 1 mM GTP (lane 7). Subsequently, the lysate was incubated with chloroplast (lanes 4-7) isolated from *P. sativum* according to standard protocols (Bionda and Schleiff, 2010). After re-isolation of chloroplasts through a Percoll cushion by centrifugation (note, lysate without chloroplast were treated the same way for control – lane 2, 3), indicated amounts of proteins were loaded onto SDS-PAGE followed by Western blotting and immunostaining with the indicated antibodies. Lane 1 shows 0.5 μg of the lysate for control of the migration of ribosomal proteins. The star in A and B marks a band that is recognized by the antibody in addition to the cytosolic ribosomal protein. (C) Cytosolic lysate from BY2-cell culture (*N. tabacum*, BY2-L, 0.5 μg lane 1) were incubated with OEP24 mRNA (lane 2, 5, 6). Subsequently, the lysate was incubated with chloroplast (lanes 5-6) isolated from *P. sativum* according to standard protocols (Bionda and Schleiff, 2010). After re-isolation of chloroplasts through a Percoll cushion by centrifugation (note, lysate without chloroplast were treated the same way for control – lane 2; Isolated chloroplasts with mRNA were treated the same way for control -lane 3,4). The asterisk in B and C marks a band that is recognized by the antibody in addition to the cytosolic ribosomal protein.

detection of RPL5 as an indicator of the ribosomal quantity, a weak binding of ribosomes in general was observed (Fig. 5.2B lanes 5-7 vs. lane 4 representing already bound ribosomes and lane 1 representing ribosomes in 0.5 μg lysate, upper panel). Interestingly, it appeared that ATP somewhat enhanced this interaction (Fig. 5.2B compare lane 5 and lane 6), while GTP did not have an impact on binding (Fig. 5.2B, compare lane 5 and 7). The latter was interesting, as the two cytosolic exposed receptor components of the protein translocation machinery of the chloroplasts are GTPases (Schleiff and Becker, 2011). Thus, it was tempting to test whether the presence of mRNA would increase the binding efficiency of ribosomes.
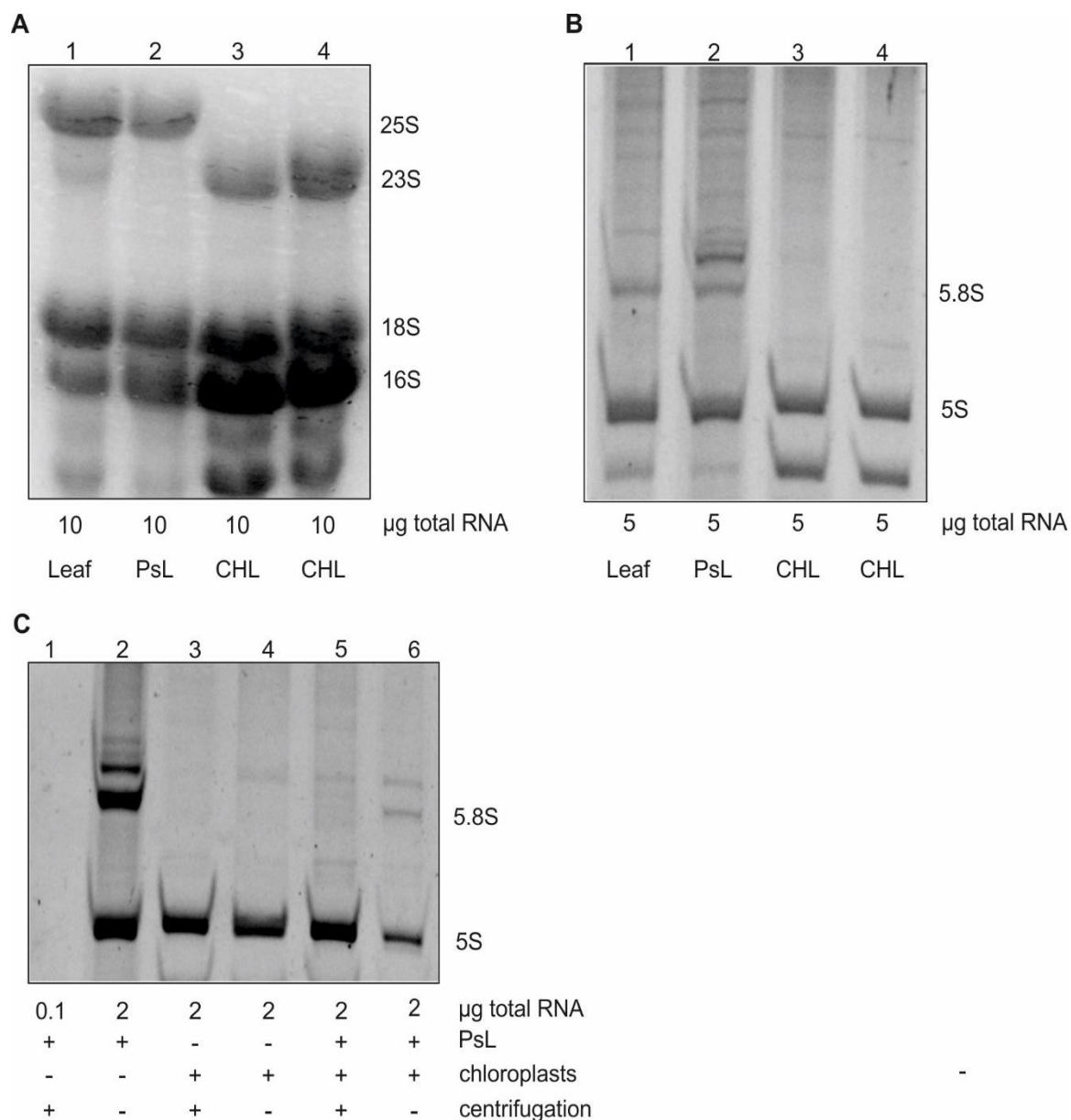
**Figure 5-3 Naked ribosomes are not considerably bound to chloroplasts under current condition.**

(A) Total RNA from leaf (lane 1), cytosolic lysate (lane 2) and chloroplast (lane 3-4) of *P.sativum* (PsL) were isolated, and 10 µg RNA was subjected to the agarose gel and stained with ethidium bromide. (B) Total RNA from leaf (lane 1), Cytosolic Lysate (lane 2) and chloroplasts (CHL) (lane 3-4) of *P.sativum* were isolated, and 5 µg RNA was subjected to the PAGE gel and stained with ethidium bromide. (C) Representative images of the binding of indicated PsL to the chloroplasts surface (lane 5-6) are shown. 20 µg PsL was added to chloroplasts for 10 min at 25 °C, followed by organelle isolation, RNA extraction, and the RNA was subjected to the PAGE gel. Lane 1 show the precipitation of ribosome in the absence of chloroplasts.

To establish this assay, the BY2-L was incubated with mRNA coding for OEP24 (an outer envelope membrane protein of chloroplasts) and tested whether this would cause precipitation of ribosomes due to the formation of polysomes. Indeed, the addition of mRNA caused the

formation of polysomes that were pelleted under the conditions used (Fig. 5.2C).Alternatively, considering the main composition of the ribosomes are proteins and rRNA, it might be feasible to use rRNA as an indicator to analyze the association of ribosomes with chloroplasts.

Firstly, the total RNA from the cytosolic fraction and isolated chloroplasts of *P. sativum* were extracted and subjected to the native gel. As shown in (Fig. 5.3 A, B), 25SrRNA and 5.8SrRNA were visualized in the cytosolic fraction and 23SrRNA was visualized in the isolated chloroplasts. These results showed that rRNA from cytosolic ribosomes were not considerably present in the fraction of isolated chloroplasts. Therefore, the unique cytosolic 5.8SrRNA was used as the indicator to evaluate the association between ribosomes and chloroplasts. Based on the established binding assay, the isolated chloroplasts were incubated with lysate of *P. sativum*, followed by re-isolation of the chloroplasts to analyze a putative interaction. The results showed that the cytosolic 5.8SrRNA could not pass through the 40% percoll cushion (Fig 5.3, C Lane 1vs 2). There was no considerable 5.8SrRNA on the surface of the freshly isolated chloroplasts (Fig 5.3, C Lane 3) and re-isolated chloroplasts (Fig 5.3, C Lane 4). After the binding assay, the 5.8SrRNA in the mixture (Fig 5.3, C Lane 6) was significantly reduced in the re-isolated chloroplasts through 40 % percoll cushion (Fig 5.3, C Lane 5), which suggested that there were no cytosolic ribosomes bound to the surface of the chloroplasts.

Taken together, with the antibody detection, low concentration of proteins from the cytosolic ribosomes were present in isolated chloroplasts; However, the binding assay showed that hardly any naked cytosolic ribosomes bound to the surface of the chloroplasts.

## 5.2 Analysis of mRNA binding to chloroplast

### 5.2.1 High quality organelle purification as prerequisite for RNA binding studies

The observed association of mRNAs with chloroplasts fractions and the *in vivo* analysis of the distribution of mRNAs (unpublished results of the Schleiff laboratory) was used as the base to formulate the hypothesis that mRNA can bind to chloroplast surface. In addition, earlier reports have discovered several proteins of unknown function in the outer envelope membrane (Simm et al., 2013). Here, for example, a protein (At3g53560) with a tetratricopeptide repeat domain, a domain known to interact with RNAs (Johnson et al., 2018), or a protein with transmembrane domain with a soluble domain annotated as ribosomal protein-related (At1g16790) were identified but not yet functionally characterized. These proteins could be involved in the recognition of mRNA at the surface. Alternatively, the docking at the outer envelope could be protein mediated in case that the mRNA is bound to cytosolic proteins. Several proteins

postulated to act in protein-protein interactions have been identified in the outer envelope membrane or in mixed envelopes, for example At1g27300 or At5g21920 (Simm et al., 2013).

To identify mRNA binding proteins or proteins that recognize mRNA targeting factors, the interaction of mRNA with chloroplasts surface was analyzed. Three different protocols were employed, namely (i) the quantitative *in vitro* transcription of mRNAs (section 4.1.3), (ii) the
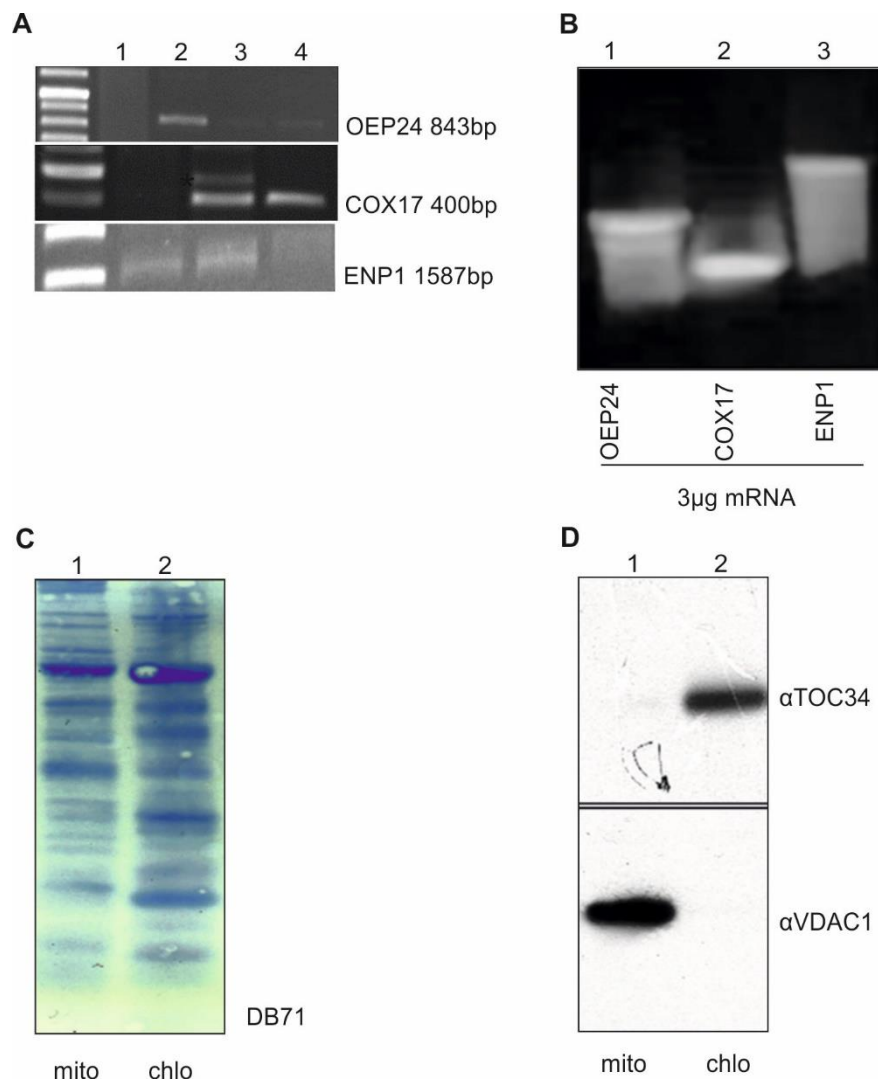


**Figure 5-4 Experimental optimization for subsequent mRNA binding**
(A) Gene sequence (CDS+3´UTR) of three mRNA was cloned with the cDNA from the *Arabidopsis thaliana*. (B) mRNA of the three indicated genes was produced by *in vitro* transcription and visualized by ethidium bromide staining after separation on an agarose gel. (C) Mitochondria (mito, lane1) and chloroplasts (chlo, lane 2) were isolated using optimized protocols. 10 µg of the proteins of the according fraction were subjected to protein separation by SDS-PAGE followed by the transfer to nitrocellulose membrane and DB71 staining. (D) The nitrocellulose membrane was subsequently immunostaining with indicated antibodies. The asterisk in A marks a band that is unspecific cloning with the primers for gene amplification.

isolation of BY2-L (section 4.2.2), (iii) the analysis of the mRNA bound to the chloroplasts by RT-PCR after mRNA re-isolation and (iv) the isolation of highly purified chloroplasts (section 4.2.3).

For the subsequent experiments, the mRNA coding for the chloroplast outer envelope transport protein Oep24 (Pohlmeyer et al., 1998) was used. In addition, the mRNA coding for the mitochondrial cytochrome c oxidase copper chaperone Cox17 was selected, because this mRNA was discovered to bind to mitochondria in yeast (Saint-Georges et al., 2008), and for the essential nuclear protein 1 (ENP1) (Missbach et al., 2013). The latter two mRNAs served as control for the specificity of the mRNA binding. The according DNA was cloned (Fig. 5.4A) and plasmid-based *in vitro* transcription yielded adequate amounts of all three mRNAs (Fig. 5.4B). Although some degradation or premature transcriptional break down was observed, the quality was considered sufficient for binding experiments.

The isolation of organelle (Fig. 5.4 C, D) was further optimized as such that mitochondrial outer membrane contaminations were not detected in the chloroplast fraction as judged from immuno-staining with antibodies detecting the mitochondrial voltage-dependent anion channel VDAC1 (Fig. 5.4 C,D).


## 5.2.2 mRNA binding to chloroplasts.

Subsequently, the established protocols (section 4.2.5.2) were used to analyze the mRNA binding to the chloroplast membrane surface. At first, the concentration-dependent association of mRNA to the chloroplasts surface was investigated. The increasing amounts of mRNA were added to chloroplasts. All the three mRNA showed the similar tendency of binding that more mRNA adding could cause more binding of the mRNA to the chloroplasts (Fig. 5.5A). However, the binding patterns of the three mRNA differed. COX17 showed a concentration-dependent unspecific binding, which was generally described by a linear behavior. The least square fit revealed a constant for nonspecific binding (Fig. 5.5A, B orange). Interestingly and unexpectedly, OEP24 (green) and ENP1 (blue) showed a combination of specific and unspecific components of binding comparable to the binding of COX17 (green vs orange; blue vs orange). Moreover, regarding the obtained dissociation constant of OEP24 ($K_D=50\pm20$ nM) and ENP1($K_D=160\pm50$ nM) (Table 1), OEP24 had a 3 fold higher affinity than ENP1 mRNA. Therefore, the binding assay revealed that COX17 does not bind specifically; the OEP24 and ENP1 showed the combination of the unspecific and specific binding, while OEP24 had a 3 fold higher affinity than ENP1 mRNA (Fig. 5.5 B).

## 5.2.3 OEP24 mRNA binding to chloroplasts is in part specific.

Next, the nature of the binding was analyzed in more detail. On the one hand it was tempting to speculate that the interaction was in part electrostatic. Thus, the interaction of the mRNA with the chloroplasts surface in the presence of an additional 75 mM or 150 mM NaCl (Fig. 5.6 A) was analyzed. However, a drastic change of the binding capacity was not observed for
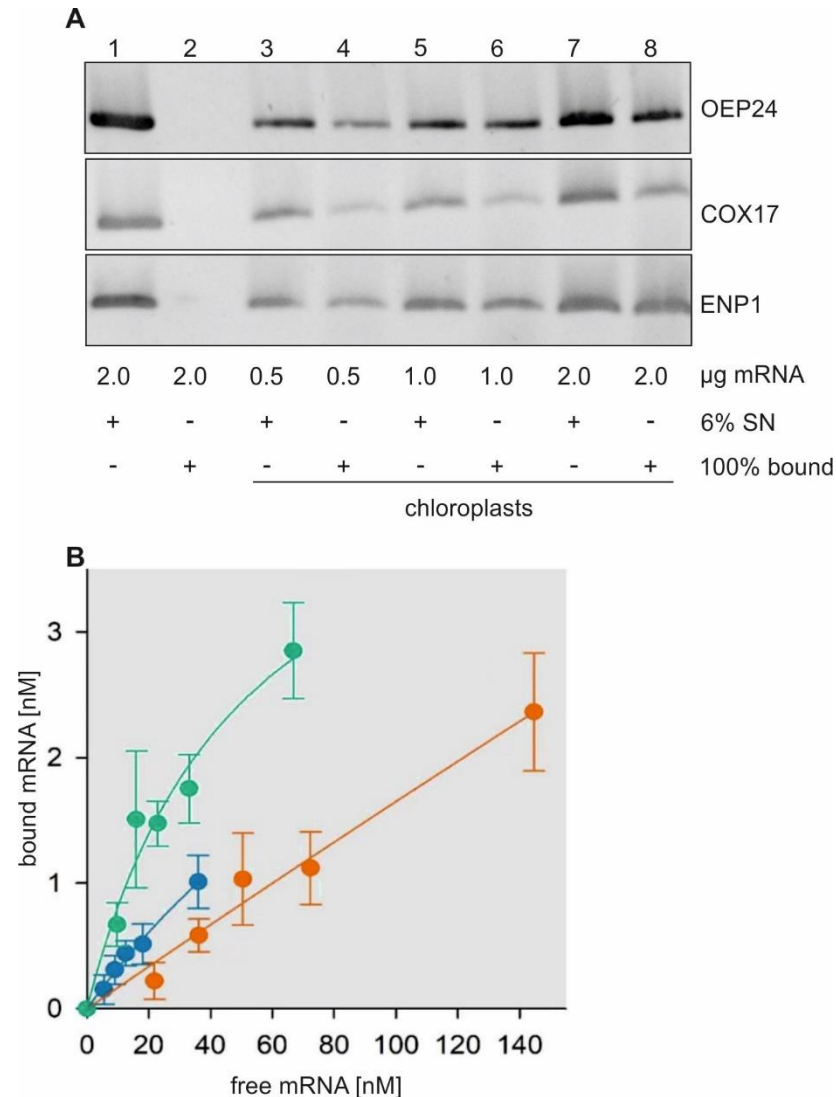


**Figure 5-5 mRNA binding to chloroplasts.**
**(A)** Representative images of the binding of indicated mRNA to the chloroplasts surface (lane 3-8) are shown. 0.5 µg (lane 3,4), 1.0 µg (lane 5,6) and 2.0 µg (lane 7,8) mRNA was added to chloroplasts for 10 mins at 25 ℃, followed by organelle isolation, RNA extraction and RT-PCR with gene specific oligonucleotides. 6% of the result the supernatant (SN) and 100% of the result for the chloroplasts pellet were subjected to agarose gel and stained with ethidium bromide. Lane 1, 2 show the precipitation of mRNA in the absence of chloroplasts. **(B)** The abundance of the transcript was quantified with Image J for multiple independent experiments. The values have been corrected for the percentage of mRNA precipitation without chloroplasts. The amount of free mRNA is plotted against the amount of bound mRNA for COX17 (orange), ENP1 (blue) or OEP24 mRNA (green). All binding curves were treated as combination of specific and unspecific binding and analyzed by least square fit analysis using $[B]=MAX*[F]/(K_D +[F])+N_s *[F]$. The results are shown as line graph and the obtained dissociation constant is indicated.
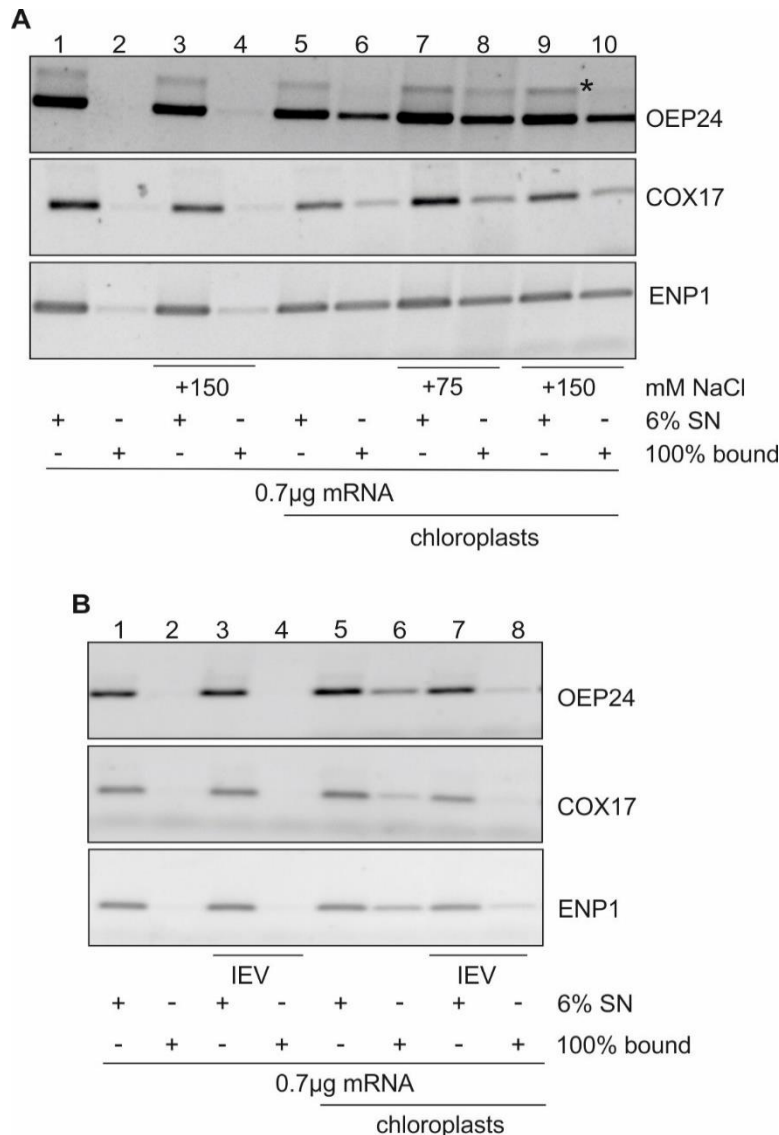
**Figure 5-6 OEP24 mRNA binding to chloroplasts is in part specific**

(A) Representative images of the indicated mRNA to the chloroplast surface (lanes 5-10) is shown. 0.7 µg mRNA was added to chloroplasts for 10 min at 25 °C in the presence of additional 75 mM NaCl (lane 7, 8) or 150 mM NaCl (lane 9, 10), followed by organelle isolation, RNA extraction and RT-PCR with gene specific oligonucleotides. 6% of the result the supernatant (SN) and 100% of the result for the chloroplast pellet were subjected to agarose gel and stained with ethidium bromide. Lanes 1-4, show the precipitation of mRNA in the absence of chloroplasts either in the absence (lane 1,2) or presence of 150 mM NaCl (lane 3,4). (B) Representative images of the indicated mRNA to the chloroplast surface (lanes 5-8) are shown. 0.7 µg mRNA was added to chloroplasts for 10 min at 25 °C in the presence of inner envelope vesicles (lane 7,8) followed by organelle isolation, RNA extraction, RT-PCR with gene specific oligonucleotides and processing as in (A). Lanes 1-4, show the precipitation of mRNA in the absence of chloroplasts either in the absence (lane 1,2) or presence of inner envelope vesicles (lane 3,4). The asterisk in A marks a band that is unspecific cloning with the primers for gene amplification.

any of the mRNAs used (Fig. 5.6A, lane 8 & 10 vs lane 6). Thus, the binding was not in part electrostatic.

On the other hand, it was interesting to check whether the unspecific binding was directed toward the lipid surface. To this end, the inner envelope membrane vesicles were used as competitor. These vesicles contain all lipids present in the outer envelope of chloroplasts (Elkehal et al., 2012). The inner envelope might contain RNA binding proteins, but these

binding proteins would not act specifically and should not have a $K_D$ that was comparable to specific interaction.

In turn, due to the different density of chloroplasts and envelope vesicles, chloroplasts and inner envelope vesicles could be separated by low speed centrifugation. Indeed, addition of inner envelope vesicles to mRNA did not yield a significant precipitation and only a minor fraction was recovered (Fig. 5.6 B Lane 4). Addition of inner envelope vesicles during mRNA binding to chloroplasts diminished the interaction of COX17 mRNA (Fig. 5.6 B, lane 8 vs. lane 6, middle panel). This confirmed the above stated assumption that the interaction of COX17 mRNA with the chloroplast surface is unspecific. Addition of inner envelope vesicles during binding of ENP1 or OEP24 mRNA to chloroplasts reduced the interaction (Fig. 5.6 B, lane 6 vs. 8, top and bottom panel), although the reduction of ENP1 mRNA binding is more pronounced. Again, this confirmed that ENP1 or OEP24 mRNA bind specifically although with different affinity. Hence, competing for the unspecific binding uncovered a specific interaction of OEP24 mRNA with the chloroplast surface.

In order to reveal the details of the specific interaction, increasing amounts of mRNA were added to chloroplasts in the presence of the inner envelope as competitor (Fig. 5.7 A). COX17 showed a concentration-dependent unspecific binding, which was generally described by a linear behavior (Fig 5.7 A, B orange). OEP24 (green) and ENP1 (blue) showed the specific components of the binding comparable to the binding of COX17 (green vs orange; blue vs orange). Moreover, regarding the obtained dissociation constant of OEP24 ($K_D$=90±20 nM) and ENP1 ($K_D$=320±200 nM) (Table 1), OEP24 had a 3 fold higher affinity than ENP1 mRNA.

Afterwards, it was interesting to reveal other features of the mRNA binding to chloroplasts. To do this, the established binding protocol was followed (section 4.2.5.2) in the absence of the 5mM ATP to check the dependence of the ATP or in the presence of the additional 20 % BY2-L to confirm the existence of the cytosolic regulatory factors. Also, the thermolysin treated chloroplasts were used for the binding assay to probe the existence of the potential receptors in the surface of the chloroplasts. A weak difference was observed in absence of the ATP (Fig 5.8 Lane 2, 6), which confirmed that the RNA binding is not dependent on the additional ATP. However, the binding efficiency was enhanced when the thermolysin treated chloroplasts were used (Fig 5.8 Lane 2 vs Lane 8).

Due to the digestion of the proteins in the outer surface of the chloroplasts, the specific binding should be erased, which resulted in the increase of the unspecific binding. Interestingly, the binding efficiency was enhanced in the presence of the additional BY2-L (Fig 5.8 Lane 2 vs Lane 4),
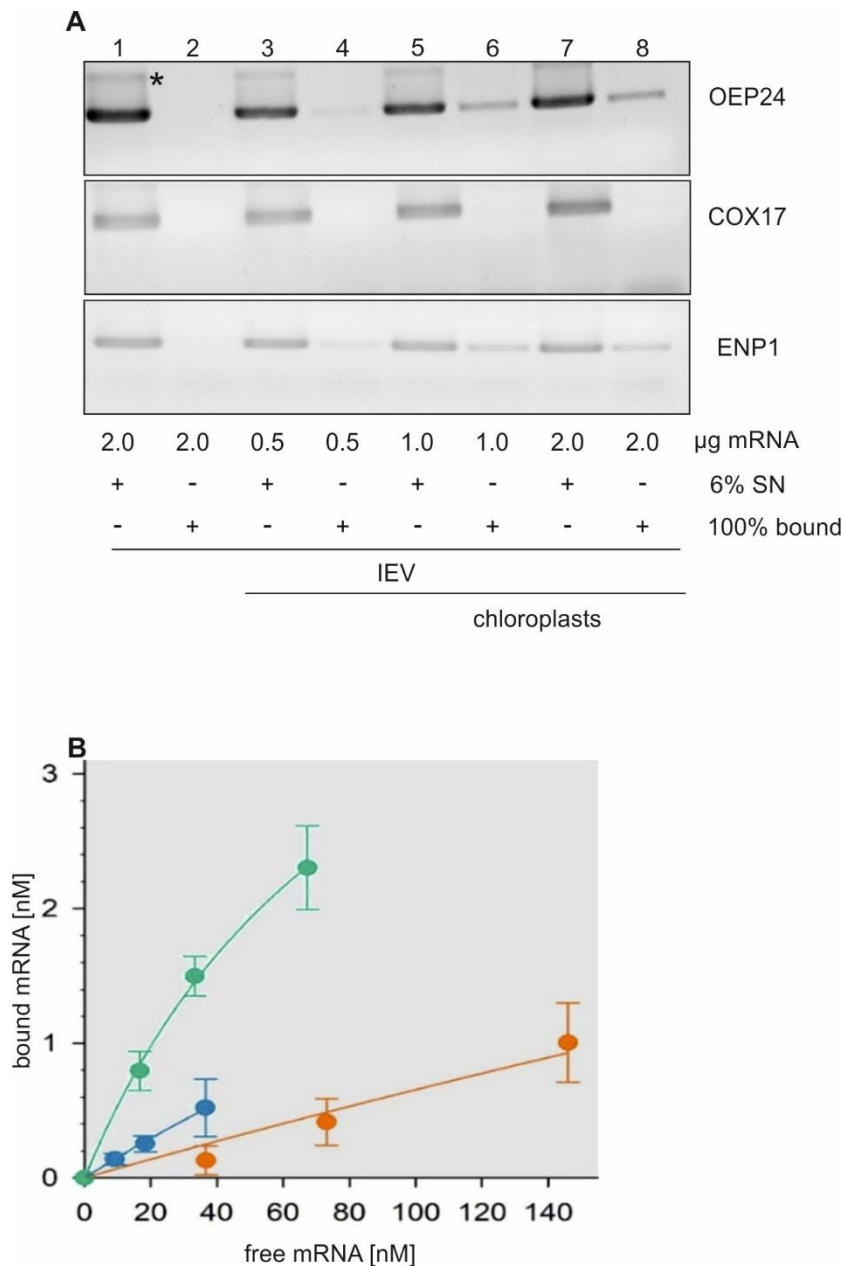
**Figure 5-7 mRNA binding to chloroplasts in the presence of inner envelope as competitor**
**(**A) Representative images of the binding of indicated mRNA to the chloroplasts surface (lane 3-8) in the presence of inner envelope vesicles (IEV) are shown. 0.5 µg (lane 3,4), 1,0 µg (lane 5,6) and 2,0 µg (lane 7,8) mRNA was added to chloroplasts for 10 mins at 25 °C, followed by organelle isolation, RNA extraction and RT-PCR with gene specific oligonucleotides. 6 % of the supernatant (SN) and 100 % of the recovered chloroplasts pellet were subjected to agarose gel and stained with ethidium bromide. Lane 1, 2 show the precipitation of mRNA in the absence of chloroplasts. **(B)** The abundance of the transcript in A was quantified with Image J for three independent experiments. The amount of free mRNA is plotted against the amount of bound mRNA for COX17 (orange), ENP1 (blue) or OEP24 mRNA (green). As a competitor was present in the reaction mixture, the binding curves were treated as specific binding and analyzed by least square fit analysis using $[B]=MAX*[F]/(K_D+[F])$. The results are shown as line graph and the determined dissociation constant is indicated. The asterisk in A marks a band that is unspecific cloning with the primers for gene amplification.

which might be caused by the precipitation of BY2-L or there might be some cytosolic factors in BY2-L that regulated the binding process.

**Table 5-1 Properties of mRNA binding to chloroplasts**

Dissociation constants ($K_D$) of mRNA to chloroplasts without inner envelope vesicles (IEV) as competitor (Fig. 5.5 B), with IEV as competitor (Fig. 5.7 B). The maximum reaction rate (MAX) was calculated by fitting data. Data represent the mean of three independent biological replicates.

| | No competitor | | With competitor | |
|---|---|---|---|---|
| | $K_D$ [nM] | MAX [nM] | $K_D$ [nM] | MAX [nM] |
| OEP24 | 50±20 | 5±1 | 90±20 | 5±1 |
| COX17 | $>10^3$ | $>10^2$ | $>10^3$ | $>10^2$ |
| ENP1 | 160±50 | 5±2 | 320±200 | 6±3 |

Therefore, more research had conducted to reveal the function of the BY2-L on the binding assay. Taken together, the mRNA binding to the chloroplasts is additional ATP independent and the thermolysin treated chloroplasts could increase the binding. BY2-L seemed to have the effect on the mRNA binding to chloroplasts, which required further research.
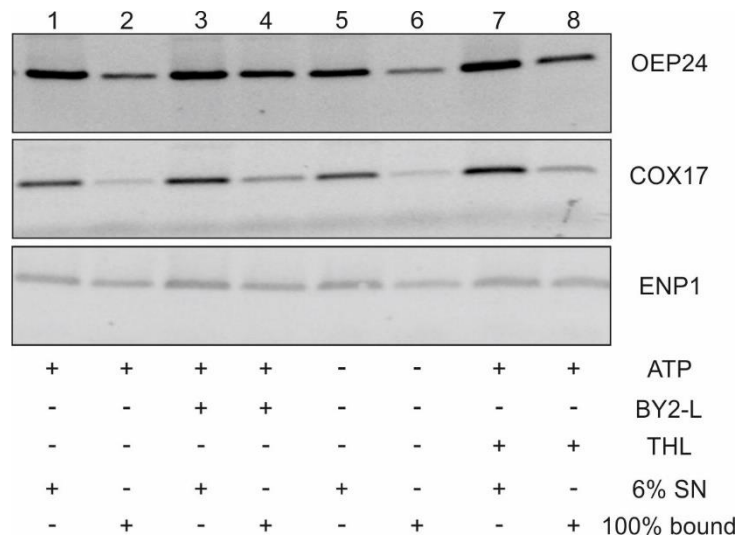


**Figure 5-8 Different properties of mRNA binding to chloroplasts**

Representative images of the indicated mRNA to the chloroplast surface (lanes 1-8) is shown. 0.7 µg mRNA was added to chloroplasts for 10 min at 25 °C in the presence of additional 20 % BY2-L (lane 3, 4), in absence of 5 mM ATP (lane 5, 6) or the chloroplasts were treated with thermolysin (lane 7, 8), followed by organelle isolation, RNA extraction and RT-PCR with gene specific oligonucleotides. 6 % of the result the supernatant (SN) and 100 % of the result for the chloroplast pellet were subjected to agarose gel and stained with ethidium bromide.

## 5.3 The function of BY-2 Lysate in the binding assay

### 5.3.1 The variation of the BY2-L function in the mRNA binding assay.

In order to probe the function of the BY2-L on the binding assay, the established protocol of the mRNA binding assay was followed in presence of additional BY2-L. However, there were opposite results observed from the binding assay with BY2-L (Fig. 5.9 A, B). Interestingly, the BY2-L could both increase the mRNA binding efficiency (Fig 5.9 A, Lane 4 vs Lane 6) and reduce the binding efficiency (Fig 5.9 B, Lane 4,6 vs Lane 8,10).

Since these two different BY2-L were not taken from the same aliquot, the composition of certain ingredients might be different, which resulted in the different function in the binding assay. Previous research suggests that the cytoskeleton is involved in the mRNA targeting process and the surface of other plastids might function as competitor in the mRNA binding process. Therefore, the amount of the cytoskeleton and the plastids might influence the function of BY2-L in mRNA binding process. Thus, the antibodies for the Actin and Toc34 were used to detect the abundance of the cytoskeleton and plastids between these two BY2-L. It was shown that there was no significant difference in the amount of cytoskeleton between the two BY2-L (Fig 5.9 C, low panel, Lane 1-4 vs Lane 5-6); However, it was obvious that BY2-L-Increase (BY2-L-I) showed significantly weaker signal than BY2-L-Reduce (BY2-L-R) in Toc34 antibody (Fig 5.9 C, upper panel, Lane 1-4 vs Lane 5-6) which might suggest that the amount of the plastids in BY2-L influenced the function of the lysate in mRNA binding assay.

### 5.3.2 The amount of envelope vesicles instead of plastids influence the binding efficiency

If the amount of the plastids was the point that influenced the function of BY2-L, the reduction of the plastids would change the behaviour of BY2-L in binding assay. To analyze this, BY2-L-R were subjected to centrifugation to remove the additional plastids. However, BY2-L-R with centrifugation treatment showed no difference in the signals detected by the Toc34 antibody (Fig 5.10 A) and still reduced the mRNA binding to chloroplasts (Fig 5.10 B Lane 2 vs Lane 5, 8, 10). Since the 15,000xg centrifugation was able to pellet the plastids but not the envelope vesicles. Therefore, it might not be the amount of plastids that influenced the BY2-L function, and the signals detected by Toc34 antibody were from envelope vesicles. Moreover, regarding the former results that inner envelope vesicles could be used as the competitor, the amount of envelope vesicles in the BY2-L might influence the behaviour of BY2-L in binding assay. To confirm this hypothesis, various BY2-L prepared through different methods (section 4.2.2) were probed with Toc 34 antibody (Fig 5.10,C) and used for the binding assay (Fig5.10, D).
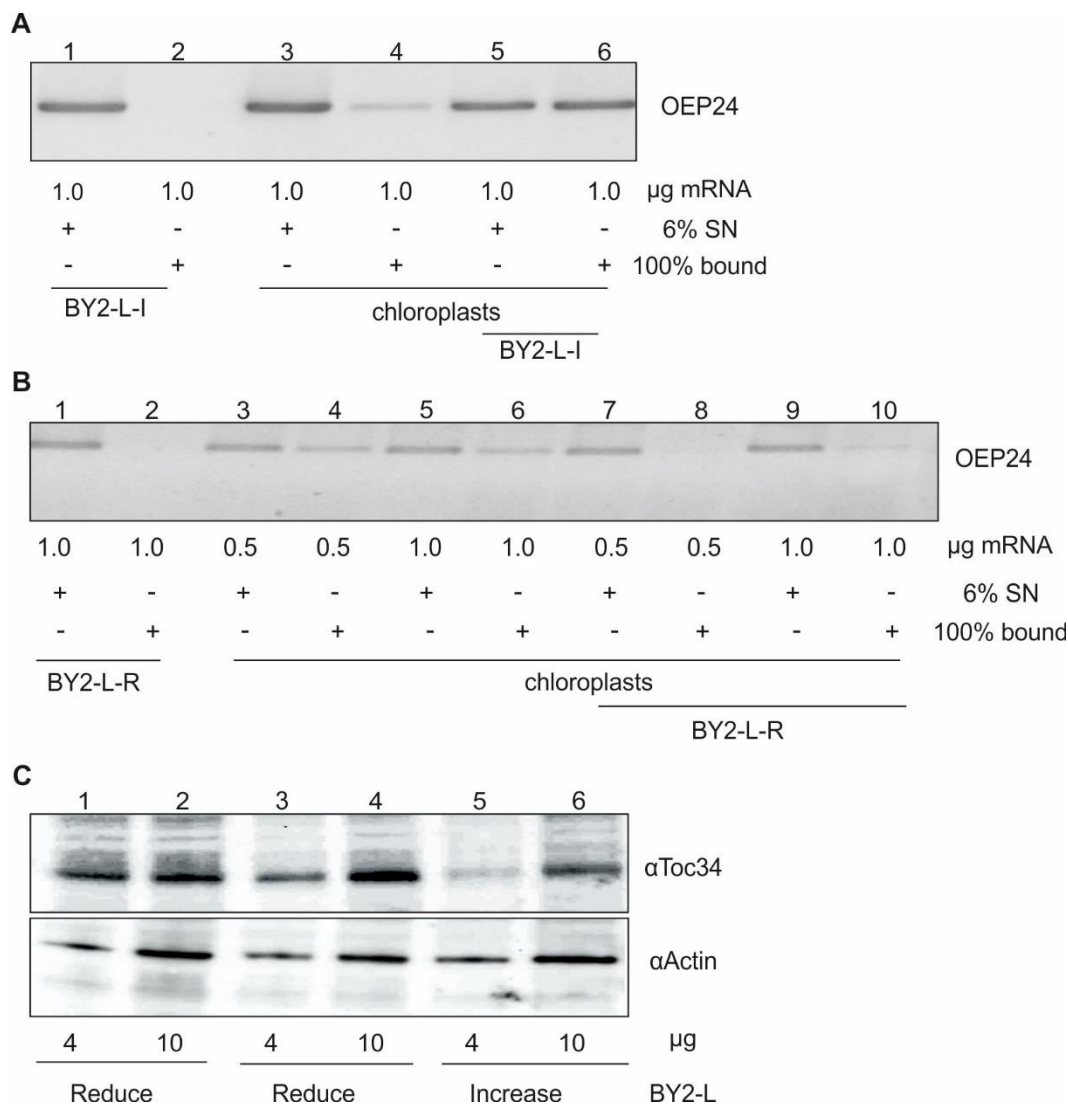
56

**A**



| | 1 | 2 | 3 | 4 | 5 | 6 | |
|---|---|---|---|---|---|---|---|
| | | | | | | | OEP24 |
| µg mRNA | 1.0 | 1.0 | 1.0 | 1.0 | 1.0 | 1.0 | |
| 6% SN | + | - | + | - | + | - | |
| 100% bound | - | + | - | + | - | + | |

BY2-L-I       chloroplasts

BY2-L-I

**B**

| | 1 | 2 | 3 | 4 | 5 | 6 | 7 | 8 | 9 | 10 | |
|---|---|---|---|---|---|---|---|---|---|---|---|
| | | | | | | | | | | | OEP24 |
| µg mRNA | 1.0 | 1.0 | 0.5 | 0.5 | 1.0 | 1.0 | 0.5 | 0.5 | 1.0 | 1.0 | |
| 6% SN | + | - | + | - | + | - | + | - | + | - | |
| 100% bound | - | + | - | + | - | + | - | + | - | + | |

BY2-L-R       chloroplasts

BY2-L-R

**C**

| | 1 | 2 | 3 | 4 | 5 | 6 | |
|---|---|---|---|---|---|---|---|
| | | | | | | | αToc34 |
| | | | | | | | αActin |
| µg | 4 | 10 | 4 | 10 | 4 | 10 | |

Reduce    Reduce    Increase    BY2-L

**Figure 5-9 The variation of the BY2-L function in the mRNA binding assay**

(A) Representative images of the binding of indicated mRNA to the chloroplast surface (lanes 3-6) are shown. 1.0 µg mRNA was added to chloroplasts for 10 min at 25 °C in the presence of additional 20% BY-2 Lysate (lane 5, 6), followed by organelle isolation, RNA extraction and RT-PCR with gene specific oligonucleotides. 6% of the result the supernatant (SN) and 100% of the result for the recovered chloroplast pellet were subjected to agarose gel and stained with ethidium bromide. Lane 1-2 show the precipitation of mRNA in the absence of chloroplasts after addition of BY2-L. Please note: only the binding of OPE24 mRNA were showed by RT-PCR. (B) Representative images of the binding of indicated mRNA to the chloroplast surface (lanes 3-10) are shown. 0,5 µg and 1.0 µg mRNA was added to chloroplasts for 10 min at 25 °C in the presence of additional 20% BY2-L (lane 7-10), followed by organelle isolation, RNA extraction and RT-PCR with gene specific oligonucleotides. 6% of the result the supernatant (SN) and 100% of the result for the chloroplast pellet were subjected to agarose gel and stained with ethidium bromide. Lane 1-2 show the precipitation of mRNA in the absence of chloroplasts after addition of BY2-L. Please note: only the binding of OEP24 mRNA were showed by RT-PCR. (C) 4 or 10 µg protein from different function BY2-L were subjected to SDS-PAGE followed by Western blotting with the antibodies indicated on the right. Please note, BY2-L increase the binding was referred as BY2-L-I, BY2-L reduce the binding was referred as BY2-L-R.
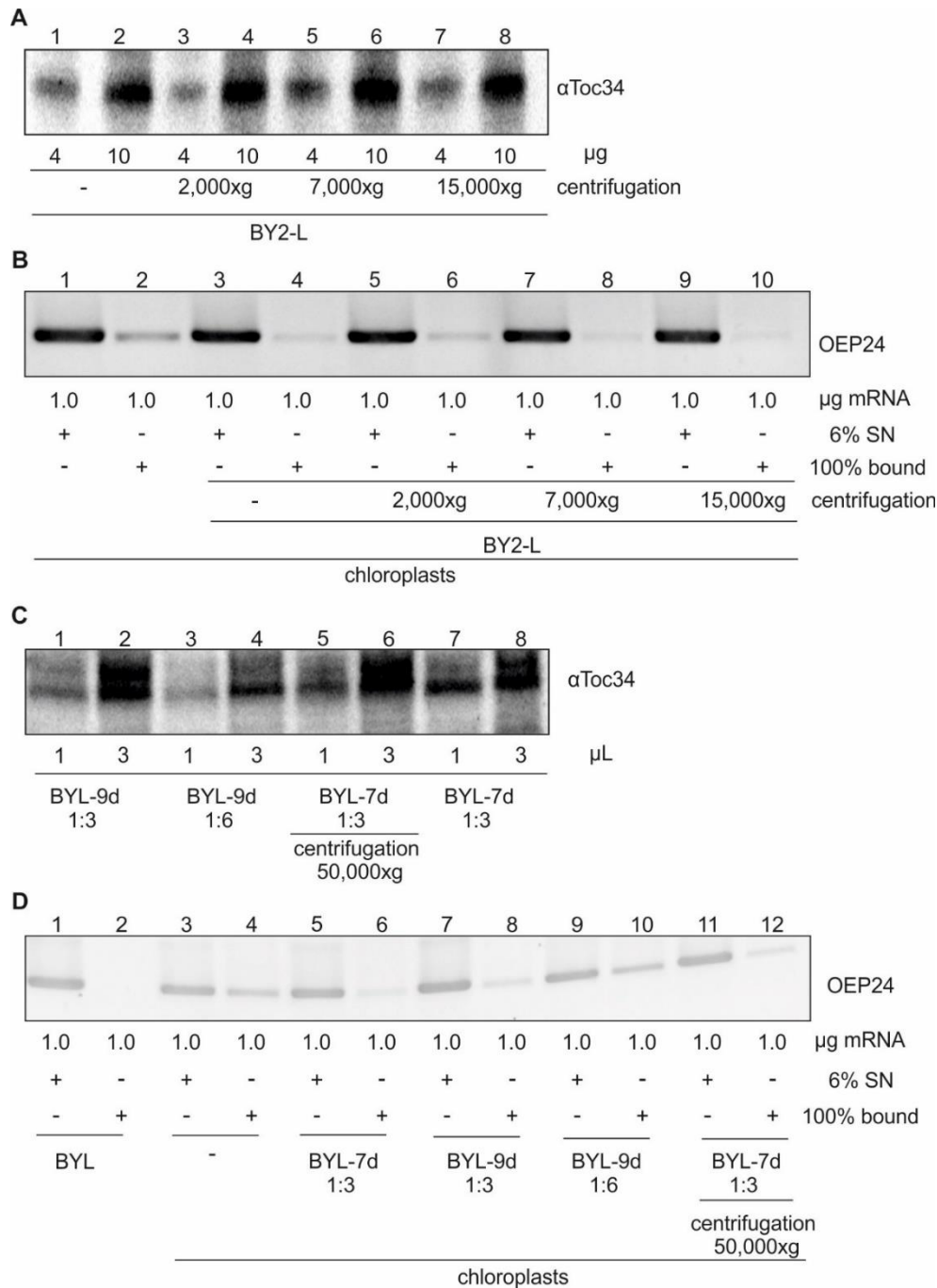
**Figure 5-10 The amount of envelope vesicles influences the BY2-L function in binding efficiency**
(A) BY2-L were treated with 10 mins centrifugation under different speed 2,000xg, 7,000xg, 15,000xg. Then the supernatant of the BY2-L was collected and 4 or 10 µg protein from the collected supernatant of BY2-L were subjected to SDS-PAGE followed by Western blotting with the antibodies indicated on the right. (B) Representative images of the binding of indicated mRNA to the chloroplast surface (lanes 1-10) are shown. 1.0 µg mRNA was added to chloroplasts for 10 min at 25 °C in the presence of additional collected supernatant of BY2-L (lane 3-10), followed by organelle isolation, RNA extraction and RT-PCR with gene specific oligonucleotides. 6% of the result the supernatant (SN) and 100% of the result for the chloroplast pellet were subjected to agarose gel and stained with ethidium bromide. (C) 1 or 3 µL from BY2-L prepared through different methods were subjected to SDS-PAGE followed by Western blotting with the antibodies indicated on the right. (D) Representative images of the binding of indicated mRNA to the chloroplast surface (lanes 3-12) are shown. 1.0 µg mRNA was added to chloroplasts for 10 min at 25 °C in the presence of differently prepared BY2-L (lane 5-12), followed by organelle isolation, RNA extraction and RT-PCR with gene specific oligonucleotides. 6% of the result the supernatant (SN) and 100% of the result for the chloroplast pellet were subjected to agarose gel and stained with ethidium bromide. Lane 1-2 show the precipitation of mRNA in the absence of chloroplasts after addition of BY2-L.

58

Interestingly, the BY2-L prepared by 9d incubation, and lysed with weight ratio of 1:6 contained the least amount of envelopes (Fig 5.10,C Lane 3-4 vs Lane 1-2,5-8) which conferred the highest mRNA binding efficiency to chloroplasts (Fig 5.10,D, Lane 10, vs Lane 6,8,12). Therefore, it seemed highly possible that the amount of the envelope vesicles might influence the function of the BY2-L in mRNA binding.
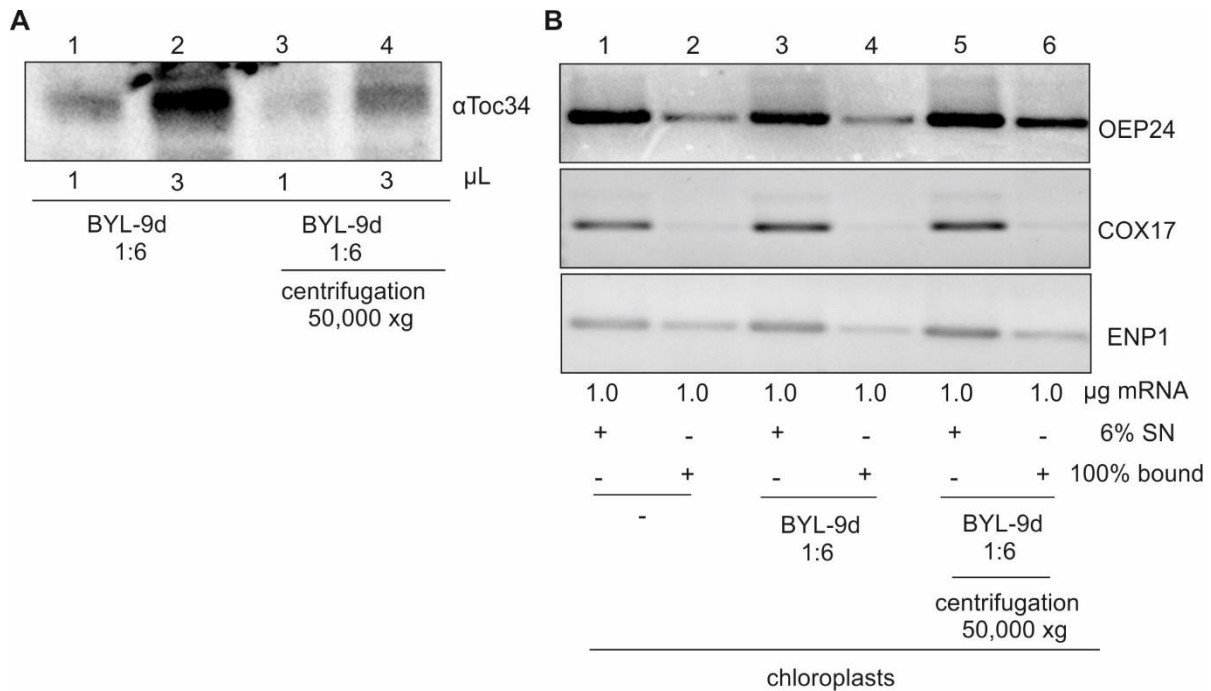


**Figure 5-11 The reduction of the envelope vesicle in BY2-L could enhance the binding efficiency**
(A) 1 or 3 µL from BY2-L prepared through different methods were subjected to SDS-PAGE followed by Western blotting with the antibodies indicated on the right. (B) Representative images of the binding of indicated mRNA to the chloroplast surface (lanes 1-6) are shown. 1.0 µg mRNA was added to chloroplasts for 10 min at 25 °C in the presence of differently prepared BY2-L (lane 3-6), followed by organelle isolation, RNA extraction and RT-PCR with gene specific oligonucleotides. 6% of the result the supernatant (SN) and 100% of the result for the chloroplast pellet were subjected to agarose gel and stained with ethidium bromide.

To further confirm the hypothesis that the amount of envelope vesicles influences the BY2-L function, 50,000xg centrifugation was used to remove the envelope vesicles and the supernatant collected after centrifugation was used for the binding assay. Surprisingly, the 50,000xg centrifugation could remove the amount of the envelope vesicles (Fig 5.11, A, Lane 1-2 vs Lane 3-4), and the reduction of the envelope vesicles in BY2-L could increase the mRNA binding efficiency to chloroplasts (Fig 5.11, B, Lane 2 vs Lane 6). Interestingly, the increasing amount of OEP24 mRNA induced by BY2-L was more obvious than that in COX17 and ENP1 mRNA. Therefore, the BY2-L with less amount of the envelope vesicles could increase the mRNA binding to the chloroplasts.

### 5.3.3 First evidence for factor mediated mRNA binding to chloroplast

Having confirmed that the BY2-L with less amount of envelope vesicles could enhance the mRNA binding efficiency. The next experiment was to investigate the existence of some cytosolic factors in BY2-L that regulated the binding process. This question is rationalized as it cannot be excluded that a cytosolic protein bound to the chloroplast is co-purified with the
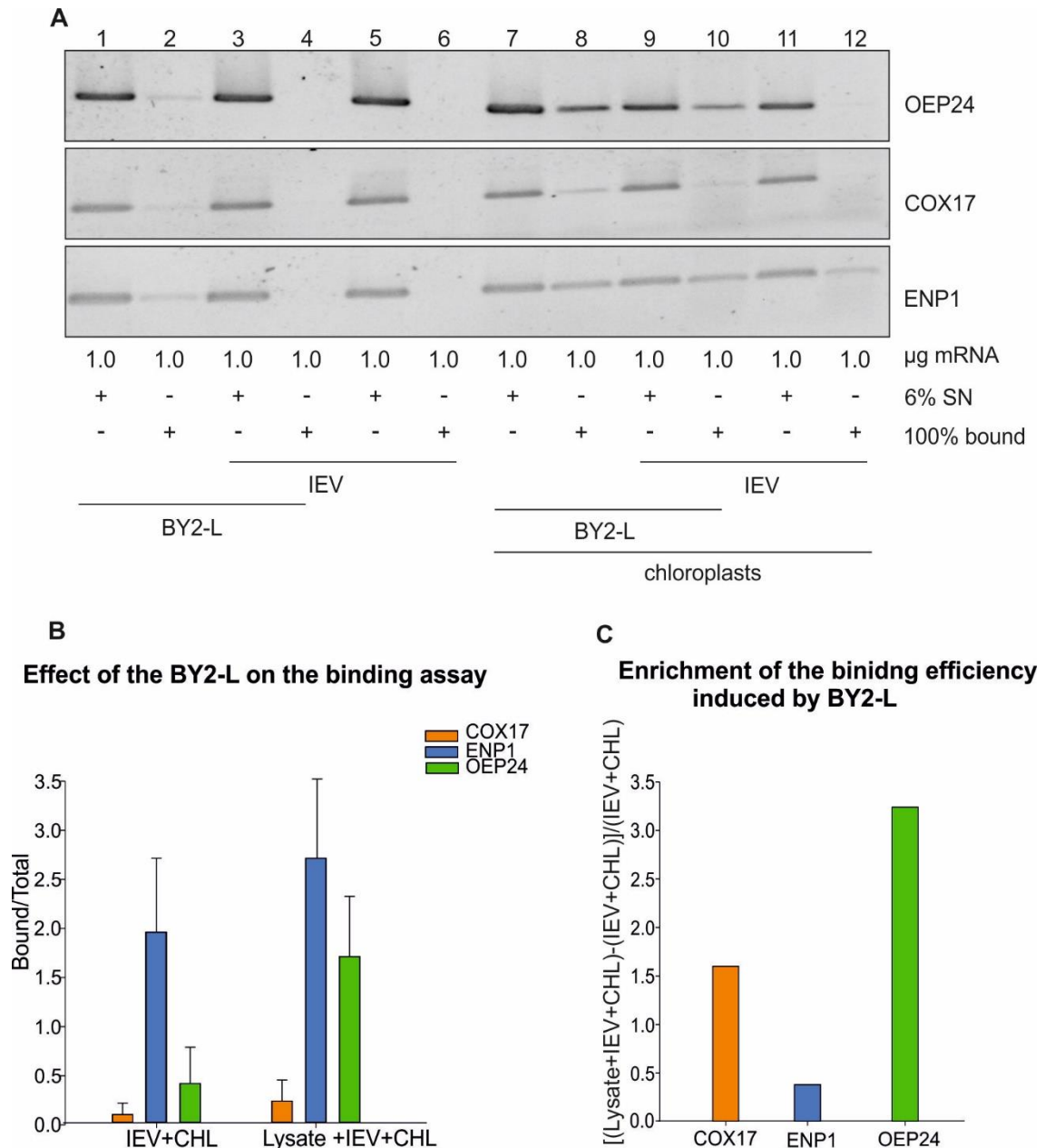


**Figure 5-12 OEP24 mRNA binding is significantly enhanced in the presence of BY2-L**
(A) Representative images of the binding of indicated mRNA to the chloroplast surface (lanes 7-12) are shown. 1.0 µg mRNA was incubated with BY2-L (lane 1-4, 7-10) before addition to chloroplasts for 10 min at 25 °C (lane 7-12) in the presence inner envelope vesicles (lane 3-6, 9-12). All samples, irrespective whether chloroplasts were added or not were pelleted for organelle isolation followed by RNA extraction, RT-PCR with gene specific oligonucleotides and processing as in Fig. 5.5A). Lanes 1-6 show the precipitation of mRNA in the absence of chloroplasts after addition of BY2-L (lane 1-4) and inner envelope vesicle (IEV) (lane 3-6). (B) The abundance of the transcript in A (lane 9-12) was quantified with Image J for three independent experiments. The amount of bound mRNA is divided by the amount of total mRNA for COX17 (orange), ENP1 (blue) or OEP24 mRNA (green).

organelle. The BY2-L isolated as described in (section 4.2.2) and the inner envelope vesicles as competitor were selected.

The analysis of the binding of the mRNA to chloroplasts in the presence of BY2-L was thus performed in the presence of inner envelope vesicles. This resulted in a minor increase of COX17 and ENP1 binding (Fig. 5.12 A, middle panel lane 10 vs 12), which suggested that the cytosolic lysate had weak influence on the efficiency of the unspecific COX17 binding and the less specific ENP1 binding. However, the binding efficiency of mRNA OEP24 to chloroplasts was significantly increased by the BY2-L in the presence of inner envelope (Fig. 5.12 A, upper panel lane 10 vs. 12). The enrichment of binding efficiency by the BY2-L showed that OEP24 has the highest binding capacity together with the BY2-L (Fig 5.12 B,C). Thus, this result was the first strong hint that cytosolic proteins were involved in the regulation of mRNA binding to chloroplasts.

## 5.4 Usage of LNA primers to find out the candidates involved in the mRNA targeting process

Based on the former results from the section 5.3, COX17 mRNA showed a concentration-dependent unspecific binding; However, OEP24 mRNA showed a concentration-independent specific binding and the BY2-L could significantly enhance the binding efficiency of OEP24 mRNA. Therefore, two hypothesis were formulated that (i) Are there cytosolic proteins that bind to mRNAs coding for chloroplast proteins that are involved in mRNA binding to the chloroplast surface? (ii) Are there receptors that specifically bind to mRNAs coding for chloroplast proteins?

The established protocol to generate translational active lysate allows to ask whether there are cytosolic factors that bind to mRNA. The mRNA will be used as the bait to conduct precipitation after UV-crosslinking by using antisense LNA/DNA mixamers as established (Rogell et al., 2017). The pull-down will be performed via magnetic beads coupled to the LNA/DNA mixamers. This will yield the associated ribonuclear Proteins bound to the mRNA. The nature of the proteins will be identified by Mass spectrometry.

Though the pull-down assay with LNA/DNA mixamers and complemented with UV-Crosslinking has been developed (Rogell et al., 2017), this system has been rarely used in plant research. Therefore, my initial objective was to try to adopt this system into the plant field and confirm its feasibility and efficiency. Taking the former knowledge into consideration, the general workflow was described (Fig. 5.13).
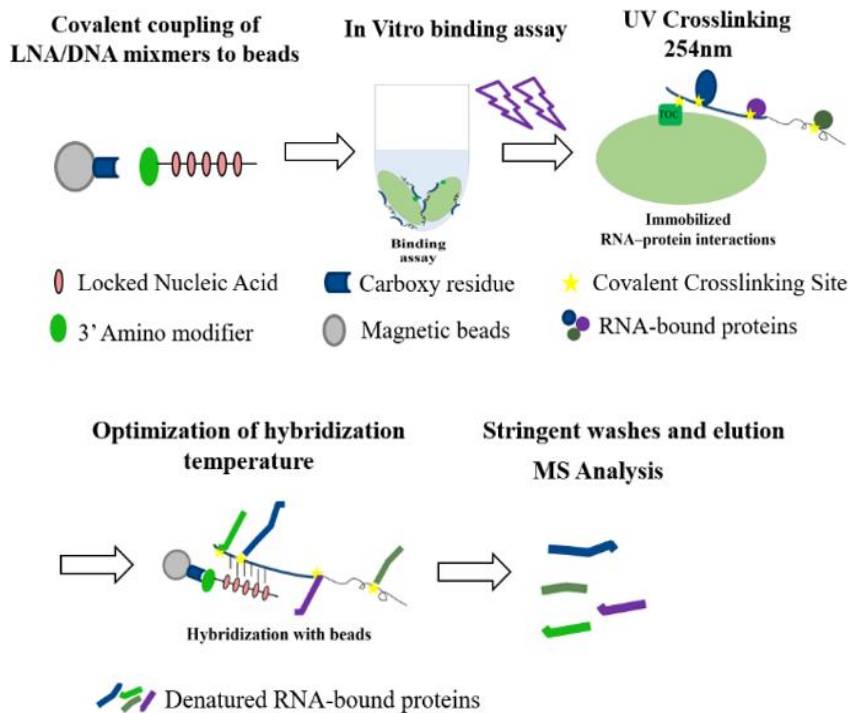
**Figure 5-13 Workflow for the setup and experiments of specific RNP capture**
Schematic overview of specific RNP capture. Specific RNP capture uses antisense LNA/DNA mixmers oligonucleotides that are covalently coupled to a magnetic resin. By applying UV crosslinking on chloroplasts at 254 nm, direct RNA–protein interactions are covalently fixed. After lysis, hybridization with the covalently coupled oligonucleotides is performed under stringent denaturing conditions at elevated temperatures. The RNA-bound proteins are identified by quantitative mass spectrometry in comparison to negative controls.

To identify this workflow, three main issues had to be analyzed (i) the feasibility of UV crosslinking to stable the interaction between mRNA and chloroplast, (ii) the hybridization specificity and efficiency test of LNA probes coupled to beads, (iii) reasonable method to read out the mRNA-binding proteins. Please note: the covalent coupling of LNA mixmers to beads was followed with the protocol (Rogell et al., 2017) mentioned in section 4.3.1.

Regarding the lower efficiency of UV-Crosslinking *in vivo* and the UV light absorbing ability of the chloroplasts, the binding efficiency of UV crosslinking in the chloroplasts surface had to be tested. The previous research of the interaction between RNA and protein showed that the UV-Crosslinking was not invertible, the size of the cross-linked RNAs was essentially unchanged and the RNA crosslinked with proteins still remained in the organic face instead of the water face during the RNA isolation process (Wagenmakers et al. 1980). Therefore, my study attempted to test the efficiency of UV-crosslinking with the usage of phenol/chloroform extraction. The theory is that the mRNA bound to the proteins of the chloroplasts surface could be isolated without UV-crosslinking, and not with UV-crosslinking. Therefore, the reduction of the isolated mRNA could be used to evaluate the efficiency of the UV-crosslinking. Following this theory, the binding assay was conducted with individual OEP24 mRNA (Fig 5.14 A upper

panel), COX17 mRNA (Fig 5.14 A, lower panel) in addition to the chloroplast, respectively. The binding assay showed that UV crosslinking could reduce the yield of the RNA isolation (Fig 5.14 A, lane 2 vs 3); with the increasing time of UV-Crosslinking, the recovery rate of
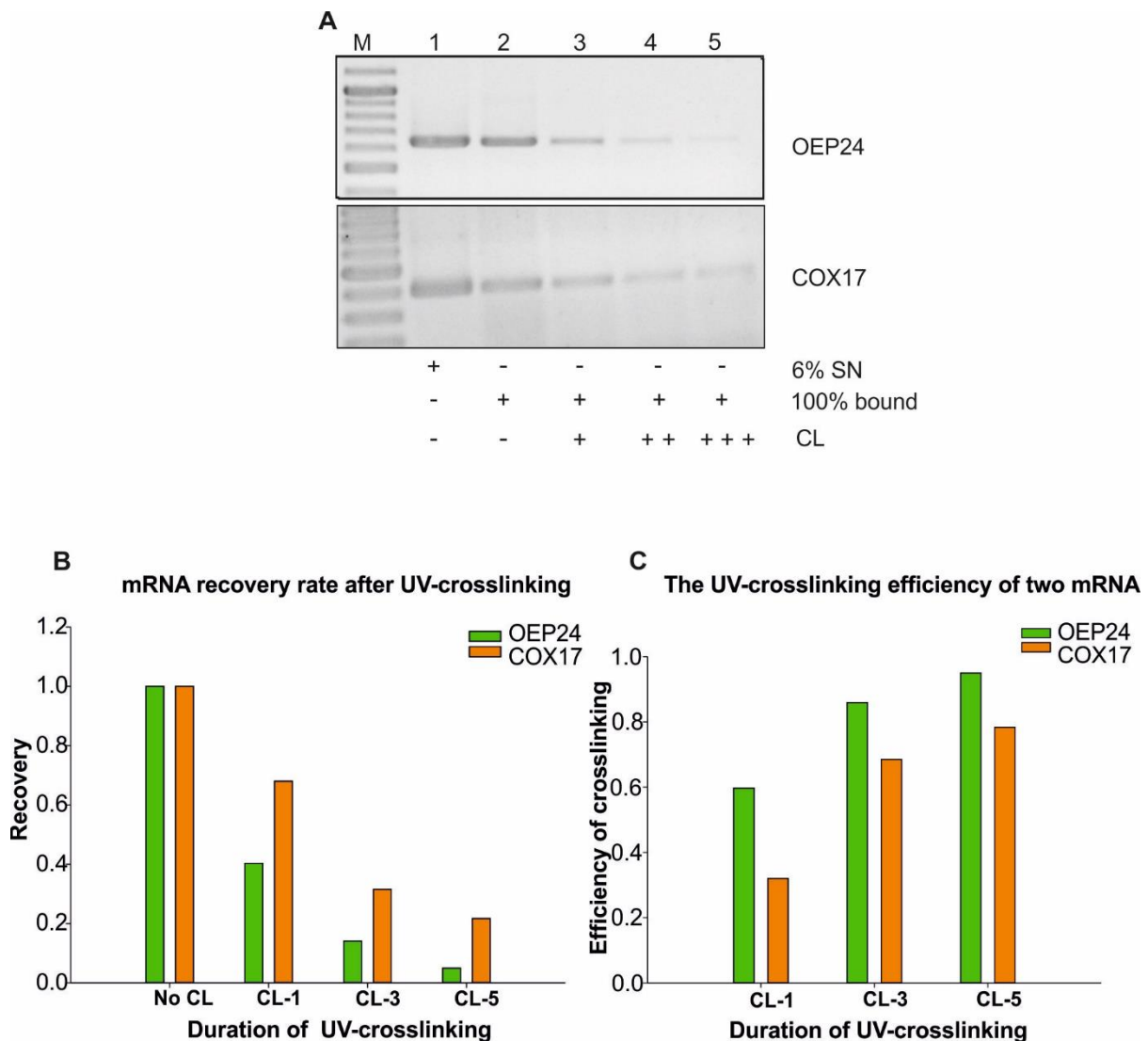


**Figure 5-14 Feasibility of UV crosslinking to stable the interaction between mRNA and chloroplast**

A: Representative images of the binding of indicated mRNA to the surface of the chloroplast. 1,0 μg mRNA was added to chloroplasts for 10 mins at 25 °C, followed by organelle isolation, UV-Crosslinking, RNA extraction, and RT-PCR with gene specific oligonucleotides. 6 % of the result the supernatant (SN) and 100 % of the result for the chloroplasts pellet were subjected to agarose gel and stained with ethidium bromide. CL samples irradiated by continuous UV for 1 (+), 3 (++) and 5 (+++) min. B: The recovery rate of the RNA isolation from the isolated chloroplasts pellet after different times of UV crosslinking treatment. C: The efficiency of the UV crosslinking to stable the interaction between mRNA and chloroplasts. The efficiency is the loss of the yield in RNA isolation with the UV-crosslinking.

RNA from the isolated chloroplasts pellets was reduced (Fig 5.14 A, lane 3 vs 4,5). The recovery rate and the efficiency of UV-crosslinking were calculated (Fig 5.14 B, C). Therefore,

UV-crosslinking was feasible to fix the interaction between the mRNA and the proteins in the surface of the chloroplasts.Since the UV-crosslinking could efficiently stabilize the interaction between mRNA and chloroplasts, the next aim is to confirm the hybridization specificity and determined the optimal hybridization temperature of the LNA primers coupled to beads (LNA$_{OEP24}$:specifically hybridize OEP24 mRNA; LNA$_{COX17}$:specifically hybridize COX17 mRNA) using the buffer conditions employed in specific RNP capture (section 4.3.3). In order to identify the optimal hybridization temperature of LNA$_{OEP24}$, the isolated chloroplasts were incubated with *in vitro* transcribed OEP24 and control COX17 mRNA in equimolar amounts, the buffer compositions of specific RNP capture was adjusted to maximize hybridization, and then specific RNP capture with the LNA coupled beads was performed. With this set-up, the hybridization temperature ranges for the LNA$_{OEP24}$ probes from 40 °C-56 °C were tested. After the pull-down assay, the relative amount and purification of the RNA in the elution were analyzed with RT-qPCR. Besides the target OEP24 mRNA, the specificity control COX17 mRNA and the endogenous 16SrRNA from the chloroplast was quantified. The results showed that LNA$_{OEP24}$ captured significantly more OEP24 mRNA than both COX17 mRNA and 16SrRNA (Figure 5.15, A). And, the highest binding efficiency occurred at 56 °C.

However, the best enrichment of OEP24 over the COX17 control was of 17 fold and 16SrRNA of almost 24 fold at 40 °C in the test set-up (Figure 5.15, B). Similarly, LNA$_{COX17}$ captured significantly more COX17 mRNA than both OEP24 mRNA and 16SrRNA (Figure 5.15, C). And the highest binding efficiency occurred at 52 °C. However, the best enrichment of COX17 over the OEP24 control was of 20 fold and 16SrRNA of almost 56 fold at 40 °C in the test set-up (Figure 5.15, D). Thus, the hybridization specificity of LNA primers was confirmed and the optimal hybridization temperature was tested. However, the higher purification rate was necessary to guarantee less background for the mass spectrometry. Therefore, an extra method had to be conducted to further remove the contamination in the elution.

Recently, colleges from Hentze team found that the pre-elution could significantly remove the unspecific binding in RNP capture and increased the enrichment of the specific mRNA. Therefore, the RNP capture was performed with an additional pre-elution step. Compared with the control COX17 mRNA and endogenous 16SrRNA, target OEP24 mRNA was strongly enriched in all the tested temperatures; especially when the hybridization was performed at 56 °C (Fig 5.16 A). LNA$_{OEP24}$ reached the best enrichment of OEP24 over the COX17 control of almost 800 fold and 16SrRNA of almost 1600 fold at 40 °C in the test set-up (Fig 5.16 B). Therefore, 40 °C was selected for further pull-down assay with LNA$_{OEP24}$.

Similarly, the optimal hybridization temperature of LNA$_{COX17}$ was determined. The isolated chloroplasts were incubated with *in vitro* transcribed COX17 and control OEP24 mRNA in equimolar amounts, following the buffer compositions of specific RNP capture, and then
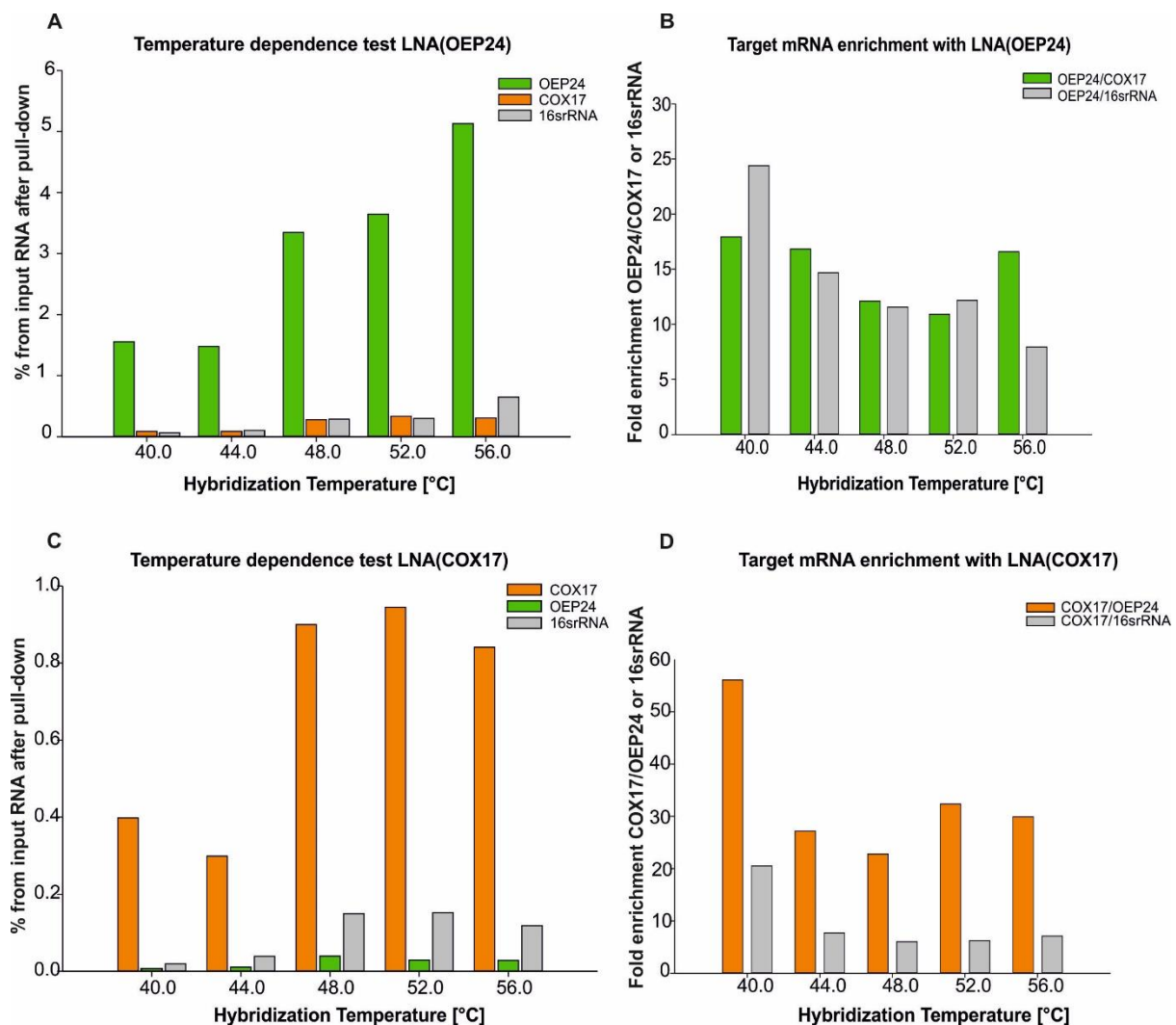


**Figure 5-15 Initial attempt for hybridization efficiency and specificity of LNA probes coupled to beads**

Different hybridization temperatures were tested in the Thermocycler. LNA$_{OEP24}$ and LNA$_{COX17}$ were designed to target OEP24 mRNA and COX17 mRNA, respectively. After stringent washes and elution, RNA from elution was isolated and analyzed by RT-qPCR. 16SrRNA, OEP24 mRNA, and COX17 mRNA were quantified in relation to the Input RNA in %. (A) Hybridization of LNA$_{OEP24}$; (B) Enrichment of OEP24 target RNA over the equimolar added COX17 control for the applied LNA$_{OEP24}$; (C) Hybridization of LNA$_{COX17}$; (D) Enrichment of COX17 target RNA over the equimolar added OEP24 control for the applied LNA$_{COX17}$.

performed specific RNP capture with the LNA$_{COX17}$ coupled beads. In the set-up, the hybridization temperature range for the LNA$_{COX17}$ probes from 40 °C-56 °C was tested. After the pull-down assay, the relative amount and purification of the RNA in the elution were analyzed with RT-qPCR. Besides the target COX17 mRNA, the specificity control OEP24 mRNA and the endogenous 16SrRNA from the chloroplast was quantified. Compared with the

control OEP24 mRNA and endogenous 16SrRNA, target COX17 mRNA was strongly enriched in all the tested temperatures; especially when the hybridization was performed at
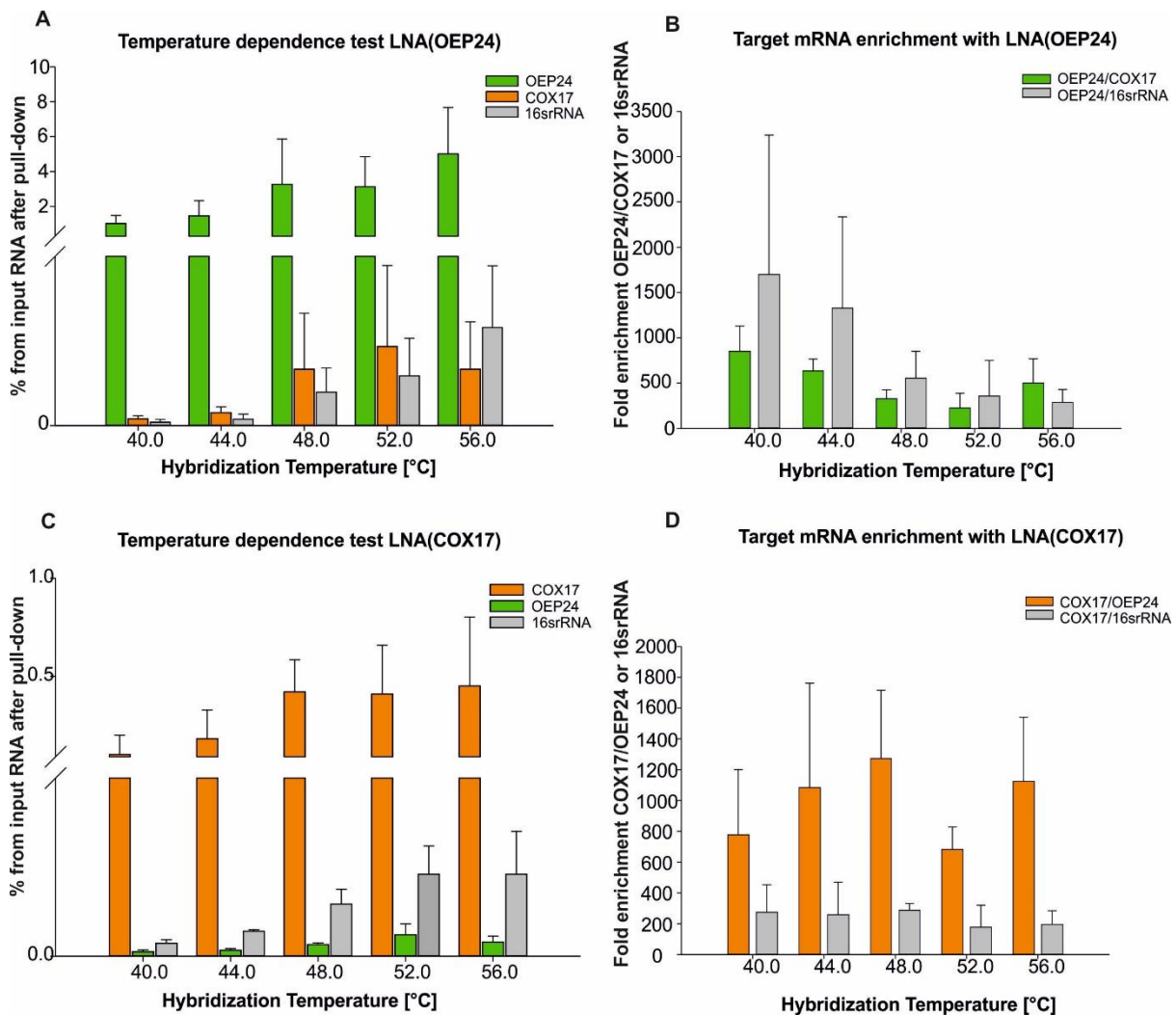


**Figure 5-16 Hybridization efficiency and specificity of LNA probes coupled to beads after pre-elution optimization**

Different hybridization temperatures were tested in the Thermocycler. $LNA_{OEP24}$ and $LNA_{COX17}$ were designed to target OEP24 mRNA and COX17 mRNA, respectively. After stringent washes and elution, RNA from elution was isolated and analyzed by RT-qPCR. 16SrRNA, OEP24 mRNA, and COX17 mRNA were quantified in relation to the Input RNA in %. Error bars represent the standard deviation of three experiments. (A) Hybridization of $LNA_{OEP24}$; (B) Enrichment of OEP24 target RNA over the equimolar added COX17 control for the applied $LNA_{OEP24}$; (C) Hybridization of $LNA_{COX17}$; (D) Enrichment of COX17 target RNA over the equimolar added OEP24 control for the applied $LNA_{COX17}$.

48 °C (Fig 5.16 C). $LNA_{COX17}$ reached the best enrichment of COX17 over the OEP24 control of almost 1250 fold and 16SrRNA of almost 250 fold at 48 °C in the test set-up (Fig 5.16 D). Therefore, the 48 °C was selected for further pull-down assay with $LNA_{COX17}$. Until now, both the feasibility of the UV-Crosslinking and the optimal hybridization temperature of LNA have

been identified. Therefore, it is feasible to use this established protocol to identify the mRNA binding proteins in the surface of the chloroplasts during the binding process.

As for the protein detection, protein band pattern should only present in the CL sample and no specific bands in non-CL sample (Zhang et al., 2016), which indicated more protein was captured with the UV-crosslinking. However, in this study, the A260 and A280 values of the CL and no CL samples were measured. In CL sample, the A260 was 0,827, which was almost the same as the value 0.78 in the CL sample. (Figure 5.17, B). However, the A280 was 1.482 in CL sample, which was much more than the value 0.397 in no-CL sample (Figure 5.17, B), indicating that mRNA was crosslinked with more proteins in CL sample. Additionally, the ratio of the A260/A280 in the No-CL sample was 1.96, which was 0.558 in the CL sample, also indicating more proteins existed in the elution with UV-crosslinking. Therefore, this confirmed the success in the pull-down assay with the LNA primers to capture the proteins interacted with the mRNA.
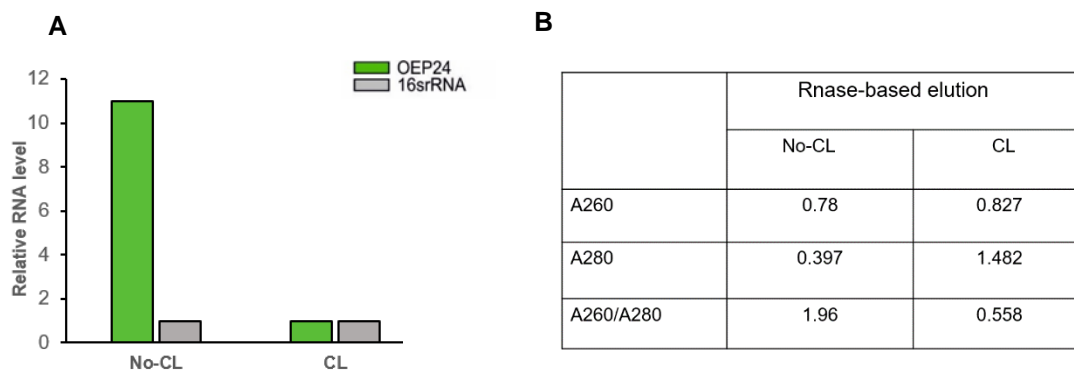


| | Rnase-based elution | |
|---|---|---|
| | No-CL | CL |
| A260 | 0.78 | 0.827 |
| A280 | 0.397 | 1.482 |
| A260/A280 | 1.96 | 0.558 |

**Figure 5-17 qRT-PCR and Nanodrop to analyze the elution from LNA$_{OEP24}$ pull-down assay**
OEP24 mRNA was added to chloroplasts for 10 mins at 25 °C, followed by organelle isolation. The bound mRNA to the isolated chloroplast surface was stabilized by the UV-Crosslinking, hybridized by the LNA$_{OEP24}$ probes, and pull-down via magnetic beads coupled to the LNA/DNA mixamers. After stringent washes and elution, RNA from elution was isolated and analyzed by RT-qPCR. Proteins crosslinked to OEP24 mRNA were pull-down and the A$_{260}$ and A$_{280}$ of the elution were measured via Nanodrop. **A**: The amount of 16SrRNA and OEP24 mRNA in the elution of No-CL and CL samples were analyzed by qRT-PCR. **B:** The A$_{260}$ and A$_{280}$ of the elution from the No UV-crosslinking and UV-crosslinking samples were measured. No-CL: non-irradiated samples, CL: irradiated samples.

# 6 DISCUSSION

## 6.1 Ribosomes binding to chloroplasts

Most proteins targeted to the mitochondria are imported post-translationally and guided by the peptide-based signal (Schleiff and Becker, 2011). However, this notion was challenged by the examples of obligate co-translational mitochondrial protein import, which was supported by the evidence that mRNAs together with cytoplasmic polysomes localize in close vicinity to mitochondria (Kellems et al., 1972; Kellems et al., 1974; Kellems et al., 1975). Moreover, it was observed that ribosomes stably bind to purified liver mitochondria *in vitro* and this was regulated by GTP and the presequence (Crowley et al., 1997), which further supported the existence of the co-translational translocation pathway for the import of mitochondrial proteins. Similarly, the post-translational process of the protein targeting to the chloroplasts was confirmed by the findings that isolated chloroplasts can import *in vitro* synthesized proteins and the absence of ribosomes in the immediate area around chloroplasts in EM images (Ulrich et al., 2012; Carde et al., 1982; Uniacke and Zerges, 2009). However, colleagues stated that none of the EM images were recorded in the presence of a translation elongation inhibitor (Uniacke et al., 2009).

In this study, different antibodies for the small and large subunits of the ribosomes were used as the indicators for the binding analysis (Figure 5.1, A). The evidence was shown that ribosomes were bound to the isolated *P. sativum* chloroplasts, although the concentration was low (Figure 5.1, B) This finding could supplement the former results that no ribosomes were observed in the immediate area around chloroplasts in EM images. Moreover, the ribosomes attached to the outer membrane could not be removed by either 300 mM salt or 5 mM EDTA (Figure 5.1, C). Which was opposite to the related researches in mitochondria that EDTA and high salt could strip the ribosomes away (Crowley et al., 1998). The resistance of the ribosomes to high salt and EDTA suggests that the interaction of the ribosome is not an electrostatic interaction and might be specifically manifested by a membrane-bound protein serving as a receptor or by translation. Since 1 mM puromycin could remove a small portion of the ribosomes (Figure 5.1, D) which is consistent with the former finding (Margulies et al., 1974). This indicated that a small portion of the ribosomes is dependent on translation for their interaction with chloroplasts. Therefore, the acquired results initially indicated that the ribosomes association with chloroplasts is slightly translation dependent.

Interestingly, with the binding assay, ATP could enhance the association between the ribosomes and chloroplasts, while GTP did not influence the binding (Figure 5.2, B). However, the two cytosolic exposed receptor components of the protein translocation machinery of the

chloroplasts are GTPases. Hence, this ribosome binding might be regulated by the other unknown machinery which is ATPases. Though, the precipitation of ribosomes due to the formation of polysomes hamper the attempt to probe whether the presence of mRNA would increase the binding efficiency of ribosomes (Figure 5.2, C), the current finding still give a hint that there might be a different machinery for the ribosome binding to chloroplasts.

Alternatively, the rRNA was also used as an indicator to reveal the association between the chloroplasts and ribosomes. The conducted research initially tested the different compositions of the rRNA in cytosol and chloroplasts (Figure 5.3, A,B). Interestingly, the chloroplasts contained its plastidic 23SrRNA and did not contain the 25SrRNA and 5.8SrRNA from the cytosol. Though, this result was opposite to the finding by the antibody that the cytosolic ribosomes are present in isolated chloroplasts fraction. This result is consistent with the former results that the ribosomes are absent in the immediate area around chloroplasts in EM images (Carde et al., 1982). The reason might be that the antibody only detected the protein part of the ribosomes and the isolated chloroplasts contained partially proteins of ribosomes instead of the rRNA. And also it might be that the intact ribosomes which are bound to the chloroplasts surface are raptured during the isolation, and the parts of the subunits stayed associated with chloroplasts. Since the chloroplasts do not contain unique rRNA from the cytosol, it is feasible to use the cytosol rRNA as an indicator to test the binding based on the established binding assay. Under the current condition, naked ribosomes are not considerably bound to chloroplasts (Figure 5.3, C), which is opposite to the finding by antibody. The reason might be that the EtBr detection is not as sensitive as the detection by the antibody. Meanwhile, ATP and GTP are not added into the binding system, which might also be the reason that no comparable signal is detected. Therefore, it will be interesting to repeat the binding assay with more sensitive detection method like Northern blot in addition to the ATP and GTP.

## 6.2 mRNA binding to chloroplasts

In spite of the ribosome binding, the post-translation protein import assumption was also challenged by the other evidences that mRNAs localize in close vicinity to mitochondria. Global analysis of transcripts bound to mitochondria in yeast or human revealed that around half of the transcripts of mitochondrial proteins displayed a high mitochondrial localization (Marc et al., 2002). And, the deletion of the Tom20 leads to mislocalization of several mRNAs encoding mitochondrial proteins (Eliyahu et al., 2010). In plants, the co-isolation assays showed the ability of mitochondrial transcripts to bind the mitochondrial surface (Michaud et al., 2010). Also, the glyceraldehyde-3-phosphate dehydrogenase (GAPDH) mRNA is able to bind to isolated mitochondria treated with proteinase K *in vitro*, which indicated Tom 40 could

interact with mRNA in the absence of *trans*-acting protein factors (Michaud et al., 2014a). Later on, the same group found that the length of the 3'UTR influences the efficiency of VDAC3 association with mitochondria (Michaud et al., 2014b). Similarly, the chloroplast localization of mRNAs encoding plastid proteins in *Chlamydomonas rheinhardtii* was revealed. A subsequent study by the laboratory of Prof. Schleiff which is yet to be published revealed a high accumulation of mRNAs coding for chloroplast proteins at the chloroplast surface. However, less research of the mRNA binding to chloroplasts *in vitro* was conducted.

In this study, it is the first time that the mRNA binding to chloroplasts was revealed *in vitro*. COX17 mRNA showed unspecific binding to the chloroplasts surface (Fig 5.5, B). Since the COX17 mRNA is a mitochondrial transcript, the unspecific binding suggested that this binding is concentration dependent. And there might be no receptors or special proteins which could specially interact with COX17 mRNA. Interestingly, the ENP1 mRNA which belongs to the nucleus showed an unexpected combination of specific and unspecific binding ($K_D$=160±50 nM) (Table 1). The reason might be the contamination of the ER membrane attached to the isolated chloroplasts, which conferred the specific binding of ENP1 to chloroplasts. Even though, the OEP24 mRNA showed more specificity than the ENP1 mRNA, which is consistent with the accumulation of mRNAs coding for chloroplasts proteins (unpublished data). Also, the binding of these three mRNAs was not influenced by adding 75 mM or 150 mM NaCl (Figure 5.6, A), which indicated that the interaction is not the electrostatic interactions. However, the interaction was affected by the inner envelope as a competitor (Figure 5.6, B), which gave a further approach to uncover the unspecific interaction. The binding assay with the inner envelope could further confirm the unspecific binding of COX17 and more specific binding of OEP24 mRNA than ENP1. Meanwhile, the specific binding of OEP24 mRNA might indicate the existence of the receptors interacting with the certain mRNA. Since the maximum velocity of the specific bound ligand is dependent on the numbers of receptors, which resulted in the platform of the binding curve. However, the unspecific bound only depended on the surface of the chloroplasts instead of the receptor numbers, which results in the huge maximum velocity bound compared with the specific bound (Table 1). In mitochondria, these receptors and ligands have been identified, like Puf family protein, and the TOM complex (Michaud et al., 2010; Eliyahu et al., 2010). Moreover, the binding efficiency of all three mRNAs was increased when the chloroplasts were treated with thermolysin (Figure 5.8, Lane 7-8). The similar observation was also detected in the mRNA binding to mitochondria assay with the Proteinase K treated mitochondria (Michaud et al., 2014a). The reason might be that the deletion of the surface protein supplies more space for the unspecific binding. The mRNA binding to the chloroplasts is additional ATP independent (Figure 5.8, Lane 5-6 vs 1-2) which might be that chloroplasts could generate the ATP by Photosynthesis. Similarly, the mRNA binding to

mitochondria is also additional ATP independent due to the production of the ATP by mitochondria in respiration (Michaud et al., 2014a).

## 6.3 Cytosolic factors affecting mRNA binding to chloroplasts

Most surprisingly, the BY2-L influenced the mRNA binding efficiency (Fig 5.8, Lane 1-2 vs 3-4). Since the whole process of the mRNA journey from the nucleus to the localization is regulated by the cytosolic proteins (Parton et al., 2014), and the BY2-L could be used for the *In vitro* protein translation (Buntru et al., 2014). Thus, there might be the cytosolic factors in BY2-L that regulate the mRNA targeting process.

Considering the existed model of the co-translational and post-translational targeting process, the cytosolic factors played the important role in both of these two machineries. During the co-translational targeting, the cytosolic factors SRP could stall translation and forms a ribosome-nascent chain complex (RNC), then transferred it to the Sec61 complex (Junne et al., 2010; Gogala et al., 2014); In the post-translational targeting process, the transport of the preprotein to chloroplasts is regulated by the collaboration of cytosolic factors, like chaperones Hsp 70, Hsp 90 and 14-3-3 proteins (May and Soll, 2000). In this study, the cytosolic factors from the BY2-L might interact with the special mRNA, then guided the mRNA to the different organelle. Since the BY2-L increased the specific binding efficiency of ENP1, COX17 by 0.5 times and 1.5 times (Fig. 5.12, A,C), respectively. However, it induced the highest increasing amount of the specific binding in OEP24 mRNA (Fig. 5.12, A,C). These factors might be able to distinguish the plastidic mRNA from the mitochondria and nuclear mRNA, and specially bind the plastidic mRNA OEP24 then guide it to chloroplasts surface. These RBPs which function in the mRNA localization has been identified in *Oryza sativa* endosperm cells. During the transportation process, RBP-P could ensure the localization of glutelin and prolamin mRNA (Tian et al., 2018, 2019). With the mediation of the cytosolic factors, mRNA could precisely localize to the different organelles, which could supply the economic benefits and guarantee the efficient translational responses to various abiotic or biotic conditions (reviewed in Weis et al., 2013). Additionally, the naked ribosomes were detected on the surface of the isolated chloroplasts, although the concentration was low (Figure 5.1, B). Since the co-translation targeting to mitochondria has been supported by the observation that ribosomes stably bind to purified liver mitochondria *in vitro* (Crowley et al., 1997). Therefore, the existence of the ribosomes in the surface of the isolated chloroplasts might also partially support the co-translation targeting to chloroplasts. The evidence found in the mRNA binding assay also showed that there might be a receptor in the surface of the chloroplasts. Considering the similarity of the mitochondria and chloroplasts in endosymbiotic organelle (Mirus and Schleiff,

2012; Ku et al., 2015), there might also be the co-translational import in chloroplasts which has been revealed in mitochondria (Lesnik et al., 2014). The co-translational import in mitochondria is not mutually exclusive with the post-translation import. And it is speculated that co-translational import is the preferred mode under most natural conditions since it enables efficient and rapid import (Lesnik et al., 2014). During the co-translational import, the cytosolic factors nascent chain-associated complex (NAC) is involved in the import reaction, which bind the ribosome-nascent chain (RNC) complexes, then transferred it to the surface of the mitochondria and recognized by the receptor OM14. Therefore, integrated all the evidence, the model of the plastidic mRNA targeting to the chloroplasts is proposed (Figure 6-1).

Once the plastidic mRNAs are transcribed in the nucleus and transported into the cytosol, the translation initiated with the association of the ribosomes. Afterwards, the signal sequence of an emerging nascent polypeptide from a translating ribosome is recognized by the unknown cytosolic factor, which stalls translation and forms a ribosome-nascent chain complex (RNC). Then, the RNC is delivered to the chloroplasts through the interaction between the cytosolic factors and unknown receptors on the surface of the chloroplasts. The interaction between the cytosolic factor and the receptor is important for the co-translational import of proteins into chloroplasts and also this association may be important for initiating specificity for those that are destined to chloroplasts.
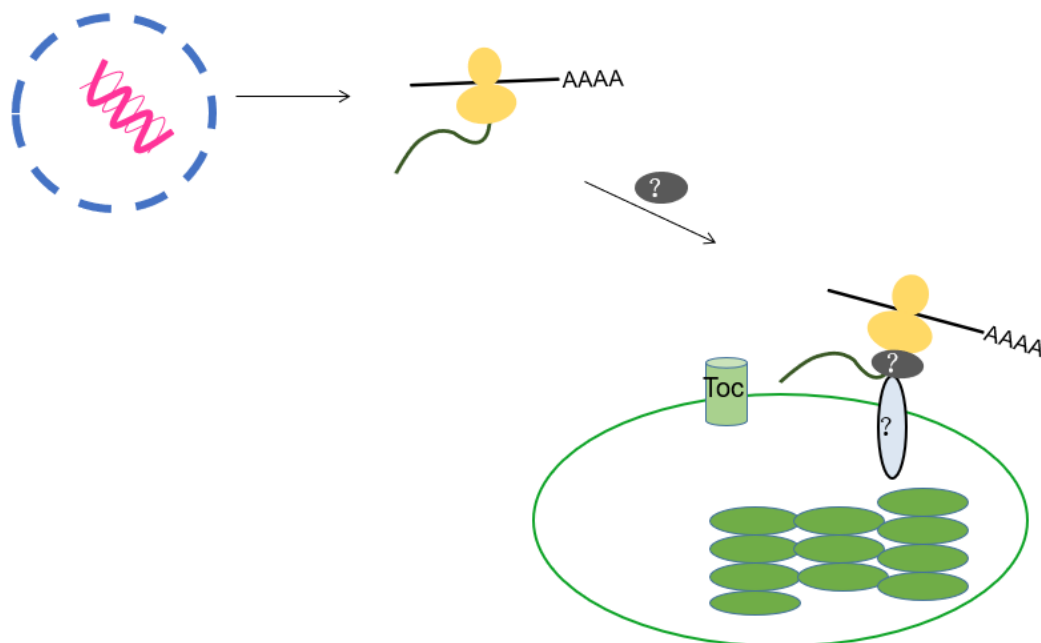


**Figure 6-1 Current model of plastidic mRNA targeting to chloroplasts.**
Cellular model of possible mRNA targeting to chloroplasts. Once the plastidic mRNAs are transcribed in the nucleus and transported into the cytosol, the translation initiated with the association of ribosomes. The RNC complexes is bound by the cytosolic factors to stall the translation. Afterwards, the mRNA-protein complexes are targeted to the chloroplasts and recognized by the receptor in the surface of the chloroplasts. The dark grey oval indicate the cytosolic factor, and the light grey oval indicate the receptor in the surface of the chloroplasts.

## 6.4 Usage of LNA primers to find out the candidates involved in the mRNA targeting process

RNA binding proteins (RBPs) are central to every aspect of gene regulation and many other processes in cell biology (Hentze et al., 2018). A recently developed approach termed RNA interactome capture (RIC) can systematically and comprehensively identify the proteins that interact with polyadenylated RNAs in living cells (Castello et al., 2013). Later, antisense locked nucleic acid (LNA)/DNA oligonucleotides are applied to *in vitro* extracts and identify the RBPs bound to the reporter mRNA with the Sex-lethal (Sxl) binding motifs (Rogell et al., 2017), which is the initial attempt to adapt the LNA primers to the RNA interactome capture. Regarding the limitations of the RIC method, Perez-Perri (2018) develop enhanced RNA interactome capture (eRIC), a method based on the use of an LNA-modified capture probe, conferring numerous advantages including greater specificity and increased signal-to-noise ratios compared to the former RIC (Perez-Perri et al., 2018). Under the condition that RNA demethylases are inhibited by dimethyloxalylglycine, eRIC identifies m6A-responsive RNA-binding proteins which is not detected in RIC (Perez-Perri et al., 2018). Furthermore, eRIC is used for the global analysis of RNA-binding protein dynamics (Perez-Perri et al., 2021). However, applying RIC to plant tissues containing the chloroplasts is challenging since the UV-crosslinking efficiency can be reduced due to the additional secondary metabolites and the presence of UV-absorbing pigments such as chlorophyll (Köster et al., 2019). Therefore, due to the characteristic of the UV-absorbing, little researches apply RIC to identify the proteins involving in the interaction between mRNA and chloroplasts.

In this study, the RIC system is firstly adapted to investigate the proteins involving in the interaction between mRNA and chloroplasts, which fills a critical void in the RNA interactome capture within chloroplasts (Figure 5.13). The previous researches showed the evaluation of the UV-crosslinking efficiency in tumor cells with phenol/chloroform extraction, and more than 80% of the mRNA were found to be cross-linked to protein (Wagenmakers et al. 1980). Following the phenol/chloroform extraction method, the efficiency of the UV-crosslinking to chloroplasts was evaluated. Theoretically, regarding the UV-absorbing by chloroplasts, the UV-crosslinking efficiency might be influenced. Surprisingly, both OEP24 and COX17 mRNA were highly crosslinked to the chloroplasts proteins (Figure 5.14, A, C). That might be the reason that the mRNA bind to the surface of the chloroplasts, and the chlorophyll which absorb the UV light is inside the chloroplasts. Therefore, the UV-crosslinking is not be influenced by the absorbance. Additionally, since the UV-crosslinking only crossed the mRNA and proteins within zero distance (Urdaneta et al., 2020), and the OEP24 mRNA showed the higher efficiency of the UV-crosslinking, which might indicate that OEP24 mRNA interact with proteins

in the different way from the COX17 mRNA. The difference in UV-crosslinking efficiency could also be explained by the specific binding of OEP24 mRNA and unspecific binding of COX17 mRNA (Fig. 5.5). Since the specific bound of OEP24 mRNA occurred between mRNA and protein receptors which could be crosslinked with UV light. However, the unspecific bound might happen between the lipids and mRNA, which might not be crosslinked with UV-light. Therefore, our study initially probe the UV-crosslinking in the chloroplasts surface and illustrate the feasibility to adapt the UV-crosslinking to chloroplasts. Additionally, as the mRNA crosslinked with the protein would remain at the inter and organic phase during the phenol/chloroform extraction. Meanwhile, the previous study has established the approach to enrich the UV cross-linked RNPs by using organic liquid-liquid extraction (Urdaneta et al., 2020). Thus, it might also be possible to enrich the mRNA binding proteins with organic liquid-liquid extraction.

The critical determination for the success in RIC is the specificity of the LNA primers which are used to hybridization the target mRNA (Rogell et al., 2017). In this study, the contamination mainly come from the plastidic rRNA and mRNA from chloroplasts during the pull-down assay, which might increase the background and influence the further Mass spectrometry analysis. Therefore, further optimization to remove the contamination and increase the signal-to-noise ratios are beneficial and still required (Perez-Perri et al., 2018). Regarding the complementary base pairing between the LNA primers and target mRNA, the specific hybridization between the LNA primers and its target mRNA should be stronger than the unspecific binding between the LNA primers and contaminations. Therefore, the pre-elution could remove more unspecific binding between the contamination (rRNA) and beads instead of the specific and tight binding between the probes and target mRNA (Perez-Perri et al., 2018). Once the contamination could be thoroughly deleted by the pre-elution, the optimal temperature for the hybridization is decided according to the purification and the amount of the target in the elution. In this study, $LNA_{OEP24}$ has the highest amount of the target but lowest purification rate in elution at 56 °C, and lowest amount of the target but highest purification rate in elution at 40 °C (Fig, 5.16. A, B). Therefore, considering both the target amount and purification rate of the elution, 48 °C is the optimal temperature for the pull-down assay. Since it has the second highest target amount and third highest purification rate. Similarly, the optimal temperature of $LNA_{COX17}$ is 48 °C. As it has the second highest target amount and the highest purification rate.

Once the pull-down assay with LNA is achieved. The amount of the mRNA and proteins in the elution should be tested with qRT-PCR and silver staining before conducting the Mass spectrometry (Perez-Perri et al., 2018; Zhang et al., 2016). Theoretically, there should be the difference in the amount of the mRNA and proteins between the samples with and without UV crosslinking. The previous study showed that the target mRNA is reduced in the CL samples

compared with the sample without CL (Zhang et al., 2016). In this study, the CL samples contained significantly less mRNA than no CL samples (Figure, 5.17, A). Regarding the UV-crosslinking could not influence the size and do not lead to extensive fragmentation of the RNA (Wagenmakers et al. 1980). The reduction of the mRNA should be caused by the proteins crosslinked to RNA, which lead to the loss of the yield in the RNA isolation. However, the amount of the 16SrRNA has no difference between the CL sample and no CL sample (Figure 5.17, A), which means that the amount of the unspecific contamination binding to the $LNA_{OEP24}$ primers is limited.

As for the proteins detection, protein band pattern should only present in the CL sample and no specific bands in non-CL sample (Zhang et al., 2016), which indicated more proteins was captured with the UV-crosslinking and LNA primer. However, in this study, the A260 and A280 values of the CL and no CL samples were measured. In CL sample, the A260 is 0.827, which is almost the same as the value 0.78 in the no CL sample (Figure 5.18, B), which indicated that the amount of mRNA was not effected under the crosslinking treatment (Wagenmakers et al. 1980). Interestingly, as for the protein level, the A280 in CL sample is 1.482 which is more than the value 0.397 in the No-CL sample, which indicated the more abundance of proteins in the CL sample. Moreover, the ration of A260/A280 is 0.558 in the CL sample and 1.96 in the no-CL samples, which also indicated that the more proteins are in the CL samples. Taken together, the analysis of the RNA level with qRT-PCR showed that the mRNA was successfully crosslinked with the UV-crosslinking, and the more abundance of proteins in the CL-sample showed the mRNA-protein complexes could be captured with the LNA primers. Therefore, these could confirm the success in the pull-down assay with the LNA primers to capture the proteins interacted with the mRNA.

# 7 OUTLOOK

## 7.1 mRNA dependent ribosome association with chloroplasts

The research so far has confirmed that ribosomes do bind to chloroplasts but with low efficiency in the absence of mRNA. This promising project will be followed with the development of a method to avoid the pelleting of the polysomes with chloroplasts. One idea could be the use of a flotation approach as used for liposomes (Schleiff et al., 2001). To this end, the isolated envelope vesicles instead of isolated chloroplasts was used. Isolated envelope vesicles do not pellet at 5,000 x g (Schleiff et al., 2001). Thus, the precipitation of the vesicles in the presence of translating ribosomes using Toc34 antibodies as established marker could be analyzed. Establishing this approach would further enable me to investigate putative binding partner. In case it can be established that translating ribosomes bind to outer envelope vesicles, this would indicate that most likely translation is one mode for the mRNA targeting to chloroplast *in vivo* and mRNA binding to chloroplast *in vitro*.

## 7.2 Properties of mRNA binding to chloroplasts

Based on the current results for the interaction of mRNA with the chloroplast surface and for an influence of cytosolic proteins. Next, the result has to be confirmed for at least two additional mRNAs coding for chloroplast localized proteins in a similar set up binding assay. The selection will be based on the unpublished analysis existing in the laboratory of Prof. Schleiff. In addition, the hybrids between COX17 and OEP24 mRNA will be created to identify the regions and motifs required for chloroplast binding. This approach will be complemented by UV-crosslinking after *OEP24* mRNA addition followed by partial mRNA digest with RNase H. Using different oligonucleotides for amplification of different regions of the gene will allow to define the region critical for chloroplast association. Moreover, the confocal microscope will be used to confirm the identified RNA motifs and to analyze whether the mRNA targeting to chloroplast is translational-based *in vivo*.

## 7.3 Cytosolic and membrane bound factors in the process of mRNA and ribosome binding

As the establishment of the transcriptional and translational active lysate has been achieved. This will supply the chance to ask whether there are cytosolic factors that bind to ribosomes or mRNA. Since the pull-down assay with the LNA/DNA mixamers has been established. This will yield the associated ribonuclear Proteins bound to the mRNA. The nature of the proteins

will be identified by Mass spectrometry. Two independent mRNA will be used, one found to be associated with chloroplasts and coding for a plastidic protein (preferentially OEP24), one coding for a mitochondrial gene (preferentially COX17). This will allow to identify specific factors by overlap of the binding partner of the two mRNA OEP24 and COX17. For the interesting candidates, it will be confirmed both *in vitro* and in mutant plants.

*In vitro*, the proteins from the candidates list will be expressed and purified, which are used for the mRNA binding assay. The function of the proteins could be confirmed by the increasing binding efficiency of the OEP24 mRNA to chloroplasts. For interesting candidates T-DNA insertion mutants will be ordered from the stock center or CrispR/CAS mutants generated to analyze the importance of the factor for plant physiology and organelle function.

# 8 REFERENCE

**Ainger, K., Avossa, D., Diana, A.S., Barry, C., Barbarese, E., and Carson, J.H.** (1997) Transport and localization elements in myelin basic protein mRNA, J. Cell Biol. 138 1077–1087.

**Ainger, K., Avossa, D., Morgan, F., Hill, S.J., Barry, C., Barbarese, E., and Carson, J.H.** (1993) Transport and Localization of Exogenous Myelin Basic Protein mRNA Microinjected into Oligodendrocytes, J. Cell Biol. 123 431-441.

**Arnon, D.I.** (1949) Copper Enzymes in Isolated Chloroplasts. Polyphenoloxidase in Beta Vulgaris. Plant Physiol. 24, 1–15.

**Bach-Pages, M., Homma, F., Kourelis, J., Kaschani, F., Mohammed, S., Kaiser, M., Castello, A. and Preston, G.M.** (2020) Discovering the RNA-binding proteome of plant leaves with an improved rna interactome capture method. Biomolecules 10, 661.

**Bach-Pages, M., Castello, A., and Preston, G.M.** (2017) Plant RNA interactome capture: Revealing the plant RBPome. Trends Plant Sci. 22, 449–451.

**Bae, W., Lee, Y.J., Kim, D.H., Lee, J., Kim, S., Sohn, E.J., and Hwang, I.** (2008). AKR2A-mediated import of chloroplast outer membrane proteins is essential for chloroplast biogenesis. Nat. Cell Biol. **10**: 220–227.

**Bausewein, T., Mills, D.J., Langer, J.D., Nitschke, B., Nussberger, S., and Kühlbrandt, W.** (2017). Cryo-EM Structure of the TOM Core Complex from Neurospora crassa. Cell **170**: 693–700.

**Becker, T., Jelic, M., Vojta, A., Radunz, A., Soll, J., and Schleiff, E.** (2004). Preprotein recognition by the Toc complex. EMBO J. 23, 520–530.

**Beckmann, B.M.** (2017) RNA interactome capture in yeast. Methods 118-119, 82–92.

**Buntru M, Vogel S, Spiegel H, Schillberg S.** (2014). Tobacco BY-2 cell-free lysate: an alternative and highly-productive plant-based *in vitro* translation system. BMC Biotechnol. 14: 37.

**Carde, J.P., Joyard, J., and Douce, R.** (1982). Electron microscopic studies of envelope membranes from spinach plastids . Biol Cell **44**: 315–324.

**Castello, A., Horos, R., Strein, C., Fischer, B., Eichelbaum, K., Steinmetz, L.M., Krijgsveld, J. and Hentze, M.W.** (2013) System-wide identification of RNA-binding proteins by interactome capture. Nat. Protoc 8: 491–500.

**Chacinska, A., Koehler, C.M., Milenkovic, D., Lithgow, T., and Pfanner, N.** (2009).

Importing Mitochondrial Proteins: Machineries and Mechanisms. Cell **138**: 628–644.

**Chu, C., Qu, K., Zhong, F.L., Artandi, S.E. and Chang, H.Y.** (2011) Genomic maps of long noncoding RNA occupancy reveal principles of RNA-chromatin interactions. Mol. Cell 44, 667–678.

**Chu, C., Zhang, QF., Rocha, S., Flynn, RA., Bharadwaj, M., Calabrese, M., Magnuson, T., Heard, E., and Chang, H.Y.** (2015) Systematic discovery of Xist RNA binding proteins. Cell 161, 404–416.

**Crowley, P.H., Cottrell, T., Garcia, T., Hatch, M., Sargent, R.C., Stokes, B.J., and White, J.M.** (1998). Solving the complementarity dilemma: evolving strategies for simultaneous hermaphroditism, J. Theor. Biol. 195 13–26.

**Daley, D.O. and Whelan, J.** (2005). Why genes persist in organelle genomes. Genome Biol. **6**.

**Dhanoa, P.K., Richardson, L.G.L., Smith, M.D., Gidda, S.K., Henderson, M.P.A., Andrews, D.W., and Mullen, R.T.** (2010). Distinct pathways mediate the sorting of tail-anchored proteins to the plastid outer envelope. PLoS One **5**.

**Eliyahu, E., Pnueli, L., Melamed, D., Scherrer, T., Gerber, A.P., Pines, O., Rapaport, D., and Arava, Y.** (2010). Tom20 mediates localization of mRNAs to mitochondria in a translation-dependent manner. Mol. Cell. Biol. **30**: 284–94.

**Faoro, C., and Ataide, S.F.** (2014) Ribonomic approaches to study the RNA-binding proteome. FEBS Lett. 588, 3649–3664.

**Gadir, N., Haim-Vilmovsky, L., Kraut-Cohen, J., and Gerst, J.E.** (2011). Localization of mRNAs coding for mitochondrial proteins in the yeast Saccharomyces cerevisiae. RNA **17**: 1551–65.

**Gakh, O., Cavadini, P., and Isaya, G.** (2002). Mitochondrial processing peptidases. Biochim. Biophys. Acta - Mol. Cell Res. **1592**: 63–77.

**Gerber, A.P., Herschlag, D., and Brown, P.O.** (2004). Extensive association of functionally and cytotopically related mRNAs with Puf family RNA-binding proteins in yeast, PLoS Biol. 2 E79.

**Gogala, M., Becker, T., Beatrix, B., Armache, J.P., Barrio-Garcia, C., Berninghausen, O., and Beckmann, R.** (2014). Structures of the Sec61 complex engaged in nascent peptide translocation or membrane insertion. Nature 506: 107–110.

**Gray, M.W.** (1999). Evolution of organellar genomes. Curr. Opin. Genet. Dev. **9**: 678–687.

**Gu, W., Deng, Y., Zenklusen, D., and Singer, R.H.** (2004) A new yeast PUF family protein,

Puf6p, represses ASH1 mRNA translation and is required for its localization, Genes Dev. 18 1452–1465.

**Hachiya, N., Komiya, T., Alam, R., Iwahashi, J., Sakaguchi, M., Omura, T., and Mihara, K.** (1994). MSF, a novel cytoplasmic chaperone which functions in precursor targeting to mitochondria. EMBO J. **13**: 5146–5154.

**Hacisuleyman, E., Goff, L.A., Trapnell, C., Williams, A., Henao-Mejia, J., Sun, L., McClanahan, P., Hendrickson, D.G., Sauvageau, M., Kelley, D.R., Morse, M., Engreitz, J., Lander, E.S., Guttman, M., Lodish, H.F., Flavell, R., Raj, A., and Rinn, J.L.** (2014) Topological organization of multichromosomal regions by the long intergenic noncoding RNA Firre. Nat. Struct. Mol. Biol. 21, 198–206.

**Hamada, S., Ishiyama, K., Choi, S.-B., Wang, C., Singh, S., Kawai, N., Franceschi, V.R., and Okita, T.W.** (2003). The Transport of Prolamine RNAs to Prolamine Protein Bodies in Living Rice Endosperm Cells. Plant Cell **15**: 2253–2264.

**Hartmuth, K., Vornlocher, H.P., and Lührmann, R.** (2004) Tobramycin afnity tag purifcation of spliceosomes. In mRNA Processing and Metabolism 47–64.

**Hentze, M.W., Castello, A., Schwarzl, T., and Preiss, T.** (2018) A brave new world of RNA-binding proteins. Nat. Rev. Mol. Cell Biol. 19, 327–341.

**Hill, K., Model, K., Ryan, M.T., Dietmeier, K., Martint, F., Wagner, R., and Pfanner, N.** (1998). Tom40 forms the hydrophilic channel of the mitochondrial import pore for preproteins. Nature **395**: 516–521.

**Hoffman, E.A., Frey, B.L., Smith, L.M. and Auble, D.T.** (2015) Formaldehyde crosslinking: a tool for the study of chromatin complexes. J. Biol. Chem. 290, 26404–26411.

**Hogg, J.R., and Collins, K.** (2007) RNA-based affinity purification reveals 7SK RNPs with distinct composition and regulation. RNA 13, 868–880.

**Huang, S., Taylor, N.L., Whelan, J., and Millar, A.H.** (2009). Refining the Definition of Plant Mitochondrial Presequences through Analysis of Sorting Signals, N-Terminal Modifications, and Cleavage Motifs. Plant Physiol. **150**: 1272–1285.


**Jambhekar, A., and Derisi, J.L. (2007)** Cis-acting determinants of asymmetric, cytoplasmic RNA transport, RNA 13 625–642.

**Jores, T., Klinger, A., Groß, L.E., Kawano, S., Flinner, N., Duchardt-Ferner, E., Wöhnert, J., Kalbacher, H., Endo, T., Schleiff, E., and Rapaport, D.** (2016). Characterization of the targeting signal in mitochondrial β-barrel proteins. Nat. Commun. **7**: 1–16.

**Jores, T. and Rapaport, D.** (2017). Early stages in the biogenesis of eukaryotic β-barrel proteins. FEBS Lett. **591**: 2671–2681.

**Junne, T., Kocik, L., and Spiess, M.** (2010). The hydrophobic core of the Sec61 translocon defines the hydrophobicity threshold for membrane integration. Mol. Biol. Cell 21: 1662–1670.

**Kellems, R.E., Allison, V.F., and Butow, R.A.** (1974). Cytoplasmic type 80 S ribosomes associated with yeast mitochondria. II. Evidence for the association of cytoplasmic ribosomes with the outer mitochondrial membrane in situ. J. Biol. Chem. **249**: 3297–303.

**Kellems, R.E., Allison, V.F., and Butow, R.A.** (1975). Cytoplasmic type 80S ribosomes associated with yeast mitochondria. IV. Attachment of ribosomes to the outer membrane of isolated mitochondria. J. Cell Biol. **65**: 1–14.

**Kellems, R.E., and Butow, R.A.** (1972) Cytoplasmic-type 80 S ribosomes associated with yeast mitochondria. I. Evidence for ribosome binding sites on yeast mitochondria, J. Biol. Chem. 247 8043–8050.

**Kim, B. and Kim, V.N.** (2019) fCLIP-seq for transcriptomic footprinting of dsRNA-binding proteins: lessons from DROSHA. Methods 152, 3–11.

**Klinger, A., Gosch, V., Bodensohn, U., Ladig, R., and Schleiff, E.** (2019). The signal distinguishing between targeting of outer membrane β-barrel protein to plastids and mitochondria in plants. Biochim. Biophys. Acta - Mol. Cell Res. **epub**.

**Kraut-Cohen, J., and Gerst, J.E.** (2010) Addressing mRNAs to the ER: cis sequences act up! Trends Biochem. Sci. 35 459–469.

**Kutik, S., Stojanovski, D., Becker, L., Becker, T., Meinecke, M., Krüger, V., Prinz, C., Meisinger, C., Guiard, B., Wagner, R., Pfanner, N., and Wiedemann, N.** (2008). Dissecting Membrane Insertion of Mitochondrial β-Barrel Proteins. Cell **132**: 1011–1024.

**Ku, C.**, **Nelson-Sathi, S., Roettger, M., Sousa, F., Lockhart, P.J., Bryant, D., Hazkani-Covo, E., McInerney, J.O., Landan, G., and Martin, W.F.,** (2015). Endosymbiotic origin and differential loss of eukaryotic genes. Nature 524: 427-32.

**Köster, T., Reichel, M., and Staiger, D.** (2019) CLIP and RNA interactome studies to unravel genome-wide RNA-protein interactions *in vivo* in Arabidopsis thaliana. Methods. 178, 63-71

**Laemmli, U.K.** (1970). Cleavage of structural proteins during the assembly of the head of bacteriophage T4. Nature 227, 680–685.

**Leliaert, F. and Lopez-Bautista, J.M.** (2015). The chloroplast genomes of Bryopsis plumosa

and Tydemania expeditiones (Bryopsidales, Chlorophyta): Compact genomes and genes of bacterial origin. BMC Genomics **16**: 1–20.

**Lee, K., and Kang, H.** (2016) Emerging roles of RNA-binding proteins in plant growth, development, and stress responses. Mol. Cells 39: 179– 185.

**Leppek, K., and Stoecklin, G.** (2014) An optimized streptavidin-binding RNA aptamer for purifcation of ribonucleoprotein complexes identifies novel ARE-binding proteins. Nucleic Acids Res. 42, e13.

**Lesnik, C., Cohen, Y., Atir-Lande, A., Schuldiner, M., and Arava, Y.** (2014) OM14 is a mitochondrial receptor for cytosolic ribosomes that supports co-translational import into mitochondria. Nat. Commun. 5, 5711.

**Lill R, Mühlenhoff U.** (2008). Maturation of Iron-Sulfur Proteins in Eukaryotes: Mechanisms, Connected Processes, and Diseases. Annu. Rev. Biochem. 77: 669–700.

**Liu, M., and Spremulli, L.** (2000). Interaction of mammalian mitochondrial ribosomes with the inner membrane. J Biol Chem. 275: 29400-29406.

**Li, X., Song, J. and Yi, C.** (2014) Genome-wide mapping of cellular protein-RNA interactions enabled by chemical crosslinking. Genomics Proteomics Bioinformatics 12, 72–78.

**Machettira, A.B., Groß, L.E., Tillmann, B., Weis, B.L., Englich, G., Sommer, M.S., Königer, M., and Schleiff, E.** (2012). Protein-Induced Modulation of Chloroplast Membrane Morphology. Front. Plant Sci. **2**: 118–129.

**Marc, P., Margeot, A., Devaux, F., Blugeon, C., Corral-Debrinski, M., and Jacq, C.** (2002). Genome-wide analysis of mRNAs targeted to yeast mitochondria. EMBO Rep. **3**: 159–164.

**Margulies, M.M., and Michaels, A.** (1974). Ribosomes bound to chloroplast membranes in Chlamydomonas reinhardtii, J. Cell Biol. 60 (1974) 65–77.

**Marondedze, C., Thomas, L., Serrano, N.L., Lilley, K.S., and Gehring, C.** (2016) The RNA-binding protein repertoire of Arabidopsis thaliana. Sci. Rep. 6, 29766

**Marondedze, C., Thomas, L., Gehring, C., and Lilley, K.S.** (2019) Changes in the Arabidopsis RNA-binding proteome reveal novel stress response mechanisms. BMC Plant Biol. 19, 1–11.

**Martin, W., Rujan, T., Richly, E., Hansen, A., Cornelsen, S., Lins, T., Leister, D., Stoebe, B., Hasegawa, M., and Penny, D.** (2002). Evolutionary analysis of Arabidopsis, cyanobacterial, and chloroplast genomes reveals plastid phylogeny and thousands of

cyanobacterial genes in the nucleus. Proc. Natl. Acad. Sci. **99**: 12246–12251.

**Martin, T., Sharma, R., Sippel, C., Waegemann, K., Soll, J., and Vothknecht, U.C.** (2006). A protein kinase family in Arabidopsis phosphorylates chloroplast precursor proteins. J. Biol. Chem. **281**: 40216–40223.

**Matia-González, A.M., Iadevaia, V. and Gerber, A.P.** (2017) A versatile tandem RNA isolation procedure to capture *in vivo* formed mRNA-protein complexes. Methods 118–119, 93–100.

**May, T. and Soll, J.** (2000). 14-3-3 Proteins Form a Guidance Complex with Chloroplast Precursor Proteins in Plants. Plant Cell **12**: 53–64.

**McHugh, C.A. and Guttman, M.** (2018) RAP-MS: a method to identify proteins that interact directly with a specific RNA molecule in cells. Methods Mol. Biol. 1649, 473–488.

**McHugh, C.A., Chen, C.K., Chow, A., Surka, C.F., Tran, C., McDonel P., Pandya-Jones, A., Blanco, M., Burghard, C., Moradian, A., Sweredoski, M.J., Shishkin, A.A., Su, J., Lander, E.S., Hess, S., Plath, K., and Guttman, M.** (2015) The Xist lncRNA interacts directly with SHARP to silence transcription through HDAC3. Nature 521, 232–236.

**Meisenheimer, K.M. and Koch, T.H.** (1997) Photocross-linking of nucleic acids to associated proteins. Crit. Rev. Biochem. Mol. Biol. 32, 101–140.

**Michaud, M., Maréchal-Drouard, L., and Duchêne, A.M.** (2010). RNA trafficking in plant cells: Targeting of cytosolic mRNAs to the mitochondrial surface. Plant Mol. Biol. **73**: 697–704.

**Michaud, M., Maréchal-Drouard, L., and Duchêne, A.-M.** (2014a). Targeting of cytosolic mRNA to mitochondria: Naked RNA can bind to the mitochondrial surface. Biochimie **100**: 159–166.

**Michaud, M., Ubrig, E., Filleur, S., Erhardt, M., Ephritikhine, G., Marechal-Drouard, L., and Duchene, A.-M.** (2014b). Differential targeting of VDAC3 mRNA isoforms influences mitochondria morphology. Proc. Natl. Acad. Sci. **111**: 8991–8996.

**Mirus O, Hahn A, Schleiff E.** (2010). Outer Membrane Proteins. In: Prokaryotic Cell Wall Compounds. Structure and Biochemistry (Eds. H. König, H. Claus and A. Varma) Springer-Verlag, pp 175-230.

**Mirus O, Schleiff E**. (2012). Recycling and Tinkering- The evolution of protein transport to and into endosymbiotically derived organelles. In: Organelle Genetics: Evolution of organelle genomes and gene expression (Ed. E. C.E. Bullerwell), Springer Verlag Berlin, pp 175–216.

**Nicolai, M., Duprat, A., Sormani, R., Rodriguez, C., Roncato, M.A., Rolland, N., and Robaglia, C.** (2007) Higher plant chloroplasts import the mRNA coding for the eucaryotic translation initiation factor 4E. FEBS Lett, 581:3921-3926.

**Nobumoto, M., Yamada, M., Song, S., Inouye, S., and Nakazawa, A.** (1998). Mechanism of mitochondrial import of adenylate kinase isozymes. J. Biochem. **123**: 128–135.

**Parrott, A.M., Lago, H., Adams, C.J., Ashcroft, A.E., Stonehouse, N.J., and Stockley, P.G.** (2000) RNA aptamers for the MS2 bacteriophage coat protein and the wild-type RNA operator have similar solution behavior. Nucleic Acids Res. 28, 489–497.

**Parton, R.M., Davidson, A., Davis, I., and Weil, T.T.** (2014). Subcellular mRNA localisation at a glance. J. Cell Sci. **127**: 2127–2133.

**Perez-Perri, J.I., Rogell, B., Schwarzl, T., Stein, F., Zhou, Y., Rettel, M., Brosig, A. and Hentze, M.W.** (2018) Discovery of RNA-binding proteins and characterization of their dynamic responses by enhanced RNA interactome capture. Nat. Commun. 9, 4408.

**Pestka S.** (1971). Inhibitors of ribosome functions. Annu Rev Microbiol. **25**: 487–562.

**Pohlmeyer, K., Soll, J., Grimm, R., Hill, K., and Wagner, R.,** (1998). A high-conductance solute channel in the chloroplastic outer envelope from Pea. Plant Cell. 10: 1207–1216.

**Popov, N., Schmitt, M., Schulzeck, S., and Matthies, H.** (1975). Eine störungsfreie Mikromethode zur bestimmung des Proteingehaltes in Gewebehomogenaten. Acta Biol. Med. Ger. **34**: 1441–1446.

**Qbadou, S., Becker, T., Bionda, T., Regar, K., Ruprecht, M., Soll, J., and Schleiff, E.** (2007) Toc64 — a preprotein-receptor at the outer membrane with bipartide function. J. Mol. Biol. 367, 1330–1346.

**Qbadou, S., Becker, T., Mirus, O., Tews, I., Soll, J., and Schleiff, E.** (2006) The molecular chaperone Hsp90 delivers precursor proteins to the chloroplast import receptor Toc64. EMBO J. 25, 1836–1847 (2006).

**Reichel, M., Liao, Y., Rettel, M., Ragan, C., Evers, M., Alleaume, A.M., Horos, R., Hentze, M.W., Preiss, T., and Millar, A.A.** (2016) In planta determination of the mRNA-binding proteome of Arabidopsis etiolated seedlings. Plant Cell. 28, 2435–2452.

**Rogell, B., Fischer, B., Rettel, M., Krijgsveld, J., Castello, A. and Hentze, M.W.** (2017) Specific RNP capture with antisense LNA/DNA mixmers. RNA 23, 1290–1302.

**Saint-Georges, Y., Garcia, M., Delaveau, T., Jourdren, L., Le Crom, S., Lemoine, S., Tanty, V., Devaux, F., and Jacq, C.** (2008). Yeast Mitochondrial Biogenesis: A Role for the PUF RNA-Binding Protein Puf3p in mRNA Localization. PLoS One **3**: e2293.

**Sambrook and Russell** (2001). Molecular Cloning: A Laboratory Manual (3rd ed.). (Cold Spring Harbor Laboratory Press: Cold Spring Harbor, N.Y.).

**Saraogi, I. and Shan, S.O.** (2011). Molecular Mechanism of Co-translational Protein Targeting by the Signal Recognition Particle. Traffic **12**: 535–542.

**Saraste, M.** (1999). Oxidative Phosphorylation at the fin de si&amp;egrave;cle. Science **283**: 1488–1493.

**Schleiff, E. and Becker, T.** (2011). Common ground for protein translocation: Access control for mitochondria and chloroplasts. Nat. Rev. Mol. Cell Biol. **12**: 48–59.

**Schleiff, E., Soll, J., Küchler, M., Kühlbrandt, W., and Harrer, R.** (2003). Characterization of the translocon of the outer envelope of chloroplasts. J. Cell Biol. **160**: 541–551.

**Schnell, D.J., Kessler, F., and Blobel, G.** (1994). Isolation of components of the chloroplast protein import machinery. Science **266**: 1007–1012.

**Shen, Z., Paquin, N., Forget, A., and Chartrand, P.** (2009) Nuclear shuttling of She2p couples ASH1 mRNA localization to its translational repression by recruiting Loc1p and Puf6p, Mol. Biol. Cell 20 2265–2275.

**Simon, M.D., Wang, C.I., Kharchenko, P.V., West, J.A., Chapman, B.A., Alekseyenko, A.A., Borowsky, M.L., Kuroda, M.I. and Klingston, R.E.** (2011) The genomic binding sites of a noncoding RNA. Proc. Natl Acad. Sci. USA 108, 20497–20502

**Simon, M.D.** (2013) Capture hybridization analysis of RNA targets (CHART). Curr. Protoc. Mol. Biol. 101, 21.25.1–21.25.16.

**Sommer MS, Schleiff E**. (2014). Protein targeting and transport as a necessary consequence of increased cellular complexity. Cold Spring Harb Perspect Biol. 6: pii: a016055.

**Sugimoto, Y., König, J., Hussain, S., Zupan, B., Curk, T., Frye, M., and Ule, J.** (2012) Analysis of CLIP and iCLIP methods for nucleotide resolution studies of protein-RNA interactions. Genome Biol. 13, R67.

**Sutherland, B.W., Toews, J., and Kast, J.** (2008) Utility of formaldehyde cross-linking and mass spectrometry in the study of protein-protein interactions. J. Mass Spectrom. 43, 699–715.

**Tian, L. and Okita, T.W.** (2014). mRNA-based protein targeting to the endoplasmic reticulum and chloroplasts in plant cells. Curr. Opin. Plant Biol. **22**: 77–85.

**Timmis, J.N., Ayliff, M.A., Huang, C.Y., and Martin, W.** (2004). Endosymbiotic gene transfer: Organelle genomes forge eukaryotic chromosomes. Nat. Rev. Genet. **5**: 123–135.

**Towbin, H., Staehelin, T., and Gordon, J.** (1979). Electrophoretic transfer of proteins from polyacrylamide gels to nitrocellulose sheets: procedure and some applications. Proc. Natl. Acad. Sci. U. S. A. 76, 4350–4354.

**Tsai, B.P., Wang, X., Huang, L. and Waterman, M.L.** (2011) Quantitative profiling of in vivo–assembled RNA-protein complexes using a novel integrated proteomic approach. Mol. Cell. Proteomics 10, M110.007385.

**Ulrich, T., Gross, L.E., Sommer, M.S., Schleiff, E., and Rapaport, D.** (2012). Chloroplast β-barrel proteins are assembled into the mitochondrial outer membrane in a process that depends on the TOM and TOB complexes. J. Biol. Chem. **287**: 27467–27479.

**Uniacke, J. and Zerges, W.** (2009). Chloroplast protein targeting involves localized translation in Chlamydomonas. Proc. Natl. Acad. Sci. U. S. A. **106**: 1439–1444.

**Urdaneta, E.C., Vieira-Vieira, C.H., Hick, T., Wessels, H.H., Figini, D., Moschall, R., Medenbach, J., Ohler, U., Granneman, S., Selbach, M., Beckmann, B.M.** (2019) Purification of cross-linked RNA-protein complexes by phenol-toluol extraction, Nat. Commun. 10 (1) 990

**Wagenmakers A. J, Reinders, R. J. and van Venrooij, W. J.** (1980) Cross-linking of mRNA to proteins by irradiation of intact cells with ultraviolet light. Eur. J. Biochem. 112, 323–330.

**Wang, Z. and Benning, C.** (2011). Arabidopsis thaliana polar glycerolipid profiling by thin layer chromatography (TLC) coupled with gas-liquid chromatography (GLC). J. Vis. Exp.: 1–6.

**Weis, B.L., Schleiff, E., and Zerges, W.** (2013). Protein targeting to subcellular organelles via mRNA localization. Biochim. Biophys. Acta - Mol. Cell Res. **1833**: 260–273.

**Yamamoto, H., Fukui, K., Takahashi, H., Kitamura, S., Shiota, T., Terao, K., Uchida, M., Esaki, M., Nishikawa, S., Yoshihisa, T., Yamano, K., and Endo, T.** (2009) Role of Tom70 in import of presequence-containing mitochondrial proteins. J. Biol. Chem. 284, 31625–31646.

**Young, J.C., Hoogenraad, N.J., and Hartl, F.U.** (2003) Molecular chaperones Hsp90 and Hsp70 deliver preproteins to the mitochondrial import receptor Tom70. Cell 112, 41–50.

**Zeng, L., Guo, J., Xu, H.B., Huang, R., Shao, W., Yang, L., Wang, M., Chen, J., and Xie, P.** (2013). Direct Blue 71 staining as a destaining-free alternative loading control method for Western blotting. Electrophoresis **34**: 2234–2239.

**Zeng, F., Peritz, T., Kannanayakal, T.J., Kilk, K., Eiriksdottir, E., Langel, U., and**

Eberwine, J. (2006) A protocol for PAIR: PNA-assisted identification of RNA binding proteins in living cells. Nat. Protoc. 1, 920–927.

Zhang, Z., Boonen, K., Ferrari, P., Schoofs, L., Janssens, E., Van Noort, V., Rolland, F., and Geuten, K. (2016) UV crosslinked mRNA-binding proteins captured from leaf mesophyll protoplasts. Plant Methods. 12, 42.

Zhang, Z., Boonen, K., Li, M., and Geuten, K. (2017) mRNA interactome capture from plant protoplasts. J. Vis. Exp. 125, e56011.

Zimorski, V., Ku, C., Martin, W.F., and Gould, S.B. (2014). Endosymbiotic theory for organelle origins. Curr. Opin. Microbiol. **22**: 38–48.

# ACKNOWLEDGEMENTS

# CURRICULUM VITAE

**Personal data**

Name          Bo Zhang

Date of birth      June. 19th 1991

Place of birth      Zheng Zhou, China

**Education**

2017/09-Now

Goethe-Universität Frankfurt am Main

Molecular Cell Biology of Plants

Project: mRNA targeting to the plants

Doctoral thesis: mRNA binding to organellar surfaces as mode of cellular surveillance

Supervisor: Prof. Dr. Enrico Schleiff (JWGU Frankfurt)

2014/09-2017/06

Department of Agriculture

Northwest Agriculture & Forestry University

Master of Crop Genetics and Breeding

Project：Functional genes and molecular regulation of reproductive process in wheat

(Projects for the 973 projects (2014CB138102)

Master thesis: Discovery of novel allelic variations at PPD and VRN locus in common wheat

Supervisor: Prof. Dr. Xiaoke Zhang (Northwest Agriculture & Forestry University)

2010/09-2014/06

Department of Life Science

Henan agriculture University

Bachelor of science

# ERKLÄRUNG

Ich erkläre hiermit, dass ich mich bisher keiner Doktorprüfung unterzogen habe.


Frankfurt am Main, den ……….……..                  ……………………………


# EIDESSTATTLICHE VERSICHERUNG


Ich erkläre hiermit an Eides Statt, dass ich die vorgelegte Dissertation über

**„mRNA binding to organellar surfaces as mode of cellular surveillance"**

selbständig angefertigt und mich anderer Hilfsmittel als der in ihr angegebenen nicht bedient habe, insbesondere, dass alle Entlehnungen aus anderen Schriften mit Angabe der betreffenden Schrift gekennzeichnet sind.

Ich versichere, die Grundsätze der guten wissenschaftlichen Praxis beachtet, und nicht die Hilfe einer kommerziellen Promotionsvermittlung in Anspruch genommen zu haben.


Frankfurt am Main, den ……….……..                  ……………………………